Exploring the Mechanisms of Regeneration in *Ptychodera flava*

Shawn M. Luttrell

A dissertation

submitted in partial fulfillment of the

requirements for the degree of

Doctor of Philosophy

University of Washington

2017

Reading Committee:

Billie J. Swalla, Chair

Olivia Bermingham-McDonogh

Sharlene Santana

Program Authorized to Offer Degree:

Biology

University of Washington

Abstract

Exploring the Mechanisms of Regeneration in *Ptychodera flava*
Shawn M. Luttrell

Chair of the Supervisory Committee:
Director Billie J. Swalla
UW Friday Harbor Laboratories

Hemichordates are marine acorn worms and a sister group to the echinoderms. Acorn worms share numerous developmental features with the chordates that the echinoderms do not share, suggesting that the common ancestor of the deuterostome clade was likely more similar to hemichordates than to echinoderms. Hemichordates possess pharyngeal gill slits that are homologous to chordate gill slits, a *Hox* specified anterior-posterior body plan, an endostyle, and a post-anal tail in some species. The hemichordate, *Ptychodera flava*, progresses from a pelagic, feeding tornaria larva to a tripartite, benthic worm with an anterior head or proboscis, a middle collar region, and a long posterior trunk. The collar houses a hollow, dorsal neural tube in ptychoderid hemichordates and numerous chordate genes involved in brain and spinal cord development are expressed in a similar anterior–posterior spatial arrangement along the hemichordate body axis. Remarkably, *P. flava* regenerates all structures, including their dorsal neural tube. This work investigates the morphological and genetic mechanisms underlying this fascinating trait

I examined anterior regeneration in the hemichordate *Ptychodera flava* and detailed the spatial and temporal morphological changes that occur. Additionally, we sequenced, assembled, and analyzed the transcriptome for eight stages of regenerating *P. flava*, and revealed significant differential gene expression between regenerating and control animals. Importantly, we

uncovered developmental steps that are regeneration-specific and do not strictly follow the embryonic program.

We also showed that *P. flava* larvae are capable of robust regeneration after bisection through the sagittal, coronal, and axial planes. We used antibody staining to show that the anterior apical region, including the eyespots and larval brain, regenerates a rich, serotonin positive complex of cells within two weeks after amputation. Cells labeled with EdU (5-ethynyl-2'-deoxyuridine) confirmed that regeneration is occurring through epimorphic processes as new cells are added at the cut site and throughout the regenerating tissue. This study verified that *P. flava* larvae can be used for future functional studies aimed at identifying the genetic and morphological mechanisms controlling CNS regeneration in a stem deuterostome.

TABLE OF CONTENTS

LIST OF FIGURES

Figure Number Page

LIST OF TABLES

Chapter 1 - Genomic and Evolutionary Insights into Chordate Origins

This chapter was published as **Luttrell, S.M**. and Swalla, B.J. (2014). Genomic and Evolutionary Insights into Chordate Origins. In "Principles of Developmental Genetics", 2nd edition. Sally Moody, ed. (Elsevier, San Diego.) pp. 116-126.

Section 1: Summary

- Hemichordates are the sister group to echinoderms, not chordates, so shared characters with chordates would have been present in the deuterostome ancestor.
- *Hox* genes are expressed in an anterior to posterior manner in hemichordates and chordates. Tunicates have lost the middle *Hox* genes and show different tissue expression patterns. Echinoderms have a rearranged *Hox* cluster and show limited co-linearity of expression in the somatapleura.
- Pharyngeal gill slits in hemichordates and chordates are homologous. Pharyngeal gill bars develop similarly in hemichordates and lancelets, but differ from vertebrates in that they are acellular and endodermal in origin.
- Post-anal tails and endostyles in hemichordates and chordates are likely to be homologous.
- Chordates specify neural and non-neural ectoderm, while all ectoderm is neural in hemichordates. Hemichordates make a dorsal neural tube in their neck region.
- Recent data suggest the stomochord may be the notochord homolog in hemichordates.
- Tunicates contain migratory cells that develop into pigment cells, so may contain neural crest cells. Tunicates also have sensory placodes, and form a secondary anus after metamorphosis, so the excurrent siphon develops from the otic placode.

Section 2: Introduction

History of Hypotheses of Chordate Origins

Vertebrates share several distinct morphological characters with three invertebrate groups: hemichordates (Figure 1A), tunicates (Figure 1B), and lancelets (Figure 1C). Tunicates, lancelets and vertebrates are a monophyletic group, the chordates (Swalla and Smith, 2008), which share five morphological features: a notochord, a dorsal neural tube, an endostyle, a muscular post-anal tail and pharyngeal gill slits (Swalla, 2007). Hemichordates share some of these chordate features; the pharyngeal gill slits (Figure 1), an endostyle, dorsal neural tube and a post-anal tail (Swalla, 2007; Brown et al., 2008). Developmental genetics and genomics have allowed re-examination of the question of chordate origins by comparing developmental gene expression in embryos of different phyla. This powerful approach has allowed new insights into the molecular mechanisms underlying morphological changes. However, as we illuminate here, comparing the correct developmental stages are critical to interpretation of the data. Genomics has allowed investigations into the phylogenetic relationships of the chordates and their invertebrate relatives, and comparison of the shared genetic pathways in related embryos. We review current research and show that our view of the chordate ancestor has changed in the past 15 years. The chordate ancestor, for years, had been considered to be a filter-feeding, tunicate-like animal with a tiny chordate tadpole larva (Figure 2). However, recent evidence from our lab and others has shown that the chordate ancestor is more likely a benthic worm, with a mouth and pharyngeal gill slits, supported by cartilaginous gill bars (Cameron et al., 2000; Gerhart et al., 2005; Rychel et al., 2006; Gillis et al., 2012). Further research in developmental genetics and genomics will be fruitful in solving some of the remaining homologies between hemichordates and chordates.

Three disparate hypotheses of chordate origins are shown in Figure 2 (Garstang, 1928; Romer, 1967; Jefferies, 1986; Jollie, 1973; Gee, 1996; Gerhart et al., 2005; Brown et al., 2008). One early scenario of chordate origins, which was quite popular, is the Garstang view of chordate origins, first hypothesized near the turn of the 20th century (Figure 2-1; Garstang, 1928). This theory espouses the notion that the echinoderm and hemichordate larvae "evolved" into the ascidian tadpole larvae, and the adults of echinoderms, hemichordates and tunicates developed independently. However, developmental gene expression data show that hemichordates and chordates share adult features, not larval (Swalla, 2006; Brown et al., 2008). These results would favor the evolution of chordates from a direct developing hemichordate (Gerhart et al., 2005; Rychel et al., 2006), not from a hemichordate tornaria larvae. Further comments on Garstang's theory, and genetic evidence against it, are nicely summarized in Lacalli (2005).

Some textbooks still carry the scenario that all deuterostomes evolved from a colonial hemichordate, a pterobranch, first published by Romer in 1967 (Figure 2-2). This theory was popularized because the fossil record has an abundance of colonial hemichordates, called graptolites, and because lophophorates were considered related to deuterostomes (Romer, 1967; Gee, 1996). Molecular phylogenetics has shown that the lophophorates are part of a large group of animals called the lophotrochozoa (Halanych, 2004), and that the colonial pterobranchs are derived hemichordates (Cameron et al., 2000). Collectively, these new data brought into question the widely held view of deuterostome evolution popularized by Romer.

We published a new hypothesis based on our molecular phylogenies and developmental gene expression patterns in 2000 (Figure 2-3; Cameron et al., 2000). In this scenario, the deuterostome ancestor is worm-like with gill slits, and the larvae of hemichordates and

echinoderms developed independent of ascidian tadpole larvae. In the ensuing years, developmental gene expression data have continued to favor a worm-like deuterostome ancestor (Lowe et al., 2003; Gerhart et al., 2005; Rychel et al., 2006; Delsuc et al., 2006; Bourlat et al., 2006). Developmental genomics and genetics can provide key pieces of evidence to understanding chordate origins. Genomic information is available for at least a single member of each of the deuterostome monophyletic groups – echinoderms (the purple sea urchin *Stronglyocentrotus purpuratus*; Sodergren et al., 2006), hemichordates (an acorn worm, *Saccoglossus kowalevskii*; Freeman et al., 2008), tunicates (solitary ascidians *Ciona intestinalis*, Dehal et al., 2002; *C. savignyi*, Vinson et al., 2005), and the pelagic appendicularian *Oikopleura dioica* (Denoeud et al., 2010), cephalochordates (the lancelet *Branchistoma floridae*; Putnam et al., 2008), and many vertebrate species (Fong et al., 2013). Deuterostomes share many of the developmental genetic networks during early embryonic and larval development (Davidson and Erwin, 2006; Swalla, 2006). Developmental genetics can be highly informative by illuminating how these similar genetic pathways are expressed in different times and places to elaborate the final morphology of the larvae and the adults (Swalla, 2006). We next review the latest findings of molecular phylogenetics and genomic analyses, examine developmental gene expression in different deuterostome phyla, and discuss the origin of the vertebrates in light of new data published in the past 15 years.

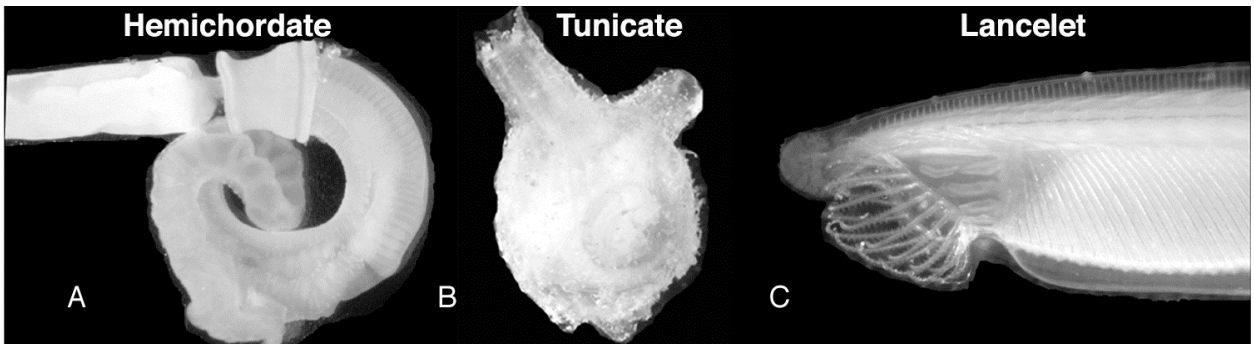

Figure 1.1 Three Distinct Invertebrate Body Plans (A) An adult enteropneust hemichordate, *Saccoglossus kowalevskii*, (B) a tunicate molgulid ascidian, *Molgula provisionalis* and (C) a lancelet, *Branchistoma viriginae*, showing the dramatic differences in their adult body plans. (A) The mouth of the enteropneust hemichordate is hidden in the collar region, directly behind the anterior proboscis, on the ventral side. Central nervous system and gill slits are dorsal, but the mouth is ventral. (B) The mouth of the tunicate is moved upwards at metamorphosis, shown here as the siphon to the top left, while the anus empties into the buccal siphon, shown to the top right. (C) The lancelet mouth has been modified for filter-feeding, as shown by the cirri at the anterior, ventral side to the left. Central nervous system is dorsal, gill slits and mouth are ventral. All animals were collected and photographed at SMS at Fort Pierce, FL.

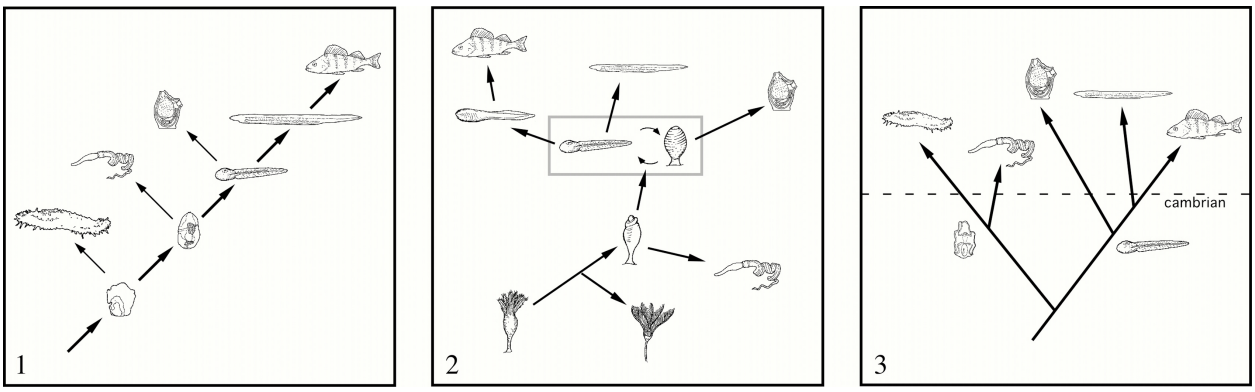

Figure 1.2. Theories of Chordate Origins: Which ones fit the available data? Several possible theories of chordate origins are depicted here. (A) Theory 1 was first proposed by Garstang (1928), and espouses the notion that the nonfeeding ascidian tadpole larva evolved from echinoderm-like and hemichordate-like larvae. However, developmental gene expression patterns in the different larvae show echinoderm larvae and hemichordate tornaria larvae are very similar, but both differ markedly from chordate expression patterns (Swalla, 2006). (B) Theory 2 was popularized by Romer (1967) and depicts the deuterostomes evolving from a pterobranch hemichordate. Phylogenetic and fossil evidence suggest that this is an unlikely scenario, since chordate, hemichordates and echinoderms all appear in the early Cambrian. (C) Theory 3 is a compilation of all available phylogenetic, fossil and gene expression data, first published in 2000 (Cameron et al. 2000). Parts of this theory were put first put forth by Jollie (1973) who considered Garstang's (Figure 1) and Romer's (Figure 2) theories extremely unlikely. The molecular evidence suggests that the chordate tadpole larva had an independent origin from an ancestor with a feeding dipleurulid larva. In this scenario, the chordate body plan would have evolved de novo in a direct-developing soft-bodied worm-like ancestor. The notochord would have evolved in the chordates from the co-option of genes used for other functions in the ancestor, or the notochord has been lost in hemichordates and echinoderms. We consider either scenario likely and are continuing to investigate it.

Molecular Phylogenetics of Deuterostomes

Phylogenetic relationships within the deuterostomes are critical to understanding evolutionary changes that have occurred during chordate and vertebrate evolution (Figure 2-3; Swalla and Smith, 2008). Deuterostome phylogenetic relationships have been reviewed extensively elsewhere (Swalla and Smith, 2008), so they will be briefly summarized here. Schaeffer (1987) examined morphological and phylogenetic evidence and concluded that the deuterostomes, the group of animals that contains the vertebrates, were monophyletic. Later, in 1994, two papers examined deuterostome relationships using 18S rDNA for the first time. Wada and Satoh (1994) showed that deuterostomes were monophyletic, presented evidence that chaetognaths were not deuterostomes, and showed echinoderms and hemichordates as sister groups, albeit with low bootstrap support. Turbeville et al. (1994) increased the deuterostome 18S rDNA data set and used the notochord as a morphological marker to place ascidians as chordates. Later, Cameron et al. (2000) greatly increased the number of tunicates and hemichordates in the deuterostome 18S rDNA database, and showed that echinoderms and hemichordates are sister groups with high bootstrap support. Morphological and molecular data since that time have continued to confirm the sister group relationship of echinoderms and hemichordates (Halanych, 2004; Smith et al., 2004; Bourlat et al., 2006; Swalla and Smith, 2008).

The tunicates, while monophyletic (Swalla et al., 2000; Tsagkogeorga et al., 2009) are difficult to place within the deuterostomes with 18S and 28S combined ribosomal sequence analysis (Swalla and Smith, 2008). Recent genome phylogenies constructed with hundreds of genes have suggested that tunicates are more closely related to vertebrates than lancelets are (Blair and Hedges, 2005; Bourlat et al., 2006; Delsuc et al., 2006). Many of the developmental

programs and gene networks that are activated in ascidian embryos for specific tissues are quite similar to vertebrate development (Swalla, 2004; Passamaneck and Di Gregorio, 2005). Ascidians have a number of important transcription factors localized in the egg cytoplasm that are necessary for some tissue development, and thus have been described as having mosaic development (Nishida, 2005). In addition, ascidians have some unique features of tissue specification, such as cellulose production by the adult ectoderm, that are not found in vertebrates (Matthysse et al., 2004; Nakashima et al., 2008). These unique characteristics of ascidian development are thoroughly reviewed in Passamaneck and Di Gregorio (2005). Examination of the timing and spatial expression of homologous genes during development can be informative in understanding which morphological structures are homologous in animals with very different body plans (Gerhart et al., 2005; Rychel et al., 2006; Swalla, 2006). In the following sections, the expression of homologous genes in different deuterostomes groups is discussed in the context of what these results tell us about the evolution of the vertebrates.

Section 3: Hox Gene Cluster Organization and Expression in Deuterostomes:

Anterior-Posterior Axis Development

The *Hox* gene complex has shed light on both deuterostome relationships and the anterior-posterior homologies between body plans of the different phyla (Figure 3; Aronowicz et al., 2006; Swalla, 2006; Brown et al. 2008; Freeman et al., 2012; Pascual-Anaya et al., 2013). The *Hox* gene complex is a group of genes that are arranged from 3' to 5' co-linearly on the chromosome, and are also expressed from anterior to posterior during embryonic development. Invertebrate deuterostomes have a single *Hox* cluster, while vertebrates have multiple copies (Swalla, 2006). The sea urchin *Hox* cluster has been mapped and has undergone an inversion so

that the most posterior gene, *Hox 11/13c* is next to *Hox* 3 (Cameron et al., 2006). Hemichordates and sea urchins share motifs in their three posterior *Hox* genes, called *Hox 11/13a*, *11/13b*, and *11/13c*, suggesting that these two groups had posterior gene duplications independent of the chordate lineage (Peterson, 2004; Cameron et al., 2006; Freeman et al., 2012; Pascual-Anaya et al., 2013).

Hox developmental gene expression provides evidence for anterior-posterior homologies between echinoderms, hemichordates, vertebrates and lancelets (Lowe et al., 2003; Swalla, 2006; Pascual-Anaya et al., 2013). Developing hemichordates express their *Hox* genes in a co-linear fashion from anterior to posterior, but instead of expression only in the dorsal neural tube, expression is seen in the entire ectoderm of hemichordates (Lowe et al., 2003). These expression patterns reflect that the hemichordate ectoderm has neural potential throughout the ectoderm, such as is seen in insects (Lowe et al., 2003). In echinoderms, co-linear expression has been reported in the developing adult somatapleura (Cameron et al., 2006), and in the adult nerve ring (Morris and Byrne, 2005). In contrast, tunicates show widely differing expression patterns of *Hox* genes, depending if the gene is expressed during the larval or adult stage (Spagnuolo et al., 2003; Passamaneck and Di Gregorio, 2005; Swalla, 2006).

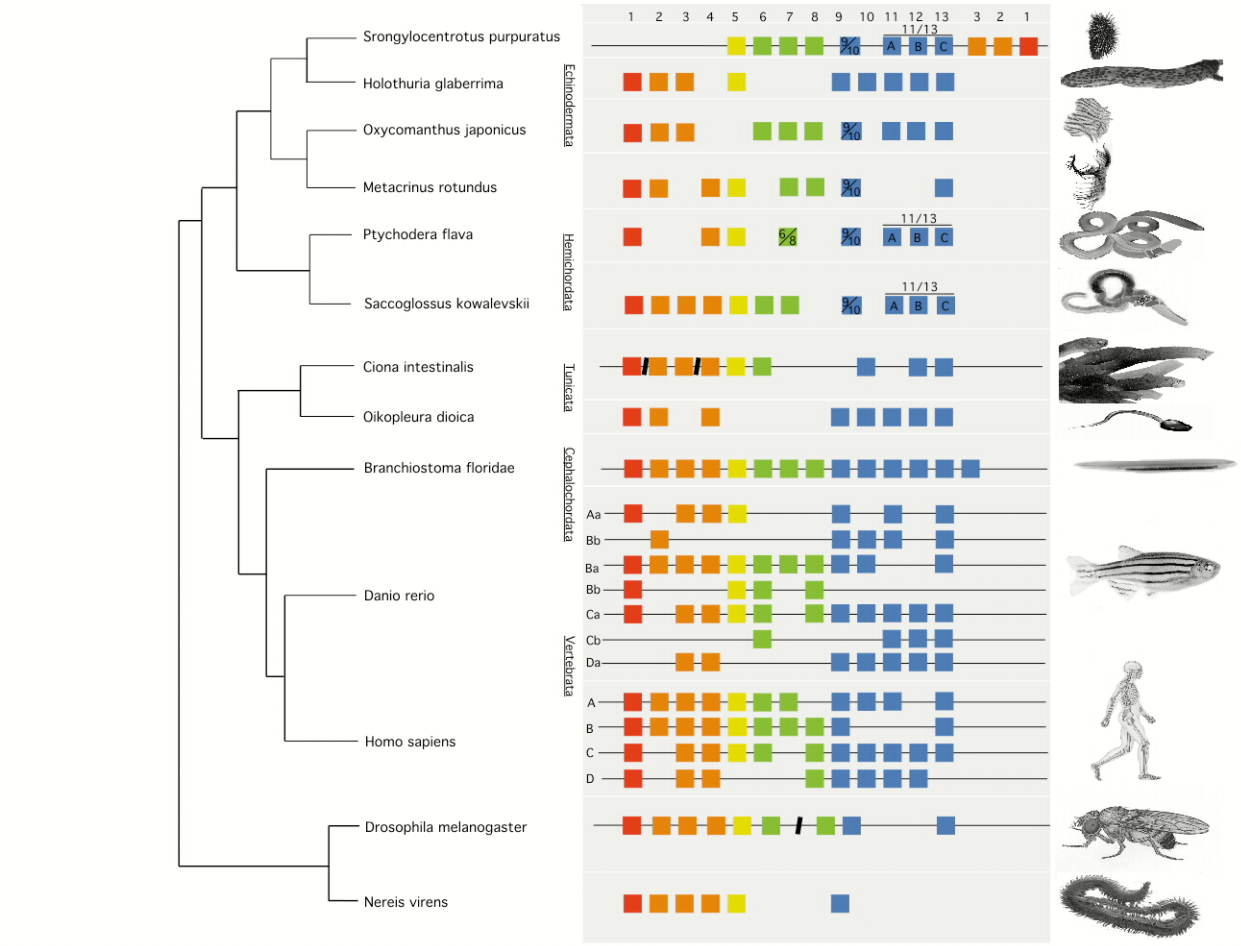

Figure 1.3. *Hox* Gene Expression in the Deuterostomes. An Ecdysozoa (fruit fly,*Drosophila melanogaster*) and a Lophotrochozoa (polychaete annelid, *Nereis virens*) are shown as outgroup protostome taxa. *Hox* clusters are shown here with all available hemichordate data and major chordate clades in 2008 (Brown et al. 2008). The two sequenced tunicates, *Oikopleura dioica* and *Ciona intestinalis* are shown with a cephalochordate, *Branchistoma floridae* and a couple of representative vertebrates. Humans have four duplicate clusters, as do all vertebrates, except teleost fishes, (*Danio rerio*), that had a second gene duplication event, resulting in eight clusters. Lines through the boxes depict that the genome has been completed, and the organization of the cluster is known. Slashes indicate genomic breaks in the clusters. Note the unusual inversion seen in sea urchins (top row). References for figure updated from an earlier review (Brown et al. 2008) (Aronowicz and Lowe, 2006; Cameron et al., 2006; Méndez et al., 2000; Mito and Endo, 2000; Passamaneck and Di Gregario, 2005; Peterson, 2004; Swalla, 2006).

Section 4: Pharyngeal Gills and Gill Bar Development

Pax 1/9 Expression and *Hox* Expression in Deuterostome Gill Slits

Pharyngeal gill slits in hemichordates were originally used as a morphological character uniting the hemichordate enteropneust worms with chordates (Figure 1; Romer, 1967; Schaeffer, 1987; Rychel et al., 2006; Gillis et al., 2012). Structures are considered to be homologous if they have similar morphology and similar function. The clear homology of pharyngeal gill slit structures is what causes the hemichordates to fall between the echinoderms and chordates by morphological analysis (Figure 2-1; Schaeffer, 1987). The pharyngeal clefts and surrounding collagen skeleton of hemichordates, cephalochordates, and vertebrates are remarkably similar in form and function (Schaeffer, 1987; Rychel et al., 2006), making it most likely that this is the ancestral morphology. In contrast, tunicates lack any cartilage skeleton in their pharyngeal structures, suggesting that they have been lost evolutionarily (Figure 1). Developmental genetics allows the comparison of morphological structures at a new level – the level of genetic pathways expressed during development of the structure. Recent work has shown that the pharyngeal slits in vertebrates, lancelets and tunicates are elaborated after the expression of specific *Pax* genes. The single gene called *Pax 1/9* in invertebrate deuterostomes has been duplicated in vertebrates to two genes, *Pax-1* and *Pax-9* (Neubüser et al., 1995; Holland and Holland, 1995; Ogasawara et al. 1999; Ogasawara et al. 2000a).

Expression of the paired box transcription factors *Pax-1* and *Pax-9* has been shown in the endodermal pharyngeal pouches during vertebrate development (Neubüser et al., 1995; Wallin et al., 1996; Peters et al., 1998; Ogasawara et al., 2000a). Furthermore, these transcription factors are necessary for proper development of the pharyngeal pouches and surrounding endodermal derivatives, such as the thymus, as seen by their absence in mice lacking either *Pax 1* or *Pax 9*

(Wallin et al., 1996; Peters et al., 1998). In both chordates and hemichordates, *Pax 1/9* is expressed in endoderm of the pharynx and later in the pharyngeal slits. Notably, in ascidians, no expression was detected during embryogenesis. The first sign of *Pax 1/9* expression was in swimming tadpole larvae that were about to begin metamorphosis (Ogasawara et al., 1999). Likewise, expression in hemichordate adults was found to be highest in the gill endoderm (Ogasawara et al., 1999; Gillis et al., 2012). Not only was *Pax 1/9* expressed, but also the downstream genes *eya* and *six 1* (Gillis et al., 2012). These results suggest that the morphological and functional similarity between the pharyngeal gill slits in hemichordates (Ogasawara et al., 1999; Gillis et al., 2012), ascidians (Ogasawara et al., 1999), cephalochordates (Holland and Holland, 1995) and vertebrates (Neubüser et al., 1995; Wallin et al., 1996; Peters et al., 1998; Ogasawara et al., 2000a) is a reflection of similar genetic programs activated in pharyngeal endoderm at the time of differentiation by the *Pax 1/9* or *Pax 1* and *Pax 9* transcription factors. In light of these results and the deuterostome phylogeny, the most parsimonious hypothesis is that the deuterostome ancestor had endodermally derived gill slits and these were subsequently lost in the echinoderm lineage (Figure 2-3). The mitrate carpoids, echinoderms from the Devonian era do appear to have gill slits (Jefferies, 1986; Gee, 1996, Smith et al., 2004). Therefore, early echinoderms may have had pharyngeal gills and then lost them (Smith et al., 2004; Rychel et al., 2006; Swalla and Smith, 2008). Further examination of Cambrian echinoderms for evidence of pharyngeal gills will be informative, as will the cloning and characterization of the expression of *Pax 1/9* in echinoderms. No expression data for *Pax 1/9* have been reported in echinoderms to date, but it will be interesting to see if this gene has expression reminiscent of gill slits or has been co-opted for other functions in echinoderms.

Not only do hemichordate pharyngeal gill slits share conserved transcription factors for their development as described above with vertebrates, they also share localization along the anterior-posterior axis. For example, in vertebrates, *Hox 1* is first expressed at the level between the first and second pharyngeal pouch (Lowe et al., 2003). When *Hox* gene expression was examined in hemichordates, *Hox 1* was expressed between the first and second pharyngeal pouch, suggesting that the location of the pharyngeal gills along the anterior-posterior axis is homologous between hemichordates, lancelets and vertebrates (Lowe et al. 2003, Freeman et al., 2012).

Pharyngeal Gill Cartilage in Hemichordates and Lancelets is Acellular

The pharyngeal gill slits themselves are homologous between hemichordates and chordates, but what about the cartilaginous gill bars that lie between the gill openings? The morphology and development of the gill bars in hemichordates is similar to lancelets (Figure 1)(Schaeffer, 1987; Ruppert, 2005; Rychel et al., 2006). The bars appear as a thickening of the basal lamina between the pharyngeal endoderm, as first reported by Libbie Hyman (1959), but also recently shown by *in situ* hybridization of *Sox* and fibrillar collagen (Rychel and Swalla, 2007). The cartilaginous bars of hemichordates stain with alcian blue (Smith et al., 2003) and are acellular (Rychel et al., 2007), while the gill bars of lamprey are made by neural crest cells and are cellular (Zhang et al., 2006). The development of gill bars in hemichordates and lancelets needs to be examined in more detail, but it appears that the ancestral cartilage may have been acellular and was secreted by the endoderm (Rychel and Swalla, 2007). Later in evolution, neural crest cells in vertebrates may have migrated into those areas and replaced the acellular cartilage with cellular cartilage. More information on the development of gill bar cartilage is

needed before any questions of homology between hemichordate and lancelet gill bars can be answered.

Section 5: The Post-Anal Tail and the Endostyle of Hemichordates: Gene Expression Studies

It is not clear how significant the post-anal tail is as a defining chordate feature. Ascidians do not have an open gut as larva, and thus do not have an anus, but both lancelets and vertebrates have a post-anal tail (Gerhart et al., 2005). The vertebrate and lancelet posterior *Hox* genes are expressed in the tissues of the post-anal tail. Phylogenetic analysis of hemichordate enteropneust worms show that they fall into two separate monophyletic groups, those that have feeding larvae similar to echinoderms and those that are direct developers (Cameron et al., 2000). The direct developing saccoglossids have post-anal tails that express the posterior *Hox* genes (Lowe et al., 2003; Freeman et al., 2012), whereas the ptychoderids lack a larval post-anal tail (Swalla, 2006). Instead, ptychoderid worms form an anus at the vegetal pole of the larvae that becomes the anus of the adult (Urata and Yamaguchi, 2004; Swalla, 2006; Röttinger and Lowe, 2012). These results could be interpreted as evidence that the vertebrates evolved from a direct developing hemichordate ancestor, as they are the only group of hemichordates that show a post-anal tail. However, since the hemichordates would have diverged from a chordate ancestor long before the Cambrian era (Blair and Hedges, 2005), there has been plenty of time for the independent evolution of a post-anal tail in both groups.

The endostyle present in lancelets and tunicates is thought to have homology to the vertebrate thyroid. For this reason, endostyle-specific genes have been isolated in an effort to examine this question with gene expression (Mazet, 2002; Ogasawara et al., 2000b; Sasaki et al.,

2003). One of these genes is the homeobox gene *TTF-1* (thyroid transcription factor 1), which regulates thyroid peroxidase, the enzyme that iodinates thyroglobulin (Mazet, 2002; Ogasawara et al., 2000b; Sasaki et al., 2003). In lancelets, *TTF-1* is expressed throughout the six morphological zones of the endostyle (Mazet, 2002), whereas in tunicates expression is limited to particular zones (Sasaki et al., 2003). Both the tunicate and lancelet endostyles also bind iodine, so their endostyles are considered to be homologous to vertebrate thyroid gland (Sasaki et al., 2003; Ruppert, 2005). When the hemichordate *TTF-1* was cloned and gene expression was characterized, there was expression seen in the pharyngeal endoderm, stomochord and hindgut (Takacs et al., 2002). The pharyngeal endoderm of hemichordates also binds iodine throughout, even in the regions that do not morphologically resemble an endostyle (Ruppert, 2005). These results could be interpreted that the entire hemichordate pharynx fulfills endostyle function (Rychel et al., 2006) or that the hemichordate endostyle is not homologous to the tunicate and lancelet endostyle (Ruppert, 2005). Further developmental and functional studies will be necessary to distinguish between these two hypotheses.

Section 6: Central Nervous System and the Dorsal-Ventral Inversion Hypothesis

Doral-ventral axis specification relies on some of the same signaling molecules in both vertebrates and invertebrates, however, there are differences in either the location or timing of expression of these molecules. Currently, there are two main hypotheses that explain these differences. In the first hypothesis, the signaling molecules directing axis specification are the same, but there is an inversion of expression localities, the Dorsal-Ventral Inversion hypothesis (Ruppert et al., 1999; Lowe et al., 2006). Bone morphogenetic proteins (BMPs) are expressed on

the dorsal side of invertebrates, whereas chordate BMPs are expressed on the ventral side of the embryo (Lowe et al., 2006). However, later in vertebrate development, BMP expression is seen in the dorsal midline, following neural tube closure (Figure 4A). Our interpretation is that the dorsal midline BMP expression seen in hemichordates (Figure 4B) is identical to the vertebrate midline BMP expression, not the earlier vertebrate ventral expression (Figure 4A). Evidence supporting axis inversion in chordates is seen in *nodal* expression analysis. *Nodal* is a gene involved in left-right axis symmetry in chordates and the gene is expressed on the right side of the chordate embryo. Conversely, *nodal* is expressed on the left side of sea urchins (Swalla and Smith, 2008). Collectively, this evidence supports the hypothesis that BMP expression was first expanded on the ventral side of a worm-like chordate ancestor. These changes in the chordate ancestor resulted in an animal with inverted dorsal-ventral and left-right axis symmetries compared to other invertebrate deuterostomes. This hypothesis assumes that the chordate ancestor did not possess a central nervous system, but merely a nerve net.

An alternative hypothesis to the inversion claim is supported by *BMP* expression studies and outlined in figure 4. This hypothesis suggests that *BMP* expression is not inverted, but is exactly the same in hemichordates and chordates, in the dorsal midline, following neurulation. The timing of expression differs among developmental stages within and between chordates and hemichordates (Marti, E., 2000; Lowe et al., 2006). During chick embryogenesis, expression of *BMP* is found in a strip down the dorsal midline, just after neurulation (Figure 4; Marti, E., 2000). Juvenile hemichordates also express *BMP* in a strip down the dorsal midline (Figure 4; Lowe et al., 2006). The similar expression of *BMP* in a dorsal strip after neurulation appears to have a role in directing neural tube differentiation in both hemichordates and chordates. This hypothesis assumes that the dorsal neural tube in hemichordates is homologous to the neural tube

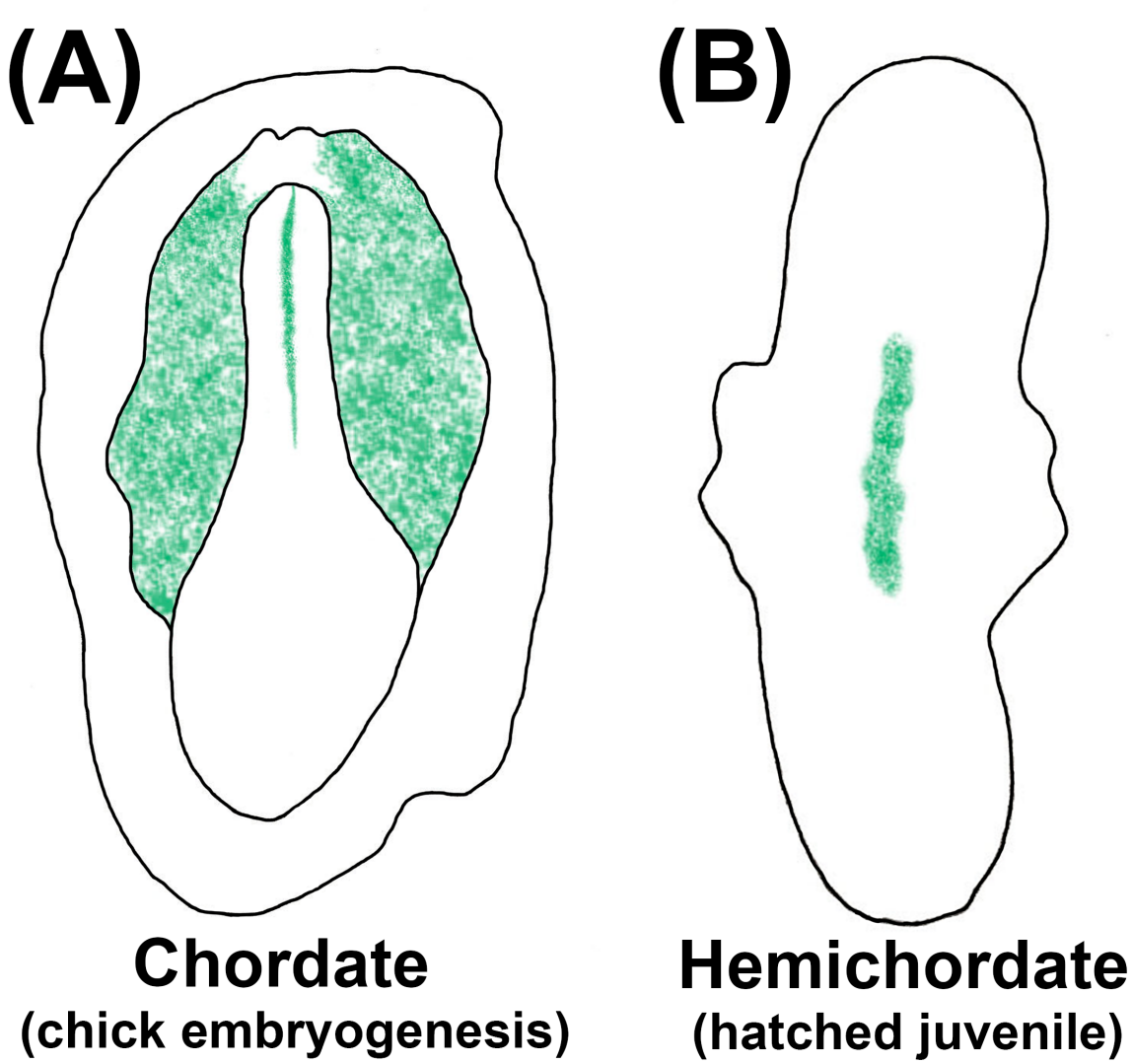

Figure 1.4. *BMP* Expressed in Dorsal Midline During Early Development. Illustrations showing the expression of *BMP* in green. (A) Dorsal view of chick embryogenesis after neurulation showing *BMP* expression in the putative ventral region and one dorsal strip in the midline of the neural tube. (B) Dorsal view of a juvenile hemichordate showing *BMP* expressed in the dorsal midline, just after neurulation. Drawings made according to published photographs of *BMP* expression in the chordate chick (Marti E., 2000) and hemichordate (Lowe et al., 2006).

in chordates (Luttrell et al., 2012; Miyamoto and Wada, 2013).

The nervous system of larval ptychoderid hemichordates develops in a similar manner to chordates (Figure 5; Luttrell et al., 2012; Miyamoto and Wada, 2013). In both groups, the neural tube develops along the dorsal midline in an anterior to posterior fashion (Figure 4, dorsal views and Figure 5, cross-sections), however in hemichordates, the neural tube is found only in the collar region (Figure 4B; Kaul and Stach, 2010; Luttrell et al., 2012). The chordate CNS forms by invaginating ectoderm that rolls up the neural tube dorsal to the notochord (Figure 5A). In hemichordates, collar ectoderm invaginates and rolls up to form the neural tube, after the development of the dorsal vessel (Figure 5B; Luttrell et al., 2012). Signaling molecules emanate from the notochord in chordates to induce neural tube formation (Figure 5C). The notochord also serves as structural support for the neural tube (Figure 5A). The notochord is dorsal to the dorsal vessel in chordates (Figure 5; Luttrell et al., 2012; Miyamoto and Wada, 2013). Hemichordates lack a notochord, so signaling molecules emanate from the dorsal vessel and the endoderm to induce neural tube formation (Figure 5D; Miyamoto and Wada, 2013). These results have always been interpreted as the chordates gaining a notochord, but evolutionarily, it is equally likely that the hemichordate ancestor lost their notochord. In the latter scenario, then the deuterostome ancestor may actually have been a chordate, with major losses in the echinoderm and tunicate lineages.

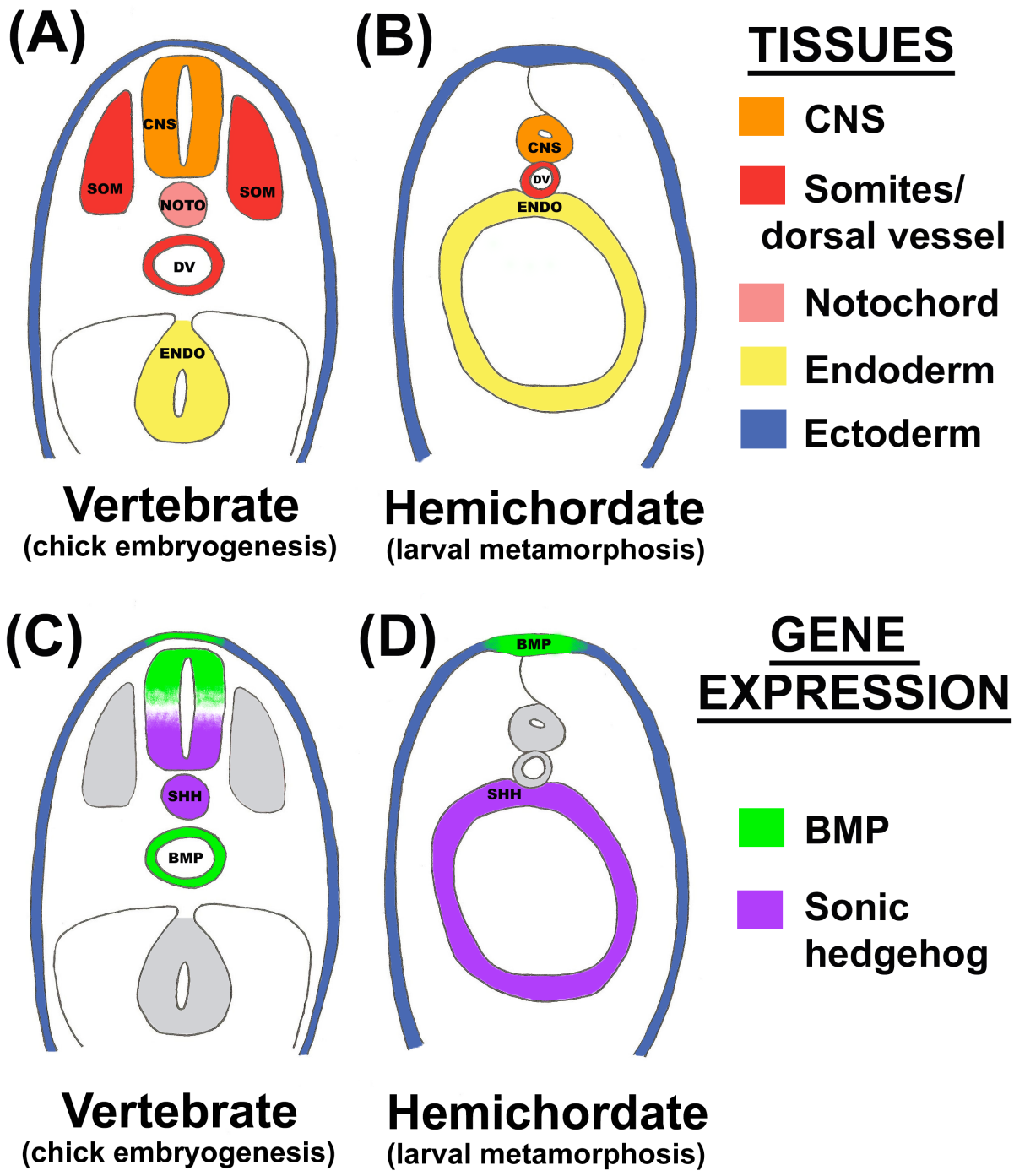

Figure 1.5. *BMP* and *Sonic Hedgehog* Expression During Neurulation. Diagrams of cross-sections of a hemichordate and a vertebrate. In all pictures, dorsal is to the top and ventral is to the bottom. The upper two illustrations show specific tissues and structures, while the bottom two illustrations show *BMP* (green) and *Sonic hedgehog* (purple) expression. In the diagram of the developing chick embryo (A), the vertebrate neural tube (orange) develops above the notochord (pink). Somites (red) surround the neural tube and notochord. The dorsal vessel (red)

is ventral to the notochord and dorsal to the endoderm (yellow). In diagram (B), the metamorphosing hemichordate neural tube (orange) develops above the dorsal vessel (red). The endoderm (yellow) is directly ventral to the dorsal vessel. Blue represents ectoderm in all images. The bottom two diagrams, show that *BMP* (green) is expressed in the dorsal ectoderm (blue) of both hemichordates (Lowe et al., 2006) and the chordate chick (Marti E., 2000). *BMP* molecules are also expressed in the dorsal vessel (DV) of vertebrates (Rickman et al., 1985; Schneider et al., 1999; Young et al., 2004). *Sonic hedgehog* is expressed in the ventral central nervous system (CNS) and the notochord (NOTO) in vertebrates (Bardet et al., 2010) and expressed in the endoderm (ENDO) of hemichordates (Pani et al, 2012).

Section 7: Evidence for the Hemichordate Stomochord Homology to Chordate Notochord

Ultrastructural studies of the hemichordate stomochord suggested that this structure could be the homolog of the chordate notochord (Balser and Ruppert, 1990). Gene expression studies of notochord-specific genes were expected to confirm this hypothesis. *Brachyury* is a T box transcription factor, first isolated during mesoderm formation in vertebrates (Wilkinson et al., 1990; Holland et al., 1995) that is expressed exclusively in the ascidian notochord (Yasuo and Satoh, 1993; Swalla, 2006). When *Brachyury T* was cloned and described in echinoderms and hemichordates, it was expressed at the site of gastrulation at the vegetal pole, which later becomes the larval anus (Peterson et al., 1999; Swalla, 2006). These results suggest that the ancestral function of *Brachyury* as a transcription factor was in promoting gastrulation and formation of the three germ layers, and that the gene was later co-opted into notochord development (Swalla, 2006). However, recent results of Miyamoto and Wada (2013) show that the presumptive stomochord endoderm expresses *sonic hedgehog*, and may induce neurulation in the hemichordate neural tube. Therefore, these researchers present evidence that the stomochord is the notochord homolog in hemichordates. Candidate gene expression studies so far do not suggest any other hemichordate structure as a candidate for the notochord homolog (Gerhart et al., 2005), but more research will be very interesting to investigate this intriguing possibility.

Section 8: Evolution of Placodes and Neural Crest in Chordates

Neural crest has been widely touted as a vertebrate innovation that allowed the development of complicated sensory structures in the anterior head and the development of the skull and pharyngeal bars (Gans and Northcutt, 1983; Theveneau and Mayor, 2014). Therefore, it has long been assumed that tunicates and lancelets lack neural crest and cranial sensory placodes.

However, in recent years, using a combination of genetic and developmental techniques, there have been a number of reports of neural crest and placodes in tunicates, but not in lancelets (reviewed in Hall and Gillis, 2013). The sister group relationship of tunicates and vertebrates that has been reported for phylogenomic analyses supports the hypothesis that tunicates may contain neural crest and placodes (Bourlat et al., 2006; Delsuc et al., 2006). It is interesting that of 615 "neural crest genes", 91% of these genes are found in invertebrates that do not contain neural crest, suggesting that these genes were co-opted into neural crest cells in vertebrates (Hall and Gillis, 2013). There are migratory and pigmented cells discovered in adult tunicates that develop from near the neural tube of the larvae and have been suggested to be neural crest by virtue of sharing parts of the neural crest gene network (Jeffery et al., 2008; Abitua et al., 2012). Recent work shows a cephalic melanocyte lineage in *Ciona intestinalis* larvae that can be reprogrammed into migrating cells by over-expression of the transcription factor *Twist* (Abitua et al., 2012). These results suggest that the gene network for neural crest is present in tunicates and that the mesenchymal property of the neural crest was most recently evolved in vertebrates (Abitua et al., 2012). However, more work remains to be done to study the exact nature and potential of these "neural crest" cells in tunicates (Hall and Gillis, 2013).

There is excellent evidence from gene expression and morphological studies that

tunicates have well-developed sensory placodes and lateral placodes (Manni et al., 2004; Bassham and Postlewait, 2005; Mazet et al., 2005). The buccal cavity and palps at the anterior of tunicates express *Six 1/2*, *Six 3/6*, *Eya* and *Pitx*, suggesting a homology to the hypophyseal and olfactory placodes of vertebrates (Manni et al., 2004; Bassham and Postlewait, 2005; Mazet et al., 2005). These results suggest that the common ancestor of vertebrates and tunicates had placodes, and that their anterior ends have homologous structures. A rather startling result is that the excurrent buccal opening in tunicates early on expresses *Six 1/2*, *Six 4/5*, *Eya*, and *Fox 1*, which are vertebrate markers for otic placodes, lateral line, and epibranchial placodes (Manni et al., 2004; Bassham and Postlewait, 2005; Mazet et al., 2005; Moody and Saint-Jeannet, 2014). As mentioned before, tunicate larvae do not have an open gut, so do not have an anus during larval life. After metamorphosis, the gut is emptied out of the excurrent buccal siphon, after the tail has retracted, and the mouth forms at the anterior of the larvae. This would suggest that the adult tunicate is defecating out of its ear, an odd symmetry twist for a chordate.

Section 9: Stem Cells and Regeneration in Hemichordates

Regeneration is a fascinating, yet common occurrence among the metazoans. The majority of animal phyla have some species that reliably regenerate certain tissues and structures (Sánchez Alvarado, 2000). All groups within the deuterostomes, with the possible exception of cephalochordates and xenoturbella, have at least some species with regenerative capabilities. Echinoderms have been shown to have a remarkable capacity for regeneration (Candia Carnevali, 2006). Every extant class within the Echinoderm lineage have been reported to regenerate to some degree (Candia Carnevali at al., 2009; D'Ancona Lunetta, 2009). Certain species of hemichordates, which are a sister group to the echinoderms, are capable of

regenerating all body structures (Rychel and Swalla, 2008; Humphreys et al., 2010; Urata et al., 2012). Some species of both solitary and colonial tunicates have been shown to regenerate either by budding or re-growing missing or damaged structures (Sánchez Alvarado, 2000; Brown et al., 2009; Jeffery, 2012). Chordates possess numerous species with some regenerative powers, including humans, which are able to regenerate bone and liver tissue (Sánchez Alvarado, 2000). While the overall understanding of regeneration in some species has improved, many of the key cellular and genetic processes controlling regeneration are still unknown.

Thomas H. Morgan classified two basic types of regeneration in metazoans. In the first mode, regeneration occurs by remodeling existing tissue without any active cell proliferation, termed morphallaxis. The second mode does require active cell proliferation and is known as epimorphosis (Morgan 1898; Morgan 1901; Sánchez Alvarado, 2000). Depending on the organism, regeneration may employ both epimorphosis and morphallaxis. Agata et al. (2007) coined the terms distalization and intercalation in order to clarify the steps in regenerating new tissue. Wound healing is often the first step in regeneration. This allows new tissue, whether in the presence of a blastema or not, to be patterned on the correct axis. The process of wound healing is termed distalization. Intercalation is the second step of regeneration and it is characterized by the replacement of missing or damaged tissue. This process can occur by morphallaxis or epimorphosis. Regeneration can be categorized further by examining the final condition of the animal and the amputated tissue. If both regenerate completely to form two new individuals, then regeneration is considered to be bi-directional and essentially asexual reproduction. If, on the other hand, only one half of the animal regenerates to form a complete individual, regeneration is said to be unidirectional.

Ptychodera flava, a solitary enteropneust hemichordate, regenerates in a bidirectional

fashion and employs both morphallaxis and epimorphosis to regenerate missing structures when bisected (Rychel and Swalla, 2008; Humphreys et al., 2010). *Glandiceps hacksi* has also been shown to regenerate with a combination of morphallaxis and epimorphosis (Urata et al., 2012). Because hemichordates are basal deuterostomes and employ both forms of regeneration, they present an exciting model to study the cellular and molecular mechanisms of regeneration. This ability to regenerate all structures in the body includes the central nervous system, hepatic sacs, heart, renal gland, and gonads (Rychel and Swalla, 2008).

The first step in hemichordate regeneration, as is seen in most animals, is wound healing. Rychel and Swalla documented that endoderm and ectoderm grow together to close the wound within 2 days post amputation. Regeneration times vary based on the temperature of the seawater and overall health of the animal, with regeneration optimized between 26°C and 30°C (Humphreys et al., 2010). Following wound healing, a blastema forms and rapidly expands to establish proboscis and collar rudiments by the fifth day of regeneration (Humphreys et al., 2010). The blastema appears to be composed of multipotent stem-like cells. Rychel and Swalla used proliferating cell nuclear antigen (PCNA) antibody staining to show actively dividing cells present and scattered throughout the tissue at two days post amputation. By the fourth day of regeneration, PCNA-positive cells were localized to the anterior regeneration site, where the proboscis and collar were forming (Rychel and Swalla, 2008). Humphreys et al. (2010) used *in situ* hybridization to show that the proboscis and collar rudiments of the blastema highly express *SoxB1* on day five of regeneration, while the surrounding non-regenerating tissue does not label with this probe. *SoxB1* is a gene that has been shown to be vital for generating induced pluripotent stem (iPS) cells (Takahashi et al., 2007). Additionally, the newly formed tissue is not pigmented, suggesting the structures were formed from newly dividing cells and not remodeled

from existing cells (Rychel and Swalla, 2008; Humphreys et al., 2010). Collectively, this evidence supports the idea that the regeneration blastema is created by proliferating stem cells. Although the cells appear to be mesenchymal, it is an open question whether they are de-differentiated cells or a population of undifferentiated cells occupying an unknown stem cell niche. Further studies will be necessary to confirm the origin and character of the blastemal cells.

By the sixth day of regeneration in *P. flava*, complete proboscis and collar rudiments were formed and the mouth was opened on the ventral, posterior end of the proboscis (Rychel and Swalla, 2008; Humphreys et al., 2010). Furthermore, internal structures were being elaborated at this stage. Dorsal to the mouth, the stomochord develops from invaginating ectoderm. This structure serves to support the heart/kidney complex, which was forming two days later, by the eighth day of regeneration (Rychel and Swalla, 2008). All structures continued to develop and increase in size until around 12 days, when the newly formed tissue approximately matched the size of the old tissue. At this stage the regenerating animal was capable of burrowing under sand, as they do in nature (Humphreys et al., 2010). The branchial region forms next and appears to combine both epimorphosis and morphallaxis. Abnormally high levels of apoptotic cells were detected approximately one cm away from the cut site in both the ectoderm and endoderm on days two through eight of regeneration using a TUNEL assay (Rychel and Swalla, 2008). However, the amount and location of programmed cell death varied over the time points sampled. In general, apoptosis was elevated in the endoderm farthest away from the cut site on day two and then progressed anteriorly towards the cut site. Additional sampling will need to be done beyond eight days to confirm the presence of apoptotic cells throughout the course of regeneration to confirm the extent of tissue remodeling during the formation of new structures. A blastema also forms between the collar and trunk between day

twelve and twenty-five. The blastema goes on to differentiate and form the new branchial section of the animal (Humphreys et al., 2010). Complete regeneration is achieved approximately five weeks post amputation and it may take up to another five weeks for the newly formed tissue to achieve the same level of pigmentation as the old tissue (Humphreys et al., 2010). In conclusion, regeneration is impressive in the basal deuterostomes. Understanding the molecular basis for this process may yield clues to unlocking extensive regeneration in other deuterostomes, including humans. Future studies will be directed at identifying the source of stem cells in hemichordates and identifying the gene networks regulated during regeneration.

Section 10: Summary and conclusions

In summary, developmental genomics and genetics have allowed new insights into the question of chordate origins (Gerhart et al., 2005; Rychel et al., 2006). Genomics and gene expression studies have been informative in understanding the homology of various structures in invertebrate deuterostomes with vertebrates. Developmental gene expression data allows one to analyze the genetic pathways that are deployed to make similar structures in genetically different organisms. Gene expression data suggest that the anterior-posterior axis of hemichordates, lancelets and vertebrates are very similar, except that the neural genes are expressed throughout the ectoderm of hemichordates (Lowe et al., 2003). Tunicates have lost some of the middle Hox genes and express some of their Hox genes as larvae and some as adults, but only a few are expressed co-linearly (Spagnuolo et al., 2003; Passamaneck and Di Gregorio, 2005; Pascual-Anaya et al., 2013). The gill slits of hemichordates, lancelets and vertebrates are homologous (Rychel et al., 2006, Gillis et al., 2012), but the gill bars of lancelets and hemichordates are both acellular and endodermal in origin. In contrast, tunicates completely lack gill bars in their

pharyngeal region, probably an adaptation that followed their acquisition of the cellulose tunic. There is good recent evidence that tunicates have cell lineages that develop next to the neural tube, migrate and develop into pigment cells. These have been interpreted as neural crest cells, due to their sharing genes identified in the neural crest gene network in vertebrates. Tunicates have been shown to have both neural and non-neural placodes, thought for many years to exist only in the vertebrates. While tunicates are clearly chordates, they have evolved some amazing changes in body plan, and are likely to have lost some structures evolutionarily at the time that the tunic evolved. Hemichordates have an anterior-posterior axis similar to chordates, but their dorsal central nervous system is restricted to the collar region (Luttrell et al., 2012; Miyamoto and Wada, 2013). Our view of the chordate ancestor is a benthic worm with gill slits and a mouth, which was able to filter feed, but also could ingest large particles. This ancestor also had a central nervous system and may or may not have had a notochord. Further research on developmental gene expression in lancelets, tunicates and hemichordates is likely to be fruitful in continuing insights into the evolution of vertebrates.

Section 11: Clinical Relevance Summary

- Chordate Ancestor - The chordate ancestor was a worm-like animal, with a through gut and the mouth at the anterior, anus at the posterior.
- Hemichordate Homologies – Hemichordates have homologies with all of the major chordate features, except the notochord, and are an excellent model system for the chordate and deuterostome ancestor.
- Tunicate Homologies – Tunicates have all of the chordate features and are an excellent model system for understanding chordate gene networks.

• Stem cells – Chordate ancestors had stem cell populations that could be co-opted for specific functions.

• Regeneration - Chordate ancestors had remarkable regeneration capacities.

Section 12: Glossary

Deuterostome – literally means "second mouth" (deutero – two; stome – mouth). The blastopore is formed first during gastrulation and the mouth is formed secondarily. This mode of development applies to all deuterostomes except Tunicata. Echinodermata, Hemichordata, Xenoturbellida and Chordata are considered deuterostome phyla.

Endostyle - an endodermal structure found in invertebrate chordates in the pharyngeal area. The endostyle secretes mucus to capture small particles and increase the efficiency of filter feeding. In lancelets and tunicates, the endostyle also accumulates iodine and is considered homologous to the vertebrate thyroid gland.

Graptolites - These abundant Cambrian fossils have been shown to be colonial hemichordates, or members of the hemichordate Class Pterobranchia.

Hemichordates – This phylum includes enteropneust worms and colonial pterobranchs. Hemichordates are tripartite as adults, having three body regions. The most anterior is the proboscis (protostome), then the collar (mesosome) and the posterior trunk (metasome). These three regions are reduced and modified in colonial Pterobranchia.

Lancelets – The common name for cephalochordates. These animals are frequently referred to by the incorrect term amphioxus.

Notochord – The key chordate morphological character is the notochord. The notochord forms a stiff rod running from anterior to posterior in chordates beneath the dorsal neural tube,

usually surrounded by a sheath of extracellular matrix. The gut is found just under the notochord in vertebrates and lancelets, but there is only an endodermal strand in the nonfeeding ascidian tadpole larvae. In lancelets and appendicularians, the notochord persists in the adult, while in ascidians the notochord undergoes apoptosis before metamorphosis and tail resorption. In vertebrates, the notochord persists as the intervertebral discs (nucleus pulposa) as the vertebrae develop from somites (Dahia et al., 2011; Dahia et al., 2012).

Pharyngeal – The area of the digestive system that serves as a respiratory organ and feeding organ in hemichordates, tunicates and lancelets. The vertebrate homolog is the pharynx, which develops into gills in early vertebrates, but is the area of the throat, including the thyroid gland and thymus in amniotes (birds and mammals).

Pharyngeal Gill Bars – Cartilaginous elements made of extracellular matrix and located between the pharyngeal endoderm, giving the pharynx of hemichordates, lancelets and vertebrates structure. Pharyngeal gill bars are secreted from endoderm in hemichordates and lancelets, but develop from neural crest cells in vertebrates.

Placodes – Area of an ectodermal thickening from which cells delaminate and eventually achieve a cell fate that is not epidermal. There are both neurogenic and non-neurogenic cranial placodes, which are associated with the peripheral nervous system in vertebrates. Placodes were thought to be found only in vertebrates, but have recently been described in tunicates, using both molecular markers and careful morphological analyses.

Pterobranch - Class Pterobranchia refers to a group of colonial hemichordates, or pterobranchs. Colonial hemichordates reproduce both sexually and asexually and have feeding tentacles to capture small particles for feeding. There are many fossil pterobranchs, called

graptolites, but only two extant families, Rhabdopleuridae and Cephalodiscidae.

Stomochord – a projection of the endoderm that juts forward into the hemichordate proboscis, against which the hemichordate heart beats. The hemichordate stomochord cells are vacuolated and make an extracellular sheath, but there is no molecular evidence that it is a notochord homolog.

Tunicates – A monophyletic group of animals that includes ascidians, appendicularians, and thaliaceans. This group of animals is also sometimes called "urochordates", but Tunicata is the preferred term. There are over 2,800 described species of tunicates.

Section 13: Acknowledgements

A special thank you to Sally Moody for putting this book together and her many helpful and insightful suggestions during writing the chapter. I would like to acknowledge the members of the Swalla lab for their many contributions to my life and my work over the past twenty years.

Chapter 2 - Head Regeneration in Hemichordates is not a Strict Recapitulation of Development

This chapter was published as **Luttrell S.M**., Gotting K., Ross E., Alvarado A.S., Swalla B.J. (2016). Head regeneration in hemichordates is not a strict recapitulation of development. *Dev Dynamics* 245: 1159-1175.

Section 1: Background

Head or anterior body part regeneration is commonly associated with protostome, but not deuterostome invertebrates. However, it has been shown that the solitary hemichordate *Ptychodera flava* possesses the remarkable capacity to regenerate their entire nervous system, including their dorsal neural tube and their anterior head-like structure, or proboscis. Hemichordates, also known as acorn worms, are marine invertebrate deuterostomes that have retained chordate traits that were likely present in the deuterostome ancestor, placing these animals in a vital position to study regeneration and chordate evolution. All acorn worms have a tripartite body plan, with an anterior proboscis, middle collar region, and a posterior trunk. The collar houses a hollow, dorsal neural tube in ptychoderid hemichordates and numerous chordate genes involved in brain and spinal cord development are expressed in a similar anterior–posterior spatial arrangement along the body axis. We have examined anterior regeneration in the hemichordate *Ptychodera flava* and report the spatial and temporal morphological changes that occur. Additionally, we have sequenced, assembled, and analyzed the transcriptome for eight stages of regenerating *P. flava*, revealing significant differential gene expression between regenerating and control animals. Importantly, we have uncovered developmental steps that are regeneration-specific and do not strictly follow the embryonic program.

Section 2: Introduction

Regeneration has captured the interest and imagination of people for centuries. Popularized in myths, science fiction, and even horror movies, regeneration of missing and damaged tissue is a common reality in the animal kingdom. Nearly every animal phyla contains at least some species that consistently regenerate all or certain tissues and structures (Bely and Nyberg, 2010; Somorjai et al., 2012; Giangrande and Licciano, 2014). All deuterostomes groups, with the possible exception of Xenoturbella, have at least some species with the capacity to regenerate (Sanchez Alvarado, 2000). Numerous chordates, including lancelets, tunicates, frogs, fish, salamanders, and even humans are able to regenerate to some degree (Brown et al., 2009; Bely and Nyberg, 2010; Somorjai et al., 2012; Giangrande and Licciano, 2014). Every extant class of echinoderms have been reported to regenerate (Candia Carnevali et al., 2009), while some species of hemichordates, which are a sister group to the echinoderms, undergo asexual reproduction and regenerate all anterior and posterior body parts when amputated (Willey 1899; Dawydoff 1902; Rao 1954; Rychel and Swalla, 2008; Humphreys et al., 2010; Miyamoto and Saito, 2010). When and in what animal lineage did the ability to regenerate first evolve? Was regeneration a stem metazoan trait that was subsequently lost or reduced in numerous taxa or has regeneration evolved independently several times across the metazoans? Porifera (Bely and Nyberg, 2010; Giangrande and Licciano, 2014), Cnidaria (Bosch, 2007; Dubuc et al., 2014), Ctenophora (Ryan et al., 2013; Moroz et al., 2014), and Placozoa (Bely and Nyberg, 2010) have extensive regenerative abilities and, as basal metazoans, these lineages suggest an ancient and ancestral mechanism of regeneration. Comparing gene regulatory networks used during regeneration across various animal phyla will help to elucidate common molecular mechanisms of regeneration.

Understanding the morphological and genetic basis of regeneration may yield clues to unlocking regeneration in animals with limited or no regenerative abilities, like humans. Millions of people suffer from neurodegenerative diseases, spinal cord injuries, and limb amputations (Brown et al., 2005; Ziegler-Graham et al., 2008; Mahabaleshwarkar and Khanna, 2014). Furthermore, aging and age-related diseases will eventually affect everyone. Regeneration may slow the aging process and stem cells present one feasible way to combat a multitude of diseases and injuries (Rando and Wyss-Coray, 2014). If regeneration is a stem deuterostomes trait, it is likely that humans possess many, if not all, of the genetic switches controlling regeneration, but those switches have been modified or inactivated in some way over evolutionary time. It may, therefore, be possible to re-activate those pathways in humans using information gained from studying genetic models made from animals with extensive regenerative capabilities.

We are seeking to identify the morphological and genetic underpinnings controlling regeneration in the solitary hemichordate, *Ptychodera flava* (Eschscholtz, 1825), which is a basal deuterostomes and capable of regenerating all anterior and posterior structures when bisected (Rychel and Swalla, 2008; Humphreys et al., 2010). It is critical to know when internal structures regenerate to use genetic knock downs and knock outs, as well as overexpression, to characterize the function of genes directing the regeneration process. Moreover, hemichordates are the only deuterostomes known to be able to regenerate an anterior head-like structure and entire central nervous system (CNS). *Ptychodera flava* progresses from a fertilized embryo to a planktonic, feeding larva that can remain in the water column for up to 300 days (Hadfield, 1978; Lin et al., 2016). Upon metamorphosis, the larva develops into a juvenile worm that settles to the ocean floor to begin a benthic lifestyle. Solitary hemichordates are exclusively marine and adult animals have a tripartite body plan with an anterior proboscis that is used for digging and

burrowing in the sand and mud, a middle collar region with a hollow, dorsal neural tube in ptychoderid hemichordates, a ventral mouth between the proboscis and collar, and a long posterior trunk with pharyngeal gill slits and gonads in the anterior trunk, a hepatic region in the mid-trunk and a terminal anus (Balser and Ruppert, 1990; Brown et el., 2008; Luttrell and Swalla, 2014).

The hemichordate nervous system is quite interesting. Upon embryogenesis in direct developing hemichordates and metamorphosis in indirect developers, dorsal and ventral nerve cords develop along the full length of the trunk and nerve rings form around the base of the collar and the base of the proboscis (Balser and Ruppert, 1990; Kaul and Stach, 2010; Miyamoto et al., 2010; Miyamoto and Wada, 2013; Kaul-Strehlow et al., 2015). Adult echinoderms also develop nerve cords throughout each arm and a circumferential nerve ring around the central disc; however, it still remains to be determined whether echinoderm and hemichordate nerve cords are homologous structures (Sly et al., 2002; Holland et al., 2013). In addition to nerve cords, *P. flava* also develops a hollow, neural tube that is positioned dorsally in the collar region. Our lab has shown this structure forms from ectoderm that invaginates and rolls up forming a hollow tube, similar to chordate neurulation (Morgan, 1894; Luttrell et al., 2012; Miyamoto and Wada, 2013; Luttrell and Swalla, 2014).

Lastly, hemichordates have a diffuse nerve net throughout the ectoderm, similar to the adult tunicate, *Ciona intestinalis* (Balser and Ruppert, 1990; Lowe et al., 2003; Dahlberg et al., 2009; Miyamoto et al., 2010; Kaul-Strehlow et al., 2015). The adult acorn worm, in light of these similarities, has aspects of the different types of nervous systems that are present in the deuterostomes. Remarkably, *P. flava* is able to regenerate all of these structures, making hemichordates a model system to study nervous system evolution and regeneration in this clade

of animals. Furthermore, as invertebrates, hemichordates lack the numerous genome duplications events present in the vertebrates (Dehal and Boore, 2005; Hughes and Liberles, 2008), thereby making functional studies of the regeneration genes more tractable in this animal.

Here, we report the spatial and temporal regeneration of internal body structures to complement the previously published external morphology regeneration data (Willey, 1899; Rao, 1954; Nishikawa, 1977; Rychel and Swalla, 2008; Humphreys et al., 2010). We also include analyses of the transcriptome from regenerating *P. flava* animals. In total, eight different stages of regeneration were sequenced, assembled, and annotated to track changes in early gene expression that direct regeneration of anterior structures. We document expression profiles and gene ontologies of hundreds of putative genes associated with anterior head regeneration. These data build a foundation for future experiments that may show what genes are sufficient and necessary to start the regeneration program in *P. flava*. Our morphological data shows the regenerative response to these early changes in gene expression and we document complete anterior regeneration of the proboscis, collar, and anterior trunk. Furthermore, we uncovered morphological differences between early development and regeneration of anterior structures, including the neural tube. The assembled transcriptomes reported here not only complement recent *P. flava* developmental transcriptomes (Shu-Hwa et al., 2014; Tagawa et al., 2014; Simakov et al., 2015), but also open the door to systematic comparisons of embryonic processes to regenerative events in hemichordates specifically, and deuterostomes in general.

Section 3: Experimental Procedures

Animal Collection and Management

Ptychodera flava were collected at Paiko Peninsula in Honolulu, Hawaii, in early

November. During low tide, when the water level was approximately 3 feet deep, animals were removed from the coral beds by snorkeling. The light sand cover was fanned by hand to expose the underlying coral and hemichordates. Animals were collected into 50-ml tubes and carried back to the lab with the tubes immersed in a cooler with sea water.

Animals were bisected at the level of the anterior hepatic sacs and allowed to regenerate for various time points (Figs. 1 and 2). Regenerating worms were kept in running seawater tanks at Kewalo Marine Laboratory at 27°C during regeneration. Some worms were collected and shipped to the University of Washington in Seattle, Washington, and kept at 26°C while regenerating. Animals were immersed in a 1:1 solution of sea water and 7.5% $MgCl_2$ for 15 min to relax muscles and constrain movement and then observed with a Nikon 1000 dissecting microscope and photographed with a Cool Snap camera. Pictures were taken daily for 15 days and near daily thereafter until 55 days post bisection.

Histology

Regenerating animals were fixed in 4% paraformaldehyde in phosphate-buffered saline overnight at room temperature and stored at -20°C in 100% methanol. They were placed into 100% ethanol for 20 min at room temperature and then moved to a 1:1 mixture of 100% ethanol and polyester wax (nine parts Poly (ethylene glycol) [400] distearate and one part 1-hexadecanol, (Polysciences, Warrington, PA) (Steedman, 1957; Norenburg and Barrett 1987) at 40°C for 1 hr. The animals were then moved to 100% polyester wax at 40°C for 1 hr and then embedded in fresh 100% polyester wax. Next, 7-µm sections were cut on a Spencer 829 microtome and mounted on gelatin subbed slides. Slides were deparaffinized, and processed through Milligan's trichrome staining, a histological stain that differentiates muscle cells, nuclei, and cartilage (Fig.

3; Presnell and Schreibman, 1997). Slides were rinsed in 95% ethanol and treated for 5 min with potassium dichromate HCl mordant and then rinsed in distilled water. Slides were then stained for 5 min in acid fuchsin (Sigma, St. Louis, MO) and rinsed again in distilled water. Slides were then stained 5 min in phosphomolybdic acid (Sigma) followed by 5 min in Orange G (Sigma) and then rinsed in distilled water. Finally, slides were treated for 2 min in 1% glacial acetic acid and stained 5 min with Fast Green FCF (Sigma) and then treated again for 3 min with 1% glacial acetic acid. Slides were dehydrated with ethanol and mounted with Permount (Fisher Scientific, Pittsburgh, PA). Sections were photographed using a Nikon Eclipse E600 microscope mounted with a Cool Snap camera.

RNA Isolation and cDNA Preparation

Following bisection, animals were allowed to regenerate for either 2 hr, 4 hr, 6 hr, 12 hr, 24 hr, 48 hr, 72 hr, or 96 hr. Between 50 and 100 mg of tissue were removed with a sterile, feather surgical blade from the cut site of the posterior segment in four regenerating animals at each time point (Fig. 1A–C). Four healthy, intact animals were bisected and total RNA was isolated from the cut site of the posterior half to serve as reference controls. RNA was isolated from the tissue using either a Promega SV Total RNA Isolation System, catalog number Z3100, or a USB PrepEase RNA Spin Kit, part number 78766 1 KT. RNA was analyzed on a NanoDrop ND-1000 spectrophotometer for nucleic acid concentration and purity and then stored at -80°C until cDNA was synthesized using the SuperScript® III First-Strand Synthesis System for RT-PCR by Invitrogen.

cDNA Library Preparation and Sequencing

mRNAseq libraries for sequencing were generated from 1 to 1.5μg of high quality total RNA, as assessed using the Agilent 2100 Bioanalyzer. RNA was purified using poly-T oligo-attached magnetic beads. Libraries were made according to the manufacturer's directions for the TruSeq RNA Sample Prep Kit v2 (Illumina, RS-122-2101). Resulting short fragment libraries were checked for quality and quantity using the Bioanalyzer. Equal molar libraries were pooled, requantified and sequenced as 100 bp paired read on the Illumina HiSeq, 2000 instrument using HiSeq Control Software 1.5.15. Following sequencing, Illumina Primary Analysis version RTA 1.13.48 and Secondary Analysis version CASAVA-1.8.2 were run to demultiplex reads for all libraries and generate FASTQ files.

Transcriptome Assembly and Annotation

To create a reference for expression analysis, paired end sequence files from all *P. flava* experimental time points were pooled (605,821,125 pairs totaling 122,164,225,000 bp) and assembled using Trinity, version r2013-02-25, (Grabherr et al., 2011), with default parameters. We vector clipped and contaminate filtered the resulting assembly with SeqClean, version, 2011-02-22, (Seq-Clean, 2011). The resulting transcriptome reference contained 527,715 sequences, with an average length of 1,022, and N50 of 1,961, 208,773 of these sequences contain an ORF of at least 60 amino acids. All sequences were used for expression analysis with sequences from the same Trinity "component," roughly equal to a gene, treated as a single gene.

To maximize the utility of this transcriptome assembly, sequences were annotated with the best BLASTx (Camacho et al., 2008) hit to Swissprot (UniProt, 2015) and NCBI's NR database, using an e-value cutoff of 0.001. We also identified PFAM (Finn et al., 2014) domains

present in *P. flava* transcripts using hmmscan, version 3.1b1, from the HMMER package (Eddy, 2011) with an e-value cutoff of 0.01. In addition, we annotated these transcripts with tmhmm, version 2.0c, (Krogh et al., 2001) signal version 4.1 (Petersen et al., 2011), and ncoils (Lupas et al., 1991). We identified putative transcription factors based on PFAM domain hits using a list from transcriptionfactor.org. For transcripts with multiple isoforms, annotations were collapsed to the gene level as determined by Trinity.

Differential Expression Analysis

To identify differentially expressed genes, single end reads from each time point were aligned to the transcriptome using Bowtie2 (Langmead and Salzberg, 2012) with default parameters. Alignments were quantified using Samtools (Li et al., 2009). Isoform counts were summed to generate a "per gene" count. Differential expression analysis and normalization was performed using the R package DESeq2 (Love et al., 2014). All time points were contrasted with the zero hour (0 hr) time point. Data used for the gene expression analysis have been deposited in the Gene Expression Omnibus (GEO) under accession number GSE70295.

Hierarchical Clustering and Heatmaps

To select genes of interest for clustering, differentially expressed genes ($P < 1e\text{-}5$), having an expression level log2 fold change greater than one or less than negative one, for one or more timepoints, and having a hit to the Swissprot protein database were identified. These genes were hierarchically clustered on the distances of the Pearson correlation of the log2 fold change, using the complete linkage method to find similar clusters (Figs. 5 and 6, 7, 8). Significantly differentially expressed genes ($P < 1e\text{-}5$) that had transcription factor domains were clustered on

the distances of the Pearson correlation of the log2 fold change, using Ward's minimum variance method to find similar clusters (Fig. 9). All heatmaps were created using the R package pheatmap (Kolde, 2013).

Gene Ontology Analysis

Gene Ontology (GO) (Gene Ontology, 2015) terms were assigned to each *P. flava* gene based upon homologous PFAM domains and significant Swissprot hits. These terms were used to impute functional categories of differentially expressed genes and calculate categorical enrichment. The GO slim terms used were from the generic GO slim terms list available at the Gene Ontology Web site. GO term enrichment was performed using the R package topGO (Alexa and Rahnenfuhrer, 2010). To examine higher-level GO terms, significantly enriched ($P < 0.01$) GO terms were mapped to select higher-level GO terms using GO.db. These select GO terms were then mapped to the significantly differentially expressed genes ($P < 1e\text{-}5$) (Fig. 10).

Section 4: Results

Regeneration of External and Internal Anterior Features in *P. flava*

Intact, healthy, adult worms (Fig. 1A) were bisected in the trunk between the branchial region and the hepatic sacs (Fig. 1B) and the posterior piece was monitored for regeneration signs at the cut site (Fig. 1C). The first observable change in tissue composition in *Ptychodera flava* is wound healing. This process is relatively rapid and takes place within the first 2 days following amputation at 26°C. Wound healing culminates in ectoderm covering and sealing the open cut site (Fig. 1D–F). Over the next 3 days, a regeneration blastema forms at the anterior end (Fig. 1G,H). Cells accumulate and proliferate in the blastema to yield a new, rudimentary

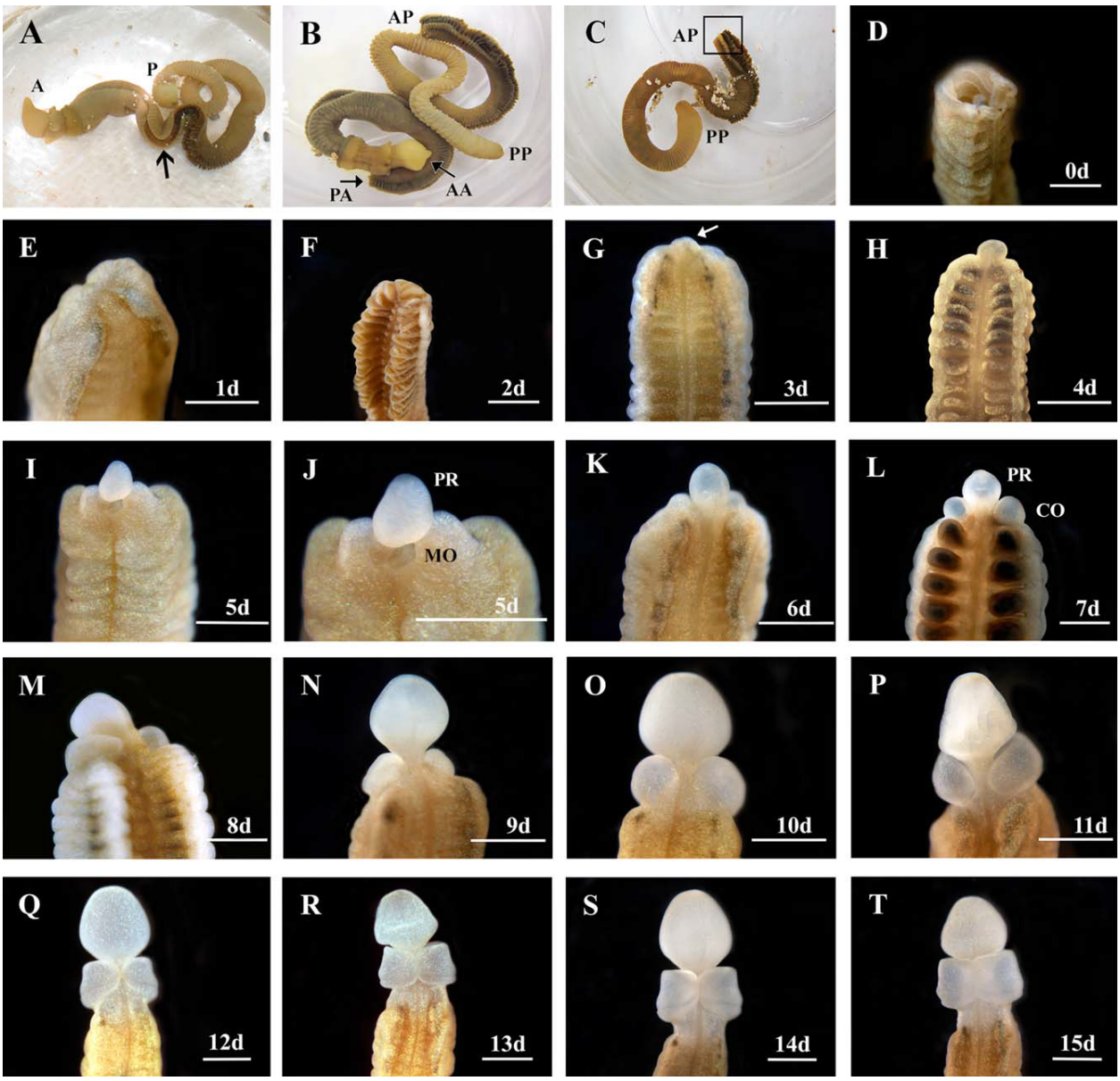

Figure 2.1. **Regenerating anterior structures on *Ptychodera flava*.** A: An intact, live animal. Anterior is to the left. The arrow indicates where the animal will be bisected. a = anterior, p = posterior. B: A bisected animal. AA, anterior end of the anterior half; PA, posterior end of the anterior half; AP, anterior end of the posterior half; PP, posterior end of the posterior half. C: The posterior half of the animal. The boxed area is the site of regeneration. D: The cut site of the posterior half of the animal. E–H: One day (1d) through 4 days (4d) postcut, showing the open wound has healed and a regeneration blastema has formed in two different animals. The arrow in (G) marks the blastema. I,J: At 5 days post bisection (5d), the blastema has formed a rudimentary proboscis (PR) and the mouth (MO) is open on the ventral side. K–T: Six days (6d) through 15 days (15d) show the proboscis (PR) the collar (CO) regenerating around the proboscis stalk in a ventral to dorsal manner. All views are dorsal and anterior is to the top except I, J, which are ventral views. Scale bars = 1 mm.

anterior head, or proboscis (Fig. 1I). Between days 4 and 5 post bisection, the mouth has opened on the ventral side (Figs. 1J, 3D1–3).

Over the next several days, cells continue to proliferate enlarging the proboscis and the collar begins to wrap around the base of the proboscis (Fig. 1K–T). The collar regenerates in the ventral and lateral positions first (Fig. 1K–P). Gill slits and gill bars start to form in the anterior most region of the trunk after 10 to 12 days, before the collar ectoderm completely regenerates and closes on the dorsal side (Fig. 1Q–T). At 13 days post bisection, the ventral and lateral collar ectoderm has fully regenerated (Fig. 2). The dorsal most region of the collar has not yet formed, but will continue to regenerate and finally close forming a continuous ring around the neck region after approximately 2 weeks of regeneration. The epibranchial nerve ring that that wraps around the posterior collar is visible in the newly regenerated tissue and forms as the collar regrows and not after the collar has fully shaped (Fig. 2).

The internal regeneration morphology of *P. flava* is striking after the first day the animal is bisected. Both ectoderm and endoderm of the trunk region come together at the cut site and form a near continuous layer (Fig. 3A1). The folds of pre-existing endoderm are still present and the neural net is maintained below the ectoderm (Fig. 3A1). Existing muscle fibers of the trunk are still obvious at the anterior end where the wound has sealed (Fig. 3A1). Hepatic collagen is visible below the ectoderm at the cut site, denoting endoderm of the existing hepatic sacculations are taking part in wound healing (Fig. 3A1). On day 2 of regeneration, the wound has completely healed and the ectoderm epithelium is smooth and continuous (Fig. 3B1,B2). Dorsal and ventral blood vessels run the length of the animal, allowing blood cells to circulate. Blood is visible in the dorsal and ventral endoderm of the cut site, indicating that both blood vessels are likely supplying blood to this region (Fig. 3B2).

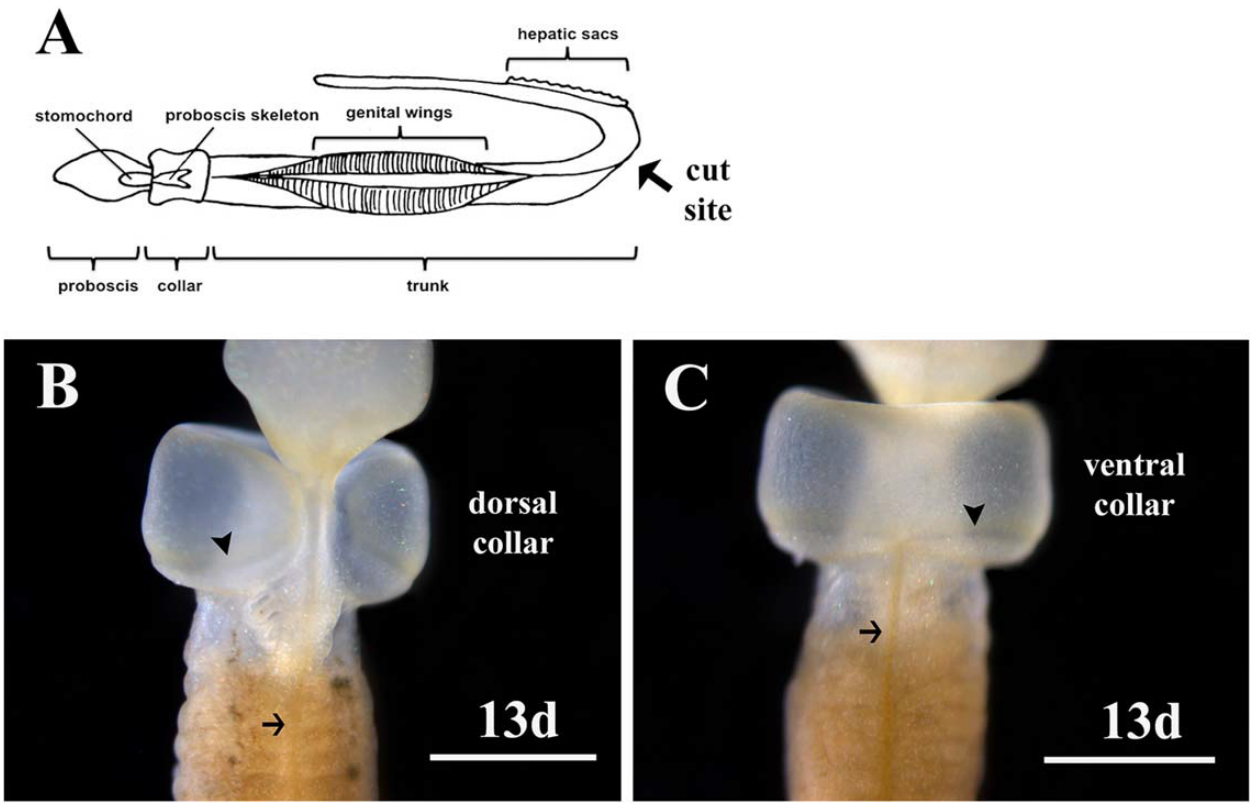

Figure 2.2. Regenerating collar on *Ptychodera flava* at 13 days (13d) postamputation. A: An illustration showing the cut site in the trunk between the genital wings and the hepatic sacs. B: Dorsal view showing the collar has not completely closed and regeneration is incomplete. Three gill slits have formed in the anterior trunk. C: Ventral view of the collar on the same animal showing complete closure and regeneration of the ectoderm. Arrows indicate the dorsal nerve cord in the trunk in (B) and the ventral nerve cord in (C). The arrowheads indicate the epibranchial nerve ring formed at the base of the collar. Scale bars are 1mm.

Hepatic collagen is still visible in the dorsal endoderm, suggesting that at least parts of this tissue have not undergone apoptosis or have been remodeled at this stage. By day 3 of regeneration, the blastema has formed a rudimentary proboscis (Fig. 3C1–4). A nerve net is present below the ectoderm in this region, at least partially originating from the existing trunk tissue and not wholly regenerated de novo (Fig. 3C1–4). At this stage, a structure resembling the presumptive stomochord appears posterior to the rudimentary proboscis and also appears to be derived from endodermal tissue (Fig. 3 C3,C4). The hepatic sacculations are clearly visible in the existing trunk denoting the dorsal side and a thick nerve net is still present on the ventral side below the ectoderm posterior to the cut site (Fig. 3C1–C4).

As the proboscis grows, anterior internal tissues continue to be elaborated. Hemichordates are tricoelomates, having separate coeloms in the proboscis, collar, and trunk regions. The proboscis coelom is fully formed after 4 days of regeneration (Fig. 3D1–3). The dorsal blood vessel flows anteriorly from the trunk, through the collar, ultimately forming the heart in the posterior proboscis (Benito and Pardos, 1997). The dorsal vessel has regenerated into the proboscis, filling the coelom with blood at 4 days postamputation (Fig. 3D1–3). The mouth, which was visible in the external morphology at day 5, is clearly open in sagittal sections at day 4 (Fig. 3D1–3). The stomochord is a stiff, rod-like structure in the posterior proboscis and provides structural support for the superimposing heart/kidney complex (Balser and Ruppert, 1990; Rychel and Swalla, 2008; Miyamoto and Wada, 2013). The stomochord is apparent in sections after 5 days of regeneration (Fig. 3E2–4). At this stage, the stomochord forms between the boundary where ectoderm and endoderm meet. At this time, the heartkidney complex regenerates in the lateral and dorsal positions around the stomochord (Fig. 3E1–4). The dorsal

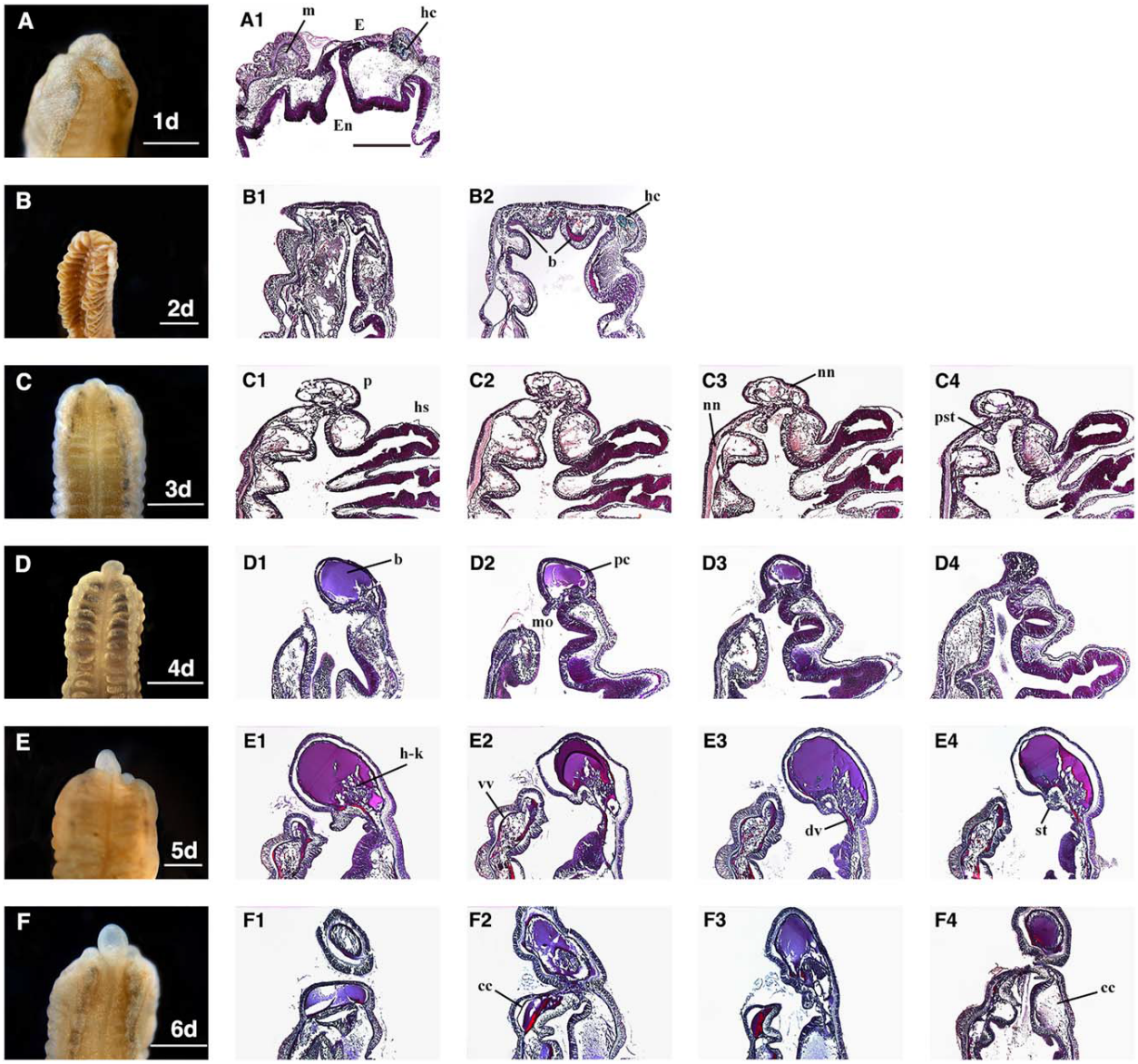

Figure 2.3. A1–F4: Sagittal sections of *Ptychodera flava* anterior regeneration days 1–6 (A-F). Sections were made through the mid-sagittal area showing the internal morphology of proboscis and early collar regeneration. cc, collar coelom; dv, dorsal vessel; E, ectoderm; En, endoderm; hc, hepatic collagen; hs, hepatic sacculations; m, muscle; mo, mouth; nn, nerve net; p, proboscis; pc, proboscis coelom; pst, presumptive stomochord; st, stomochord; vv, ventral vessel. Scale bars = 1 mm and all sections are at the same magnification. All sections are anterior up and dorsal to the right and ventral to the left. All sections are stained with Milligan's trichrome stain. Collagen = green; nuclei, muscle = magenta.

blood vessel is obvious at this stage, flowing into the proboscis just above the stomochord where the heart/kidney complex is regenerating (Fig. 3E1–4). The ventral blood vessel is supplying blood and cells to the presumptive ventral collar coelom as well (Fig. 3E1–4). One day later, the regenerated collar coeloms can be seen in the dorsal and ventral regions (Fig. 3F1–4). The proboscis skeleton provides structure and support for the collar and overlying dorsal blood vessel and neural tube (Luttrell et al., 2012). The proboscis skeleton regenerates from endoderm in the collar region and is visible in endodermal inpocketing at 13 days postamputation (Fig. 4P). The hollow, dorsal neural tube, which is found only in the collar region in ptychoderid hemichordates, begins to form in the posterior collar as the ectoderm closes on the dorsal side at 13 days postbisection (Fig. 4T). These morphological regenerative events are summarized in Table 1.

Dynamic and Discrete Cohorts of Gene Expression Patterns Are Observed During Early Stages of Head Regeneration

Regeneration of these morphological structures is driven by a significant change in gene expression as evidenced by the transcriptomes data. A line graph was constructed to show clusters of upregulated, putative genes showing similar expression profiles along all time points sampled (Fig. 5A). Nearly all genes in cluster A are significantly up-regulated 2 hr after the animal is bisected; however, the expression level of these genes steadily and drastically declines beginning 6 hr into the regeneration process. A heatmap of cluster A identifies the individual, putative genes and their expression profile across all time points (Fig. 5B). Heatmaps of the

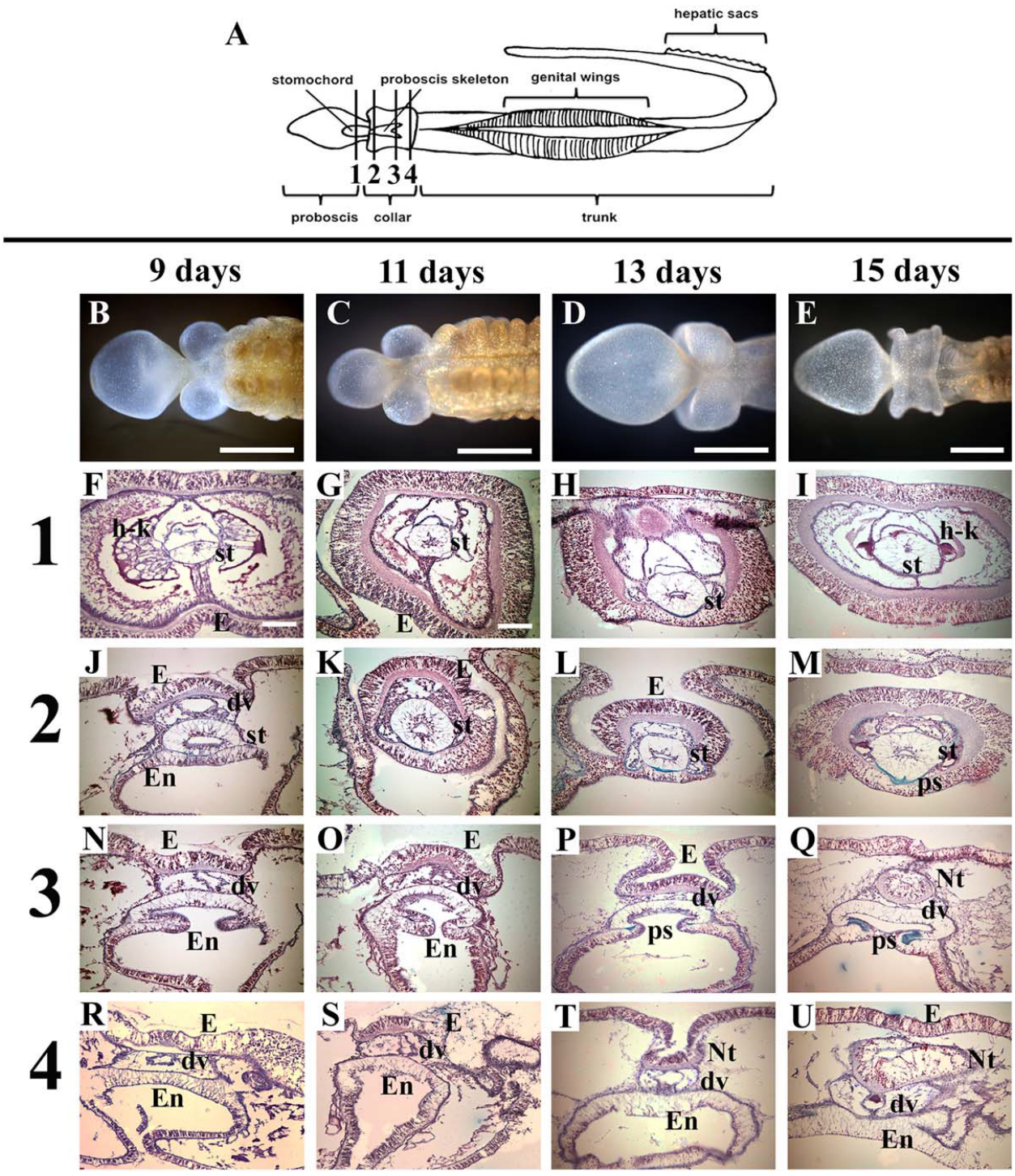

Figure 2.4. Cross-sections of *Ptychodera flava* anterior regeneration days 9–15. All sections are stained with Milligan's trichrome at four different stages of regeneration: 9 days, 11 days, 13 days, and 15 days postamputation. A: Diagram of *P. flava* showing approximate locations of sections. Row (1) is taken through the posterior proboscis in all four regeneration stages. Row (2) is taken through the anterior collar. Row (3) is taken through the mid collar. Row (4) is taken through the posterior collar. dv, dorsal vessel; E, ectoderm; En, endoderm; h-k, heart-kidney

complex; Nt, neural tube; ps, proboscis skeleton; st, stomochord. Scale bars = 1 mm in B–E; 0.1 mm in F–U. B–U: Dorsal views with anterior to the right in (B– E) and dorsal to the top in (F–U). Collagen = green; nuclei, muscle = magenta.

Table 2.1

***Ptychodera flava* Anterior Regeneration Timetable at 26°C**							
Regeneration Events	**Days of Regeneration**						
	1-2	3-4	5-6	7-8	9-10	11-12	13-15
Wound healing	X						
PCNA positive cells (Rychel and Swalla, 2008)	X	X	X	X			
Nerve net	X	X					
Blastema		X					
Proboscis		X	X	X			
Proboscis coelom		X					
Dorsal vessel		X					
Mouth		X	X				
Stomochord			X	X			
Collar coelom			X				
Ventral and lateral collar			X	X	X	X	
Heart/kidney complex			X	X	X		
Proboscis skeleton						X	X
Gill slits						X	X
Dorsal collar							X
Neural tube							X

genes in cluster B shows overall expression is near baseline values at the 2-hr time point, but then expression increases significantly after 6 hr and is elevated approximately 8-fold higher than control animals after 4 days of regeneration (Fig. 5C). Heatmaps of the cluster C and cluster D genes show similar expression profiles, both being only slightly elevated after 2 hr of regeneration and then progressively increasing until the 24-hr time point, at which time both clusters begin to show decreased expression levels, with cluster C displaying the most dramatic decrease (Fig. 5D,E). However, expression of putative genes in both clusters still remain over two log fold change higher than controls after 4 days of regeneration.

Down-regulated, putative genes were also identified and grouped into clusters of similar expression domains. A line graph shows four clusters of predicted genes with very different expression profiles (Fig. 6A). Heatmaps of cluster A show overall expression levels slightly below baseline values between 2 and 6 hr of regeneration and then expression gradually decreases with a steep decline between 3 and 4 days of regeneration. A detailed listing of these putative genes is included in Figure 7. Cluster B genes also start off at near baseline values and expression steadily decreases; however, this group of genes reverses at the 48-hr time point and expression levels begin to increase, although overall expression of this cluster remains significantly down-regulated at the 96-hr time point compared with control animals (Fig. 8).

Predicted genes in cluster C show an interesting expression pattern along all sampled time points. Expression is initially significantly reduced by over three log fold compared with control animals at the 2-hr time point and then expression sharply increases over the next 2 hr, only to abruptly decrease again to nearly an 8-fold change from control animals at the 6-hr time point. Expression levels then steadily elevate again over the next 18 hr, at which point expression sharply declines again between 24 and 48 hr of regeneration, with expression values greater than

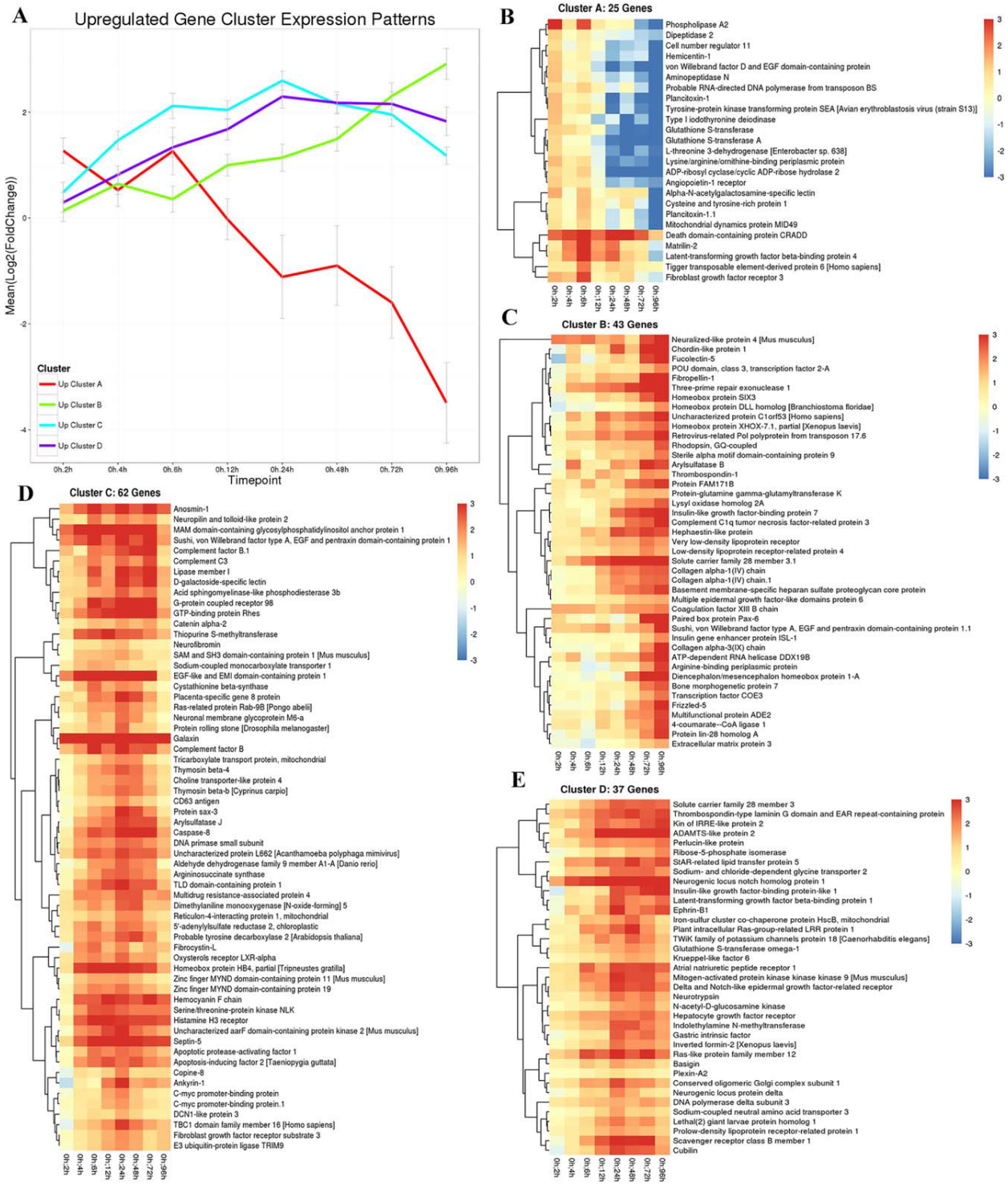

Figure 2.5. Up-regulated gene cluster expression patterns in regenerating *Ptycodera flava*. A: The line graph shows all putative genes that are initially up-regulated and cluster together in their expression profiles along all time points sampled. Red, cluster A genes; green, cluster B genes; blue, cluster C genes; and purple, cluster D genes. The X-axis is time of regeneration and the Y-axis is the log2 fold change in gene expression compared with control animals. B–E:

Heatmaps showing the individual genes identified in clusters A, B, C, D, respectively.

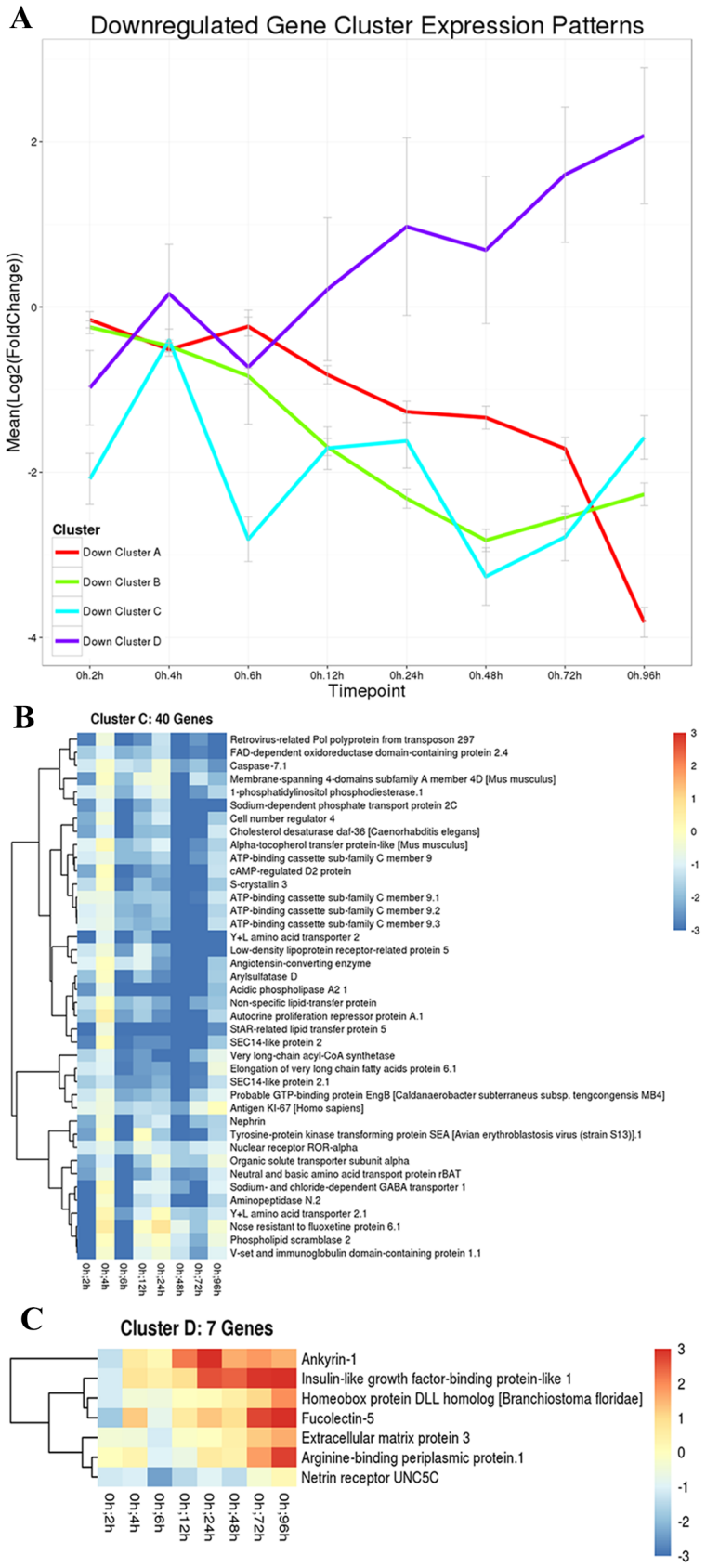
A
Downregulated Gene Cluster Expression Patterns
Mean(Log2(FoldChange))
Timepoint
0h.2h
0h.4h
0h.6h
0h.12h
0h.24h
0h.48h
0h.72h
0h.96h
Cluster
Down Cluster A
Down Cluster B
Down Cluster C
Down Cluster D
B
Cluster C: 40 Genes
Retrovirus-related Pol polyprotein from transposon 297
FAD-dependent oxidoreductase domain-containing protein 2.4
Caspase-7.1
Membrane-spanning 4-domains subfamily A member 4D [Mus musculus]
1-phosphatidylinositol phosphodiesterase.1
Sodium-dependent phosphate transport protein 2C
Cell number regulator 4
Cholesterol desaturase daf-36 [Caenorhabditis elegans]
Alpha-tocopherol transfer protein-like [Mus musculus]
ATP-binding cassette sub-family C member 9
cAMP-regulated D2 protein
S-crystallin 3
ATP-binding cassette sub-family C member 9.1
ATP-binding cassette sub-family C member 9.2
ATP-binding cassette sub-family C member 9.3
Y+L amino acid transporter 2
Low-density lipoprotein receptor-related protein 5
Angiotensin-converting enzyme
Arylsulfatase D
Acidic phospholipase A2 1
Non-specific lipid-transfer protein
Autocrine proliferation repressor protein A.1
StAR-related lipid transfer protein 5
SEC14-like protein 2
Very long-chain acyl-CoA synthetase
Elongation of very long chain fatty acids protein 6.1
SEC14-like protein 2.1
Probable GTP-binding protein EngB [Caldanaerobacter subterraneus subsp. tengcongensis MB4]
Antigen KI-67 [Homo sapiens]
Nephrin
Tyrosine-protein kinase transforming protein SEA [Avian erythroblastosis virus (strain S13)].1
Nuclear receptor ROR-alpha
Organic solute transporter subunit alpha
Neutral and basic amino acid transport protein rBAT
Sodium- and chloride-dependent GABA transporter 1
Aminopeptidase N.2
Y+L amino acid transporter 2.1
Nose resistant to fluoxetine protein 6.1
Phospholipid scramblase 2
V-set and immunoglobulin domain-containing protein 1.1
0h:2h
0h:4h
0h:6h
0h:12h
0h:24h
0h:48h
0h:72h
0h:96h
C
Cluster D: 7 Genes
Ankyrin-1
Insulin-like growth factor-binding protein-like 1
Homeobox protein DLL homolog [Branchiostoma floridae]
Fucolectin-5
Extracellular matrix protein 3
Arginine-binding periplasmic protein.1
Netrin receptor UNC5C
0h:2h
0h:4h
0h:6h
0h:12h
0h:24h
0h:48h
0h:72h
0h:96h

Figure 2.6. Down-regulated gene cluster expression patterns in regenerating *Ptycodera flava*. A: The line graph shows all putative genes that are initially down-regulated and cluster together in their expression profiles along all time points sampled. Red, cluster A genes; green, cluster B genes; blue, cluster C genes; and purple, cluster D genes. The X-axis is time of regeneration and the Y-axis is the log2 fold change in gene expression compared with control animals. B,C: Heatmaps showing the individual genes in clusters C and D, respectively. Heatmaps and identities of genes in clusters A and B are included in Figures 7 and 8, respectively.

Figure 2.7. Down-regulated gene cluster A expression patterns in regenerating *P. flava*. The heatmap shows the individual genes in cluster A of Figure 6 and their expression profile along all time points sampled compared with control animals.

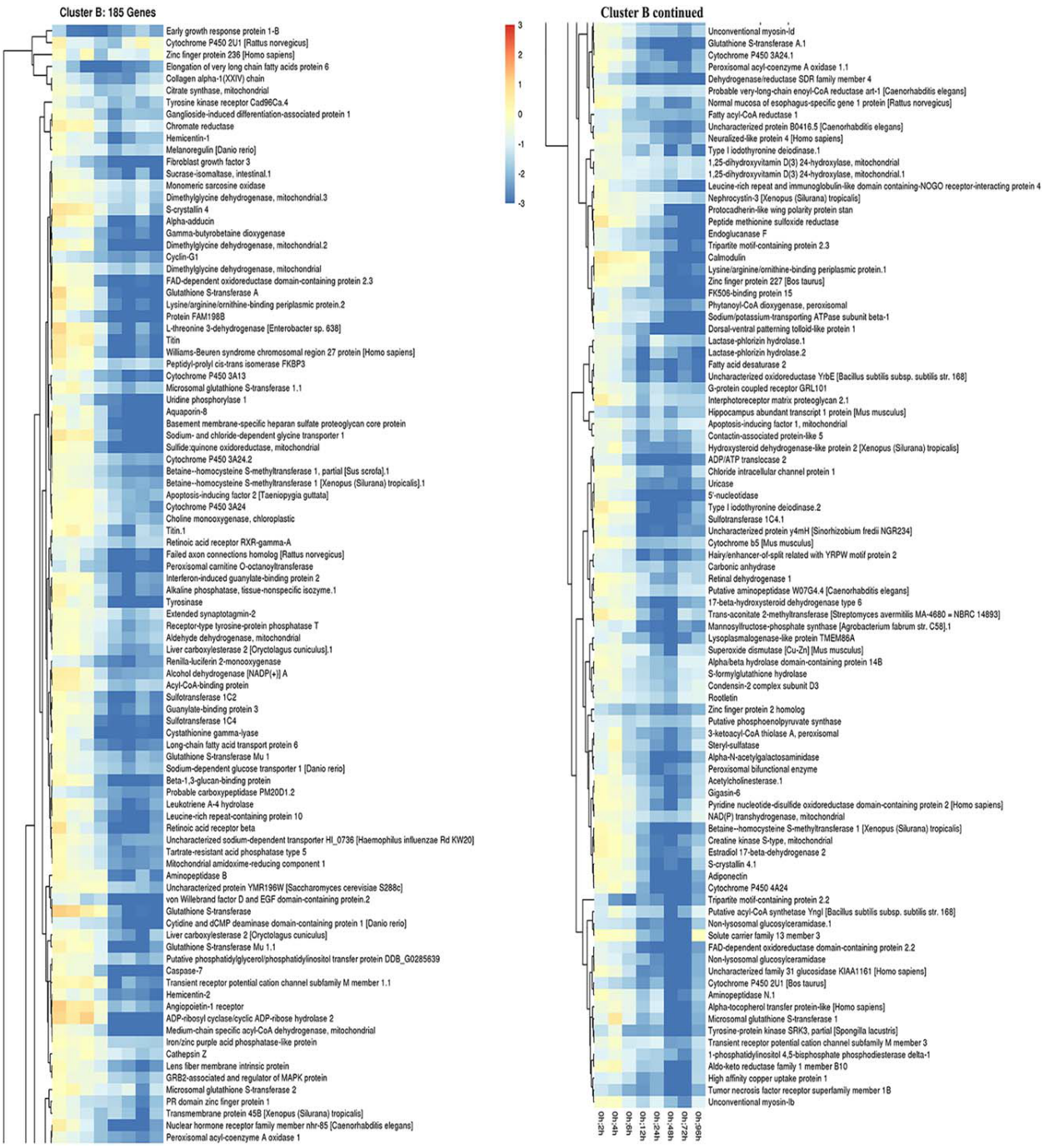

Figure 2.8. Down-regulated gene cluster B expression patterns in regenerating *P. flava*. The heatmap shows the individual genes in cluster B of Figure 6 and their expression profile along all time points sampled compared with control animals.

8-fold lower than control animals. Expression then rebounds over the next 48 hr and returns to around the same levels measured at the 2-hr time point, which is still nearly four log fold lower than expression in control animals (Fig. 6B). Cluster D genes are initially down-regulated after 2 hr of regeneration, but are significantly up-regulated from baseline levels at the 96-hr time point (Fig. 6C). Additionally, a heatmap was constructed for putative transcription factors and their relative expression compared with control animals over all time points (Fig. 9).

Gene Activity Associated With Cell Proliferation and Metabolic Changes is Prominently Detected in the Early Stages of *P. flava* Head Regeneration

Gene ontology (GO) analysis was completed to categorize the function of differentially expressed putative genes. We display the number of genes per significantly enriched GO term for 72 hr and 96 hr and no other time points because there was no enrichment for the other time points. Over half of the significantly enriched genes for which we have GO annotations play a role in cell proliferation and differentiation, as well as organ morphogenesis (Fig. 10A). Approximately 12% of the significantly enriched genes for which we have GO annotations are involved with cell signaling (Fig. 10A). Predicted orthologs of highly conserved developmental pathways were detected, including members of the Wnt signaling pathway, the fibroblast growth factor signaling pathway, and the Notch signaling pathway (Fig. 10A).

We further classified the amount of both up and downregulated genes at the 72-hr time point and 96-hr time point into biological processes, molecular function, and cellular component categories (Fig. 10B). The vast majority of up-regulated genes at the 3- and 4-day time points are involved with extracellular space and matrix roles (Fig. 10B). At 72 hr post bisection, hundreds of genes are up-regulated for biological processes, such as cell adhesion and lipid metabolism

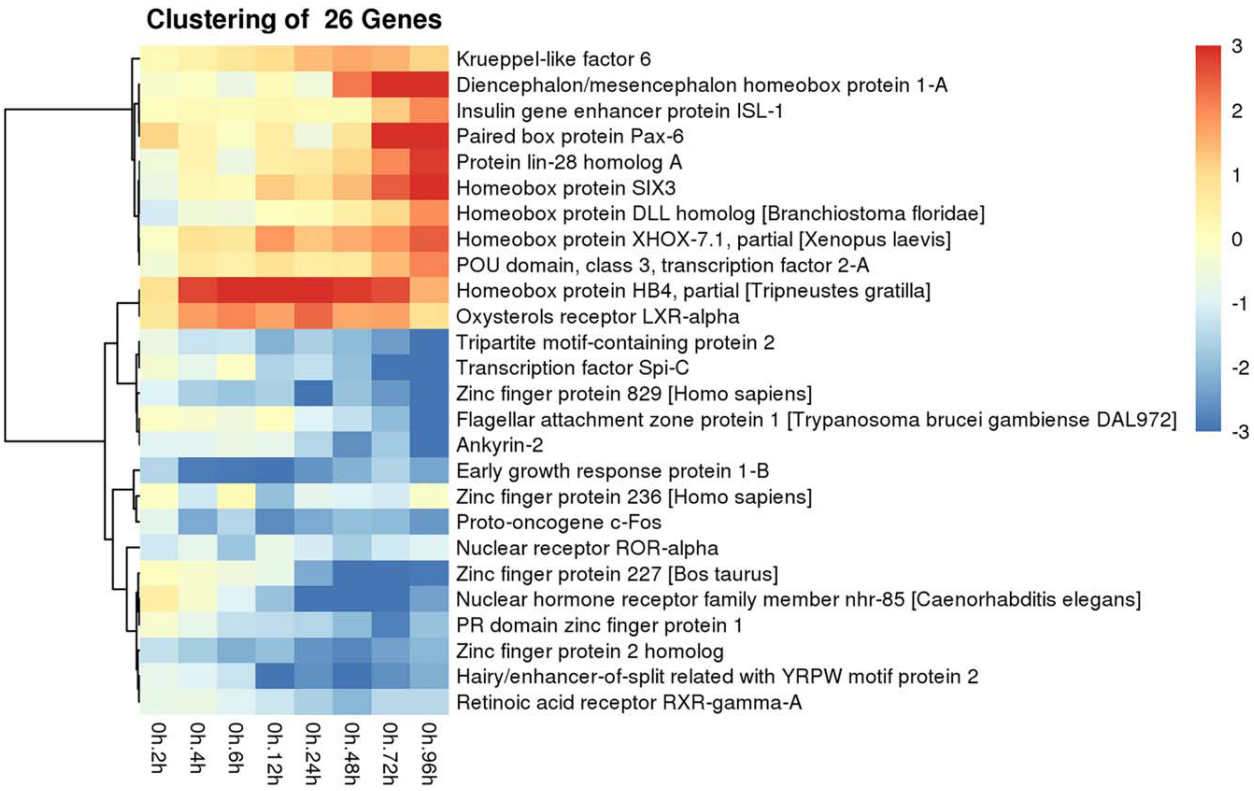

Figure 2.9. Differential gene expression of putative transcription factors in regenerating *P. flava*. A heatmap showing the identity and expression profile of all transcription factors that were both up and down-regulated across all time points sampled compared with control animals.

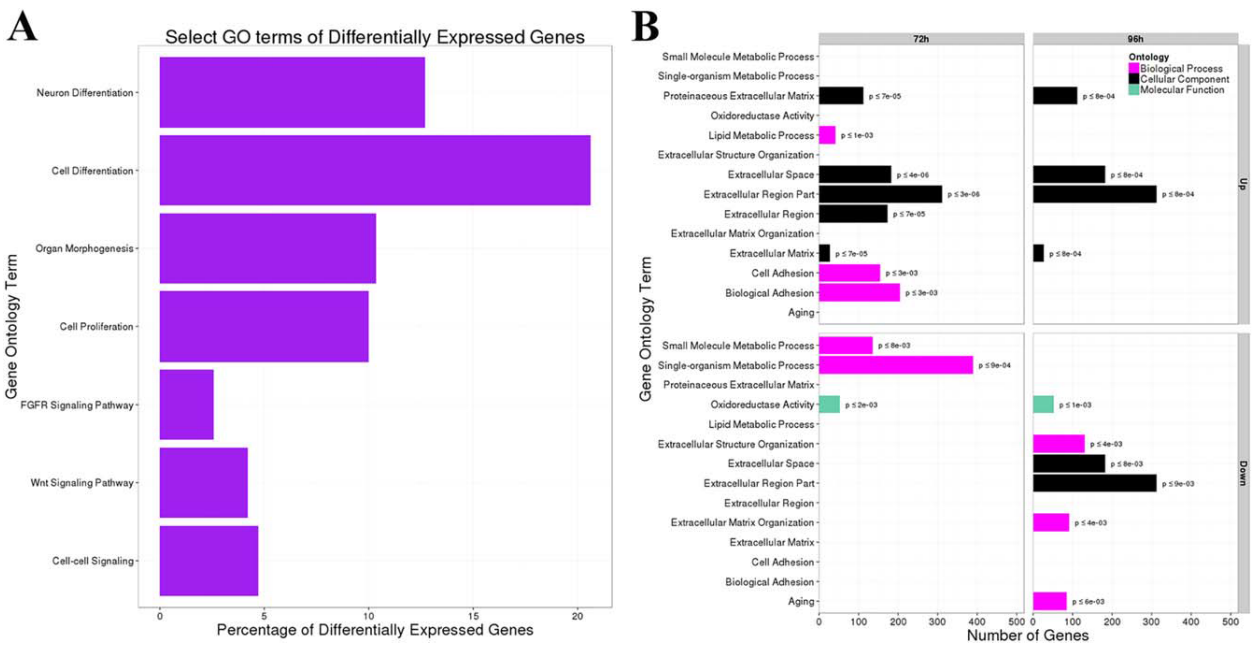

Figure 2.10. Select GO terms of differentially expressed genes in regenerating *P. flava*. A: The X-axis is the percentage of genes that are differentially expressed in the biological processes on the Y-axis. B: The X-axis is the number of genes that were grouped into each gene ontology term on the Y-axis.

(Fig. 10B). Genes regulating small molecule and single organism metabolic processes on the other hand are down-regulated after 72 hr of regeneration, as well as numerous genes involved with oxidoreductase activity (Fig. 10B). Biological process genes aligned with aging, extracellular structure organization and matrix organization are down-regulated at the 96-hr time point (Fig. 10B). The cellular component categories of extracellular space and region part, as well as oxidoreductase activity in the molecular function category are also down-regulated at 96 hr post bisection (Fig. 10B).

Section 5: Discussion

External Regeneration Morphology

Ptychoderid hemichordate regeneration is a remarkable process that results in external structures regenerating in an anterior to posterior manner patterned off the existing body axis. This is similar to juvenile worm development in *P. flava* and another ptychoderid hemichordate, *Balanoglossus simodensis*, when the proboscis forms first during metamorphosis (Miyamoto et al., 2010; Lin et al., 2016). The collar and trunk then differentiate and the trunk elongates. One difference between development and regeneration, however, is that gill slits start to regenerate before the collar has fully formed, unlike early development in direct developing hemichordates when gill slits form after the collar and trunk have delineated from one another (Kaul-Strehlow and Stach, 2013; Kaul-Strehlow et al., 2015).

Furthermore, during direct development, the neural tube also starts to invaginate from dorsal, collar ectoderm in the posterior region of the collar before the first gill slit formation (Kaul-Strehlow and Stach, 2013); however, we show in this study that the first gill slit regenerates at least 2 days before the neural tube begins to form in the indirect developing *P.*

flava. Few studies directly compare development or regeneration of the neural tube and gill slits in ptychoderid worms, but two studies state that the collar develops or regenerates before the branchial region (Nielsen and Hay-Schmidt, 2007: Humphreys et al., 2010). This is not evidence that the neural tube specifically has developed at this point and future studies will need to confirm the timing of development of the neural tube compared with development of the branchial region in *P. flava*. These differences, however, do show a potential temporal plasticity during regeneration of anterior structures in *P. flava*.

During regeneration, cells proliferate and accumulate to form a blastema at the cut site, which then differentiate to replace missing or damaged tissue. The question remains whether these proliferating cells are bona fide stem cells occupying an unknown niche that are recruited to the cut site or are these somatic cells that have undergone de-differentiation and returned to a progenitor cell state and then assigned new fates in the regenerating tissue? Numerous genes in *P. flava* are both up- and downregulated beginning just 2 hr after the animal is bisected. Differential gene expression increases rapidly during the early time points sampled in this study resulting in wound healing and may drive regeneration through the recruitment of stem cells to the cut site forming the regeneration blastema within 3 to 4 days postamputation. Rychel and Swalla (2008) showed that proliferating cell nuclear antigen positive cells are found in scattered mesenchyme cells throughout the tissue near the cut site by day 2 of regeneration at 28°C in *P. flava*. There is some slight variation in wound healing and blastema growth times between the results reported by Rychel and Swalla (2008) and here, but the overall results are consistent. Our lab is currently working to determine the origin and molecular profile of these proliferating cells to verify whether these are stem cells or de-differentiated somatic cells. We are using stem cell markers in regenerating and nonregenerating animals to detect molecular signatures consistent

with known stem cell lines.

Internal Regeneration Morphology

While epidermal tissue regenerates anterior to posterior, internal structures appear to regenerate based on need and function. The mouth, which is critical to feeding and thereby supports the high metabolic cost of regeneration, forms and opens after just 4 days. The worm does not burrow and ingest sand to deposit feed at this point; however, they are likely taking in organic nutrients suspended in the water column. Regenerating worms start to burrow in sand around 10 days postbisection. Blood vessels and mechanical support elements for vital organs and tissues also seem to be essential as these are among the first internal structures in the new tissue.

The stomochord in the posterior proboscis is vacuolated and acts as a hydrostatic skeleton, providing support for the heart-kidney complex (Miyamoto and Wada, 2013). Several studies have shown that, in both direct and indirect developing acorn worms, the stomochord is elaborated from endoderm during juvenile worm development (Kaul-Strehlow and Stach, 2013; Miyamoto and Wada, 2013; Satoh et al., 2014). At 3 days postbisection, we show what may be the presumptive stomochord regenerating from endoderm; however, the identity of this structure is not clear. At this stage, it is not positioned directly below the future heart/kidney complex in the proboscis as the stomochord should be, but rather it is more internal in the presumptive collar region. This structure could also be the hydropore, which is a rounded tube, but that is also not in the correct position, as the hydropore is in the dorsal proboscis/collar ectoderm region and expels circulating waste from the proboscis coelom to the environment (Röttinger and Martindale, 2011). It may be that the angle of the sections is not exactly sagittal, at which point internal

structures may appear skewed. It may also be that regenerating structures look out of place during the early stages. Future studies will be needed using molecular markers to confirm the identity of this structure.

This study does clearly show, however, that the stomochord is elaborated from tissue at the ectoderm/endoderm boundary at 5 days postbisection. Tracing the anterior proboscis ectoderm to the anterior stomochord shows that ectoderm is definitely connected to this structure. Conversely, tracing the endodermal tissue to the posterior stomochord also shows that it is definitely connected to this tissue. So the question remains; at what point does endoderm become ectoderm? Our lab is using endodermal and ectodermal molecular markers to answer this provocative question and determine from what tissue type the stomochord regenerates.

The proboscis skeleton is cartilaginous and provides a rigid framework to protect the collar and overlying dorsal blood vessel and neural tube. The proboscis skeleton regenerates from endoderm, similar to early development (Luttrell et al., 2012; Miyamoto and Wada, 2013). A key difference is that the proboscis skeleton and dorsal vessel regenerate before neural tube regeneration. During normal development this process is reversed and the dorsal vessel and neural tube develop before the proboscis skeleton (Luttrell et al., 2012). Another major difference is the way the neural tube regenerates. During normal development, dorsal collar ectoderm invaginates, rolls up forming a hollow tube. During regeneration, the neural tube begins to form at day 13 as the collar ectoderm nears closure on the dorsal side. It is the closure of this ectoderm that actually forms the tube and not from invaginating ectoderm after the collar fully regenerates and closes.

This study shows that regeneration in *P. flava* does not strictly follow the developmental program and there are morphological steps that are regeneration specific. Furthermore, Arimoto

and Tagawa (2015) showed that the *hedgehog* gene, which is highly conserved in the metazoans (Adamska et al., 2007) and involved with both morphogenesis and regeneration (Huangfu and Anderson, 2006; Rink et al., 2009), is expressed in both the pharyngeal endoderm and anterior tip of *P. flava* larvae, however, it is only expressed in the pharyngeal region during regeneration in *P. flava*. The regenerating proboscis tip does not express *hedgehog* and this evidence suggests there are different gene expression patterns that are regeneration specific in *P. flava* as well.

In the vertebrates, the notochord and dorsal vessel secrete signaling molecules to partially pattern the neural tube and peripheral nervous system, respectively. The notochord secretes sonic hedgehog, signaling the overlying ectoderm to become neural, invaginate and roll up forming the neural tube, while the dorsal blood vessel secretes bone morphogenetic protein molecules that signal neural crest cells to become peripheral neurons (Rickmann et al., 1985; Altaba et al., 1995; Briscoe et al., 1999; Schneider et al. 1999; Young et al., 2004). Hemichordates lack a notochord; therefore, the dorsal vessel may play a pivotal role in guiding CNS formation in the collar region during early development. The dorsal vessel may still be directing this process during regeneration as this structure is formed and has regenerated into the proboscis by day 4. The tissue directly above the dorsal vessel in the collar region is thickened with a rich nerve net by 9 days postbisection and this tissue will become the ventral part of the neural tube. It is likely that signals directing a neural tube fate are coming on early during collar regeneration, before the dorsal, collar ectoderm being present, and these signals may be emanating from the dorsal vessel.

Regeneration of the branchial region starts to occur before the collar closes dorsally and the neural tube forms. Between days 10 and 12, the first gill slit appears directly between the regenerating collar and the existing hepatic sacs. The regenerating branchial region in *P. flava* contains both pigmented and unpigmented cells. The anterior most branchial region closest to the

collar is clear to white, while the posterior regenerating branchial region closest to the original cut site contains pigmented cells. Rychel and Swalla (2008) used a TUNEL (terminal deoxynucleotidyl transferase–mediated deoxyuridinetriphosphate nick end-labeling) assay to show numerous apoptotic cells in the endoderm of the hepatic sacs near the cut site 8 days after amputation. This suggests that, while the anterior most branchial tissue is likely elaborated from newly generated, unpigmented proliferating cells, the cells in the tissue closest to the cut site undergo apoptosis and the tissue is remodeled from the existing cells in the hepatic region. This hypothesis remains to be confirmed, but it will be exciting if internal structures regenerate using both stem cells and somatic cells in *P. flava* because it will provide a model to study two different modes of regenerating tissue in a stem deuterostome.

Expression of Putative Vertebrate Anterior Head Genes

Understanding the genetic and morphological basis of regeneration in hemichordates is vital to unlocking more extensive neural regeneration in humans. No vertebrate has been shown to be able to regenerate an anterior head or an entire CNS. Vertebrates that are capable of regenerating a small part of their CNS, like fish and amphibians (Slack et al., 2008; Sîrbulescu and Zupanc, 2010; Kroehne et al., 2011; Lau et al., 2013), possess numerous copies of single genes due to whole genome duplication events (Dehal and Boore, 2005; Hughes and Liberles, 2008). This genetic redundancy complicates functional studies of key genes controlling the regeneration process. Hemichordates not only lack whole genome duplications, but consistently regenerate their anterior head and complete CNS and, therefore, present a remarkable model system to study and uncover key genetic switches directing regeneration of anterior structures in the deuterostomes.

Several studies have detailed expression of genes involved with chordate brain and spinal cord development in the direct developing hemichordate, *Saccoglossus kowalevskii* (Lowe et al., 2003; Pani et al., 2012: Röttinger and Lowe, 2012). These orthologous genes show a similar spatial distribution of chordate patterning along the anterior–posterior body axis in *S. kowalevskii*. Numerous chordate forebrain genes are expressed in the developing hemichordate proboscis region while chordate midbrain genes are expressed in the hemichordate collar region and chordate hindbrain and spinal cord genes are expressed in the hemichordate trunk region (Lowe et al., 2003; Pani et al., 2012; Röttinger and Lowe, 2012). These overlapping similarities suggest that at least parts of the gene regulatory networks that pattern the chordate CNS were likely present in the common ancestor of the deuterostomes and the hemichordate proboscis and collar could be considered an early representation of the chordate head. No chordate has been shown to regenerate an anterior head or CNS after complete amputation and, therefore, hemichordates are vital to revealing gene networks regulating CNS regeneration in the deuterostomes.

We compared regeneration in *P. flava* and identified several putative orthologs of chordate CNS patterning genes that are upregulated after 3 and 4 days of regeneration. The regeneration blastema has formed at these time points, and cells continue to proliferate to generate a rudimentary proboscis at 3 to 4 days postbisection of the animal. *Sine oculis homeobox 3* (*six3*), *distal-less* (*dll*), *paired box homeobox 6* (*pax6*), and *frizzled-5* are all significantly up-regulated at the 96-hr time point, which is just as the proboscis begins to form. *Six3*, *Pax6*, and *dll* are transcription factors that are involved with patterning the chordate forebrain (Echevarria et al., 2003; Wilson and Houart, 2004; Paek et al., 2009). Frizzled-related Wnt antagonists have been shown to be necessary and sufficient to establish the telencephalon

region of the chordate brain (Houart et al., 2002; Paek et al., 2009). Of the 26 putative transcription factors identified as being differentially expressed in this study, 7 of them are known to be involved in head and neural development and they are all significantly up-regulated 3 and 4 days into regeneration as the rudimentary proboscis is beginning to form. It is likely that other chordate head genes are up-regulated during anterior regeneration in *P. flava*, but they are possibly expressed at later time points as the proboscis continues to regenerate and the collar begins to form. Future studies will be aimed at identifying these transcripts and their expression domains.

Section 6: Conclusions

We have shown that *Ptychodera flava* regeneration is not strictly a morphological recapitulation of development. There is extensive temporal plasticity during regeneration, as well as different modes of acquiring the same anterior structures. Putative orthologs of chordate head genes are also significantly up-regulated just before anterior proboscis regeneration. It will be interesting and informative to discover whether additional head genes are expressed as the proboscis and collar undergo regeneration and we will then use in situ hybridization to localize gene expression in regenerating tissues.

The origin of blastemal cells in *P. flava* still remains to be determined. Our lab is currently working to determine whether this animal uses genuine stem cells or dedifferentiated somatic cells to propagate missing tissue. In humans, when a cell differentiates into a particular cell type, the cell fate assignment normally cannot be reversed or transformed. If hemichordates are using dedifferentiated cells to elaborate new tissue, this may reveal cell signaling pathways necessary for the gain and loss of cell fates in the deuterostomes.

Section 7: Acknowledgments

We thank Dr. Michael Hadfield for allowing us to use his seawater tanks, microscopes, and lab space at Kewalo Marine Laboratory. We also thank the Seeley family for their encouragement and their generous donation from the Seeley Fund for Ocean Research on Tetiaroa. This work was also funded in part by NIH to Dr. Alejandro Sánchez Alvarado. Dr. Alejandro Sánchez Alvarado is a Howard Hughes Medical Institute and Stowers Institute for Medical Research Investigator. This material is based upon work supported by the National Science Foundation Graduate Research Fellowship Program to Shawn Luttrell. Additionally, this material is also based in part upon work supported by the National Science Foundation. Any opinions, findings, and conclusions or recommendations expressed in this material are those of the author(s) and do not necessarily reflect the views of the National Science Foundation. Shawn Luttrell is a Ph.D. candidate in the Swalla Lab at the University of Washington and collected all animals and performed all regeneration experiments, RNA isolation, sectioning and histology, constructed the figures, and wrote the manuscript, including the figure legends. Dr. Billie J. Swalla is a Principal Investigator and oversaw all aspects of animal collection and disposition, regeneration experiments, histology, and manuscript preparation and editing. Dr. Alejandro Sánchez Alvarado is a Principal Investigator at the Stowers Institute for Medical Research in Kansas City, Missouri, and oversaw all aspects of the sequencing, assembly, and annotation of the transcriptome. Eric Ross is a Bioinformatics Specialist in the Sánchez Lab who, along with Kirsten Gotting, a Bioinformaticist also in the Sánchez Lab assembled and analyzed the transcriptome data. They also wrote the methods for the transcriptomes sequencing, assembly and annotation and generated the heatmaps, transcriptome line graphs, and gene ontology graphs. All authors were involved in the writing of this manuscript and page proofs. S.M.L. was funded

by the DGE, A.S.A. was funded by the NIH and HHMI, B.J.S was funded by the DBI, and B.J.S. and S.M.L. were funded by the Seeley Fund for Ocean Research on Tetiaroa.

Chapter 3 - Getting a Head with *Ptychodera flava* Larval Regeneration

Section 1: Abstract

Severe injury to the central nervous system (CNS) of chordates often results in permanent and irreversible mental and physical challenges. While some chordates are able to repair and/or regenerate portions of their nervous system, no chordate has been shown to be able to regenerate all regions of their CNS after catastrophic injury or amputation. In contrast, some hemichordates, on the other hand, are able to efficiently regenerate all neural structures, including their dorsal, hollow neural tube after complete ablation. Hemichordates are marine acorn worms and a sister group to the echinoderms. Acorn worms share numerous developmental features with the chordates that the echinoderms do not share, suggesting that the common ancestor of the deuterostome clade was likely more similar to hemichordates than to echinoderms. The hemichordate, *Ptychodera flava*, progresses from a pelagic, feeding tornaria larva to a tripartite, benthic worm with an anterior head or proboscis, a middle collar region, and a long posterior trunk. The adult worm regenerates all anterior and posterior body parts when bisected in the trunk. It is an open question whether *P. flava* regenerates during the larval stage or whether the regeneration program becomes active post metamorphosis. We show that *P. flava* larvae are capable of robust regeneration after bisection through the sagittal, coronal, and axial planes. We also use antibody staining to show that the anterior apical region, including the eyespots and larval brain, regenerates a rich, serotonin positive complex of cells within two weeks after amputation. Cells labeled with EdU (5-ethynyl-2'-deoxyuridine) confirm that regeneration is occurring through epimorphic processes as new cells are added at the cut site and throughout the regenerating tissue. This study verifies that *P. flava* larvae can be used for future functional studies aimed at identifying the genetic and morphological mechanisms controlling CNS

regeneration in a stem deuterostome.

Section 2: Introduction

One of the great marvels in biology is the ability to regenerate a fully functional nervous system after damage from disease or injury. Scientists have studied this remarkable process for decades, but it is still largely a mystery how some animals accomplish this incredible feat. Humans have limited regenerative abilities, particularly in the central nervous system (CNS; Chernoff et al., 2002; Stocum, 2006; Poss, 2010). Some peripheral neurons can regenerate to a certain degree however, damage to the brain or spinal cord usually results in permanent, catastrophic impediments that are not corrected though regenerative mechanisms (Yannas IV, 2001). Animal models that are capable of extensive and complete nervous system regeneration are needed to effectively make strides in understanding the molecular mechanisms underlying this trait. Moreover, models that are closely related to humans will likely provide greater insight to achieving extensive mammalian CNS regeneration as many of the same genes, gene networks, and developmental programs are shared between the deuterostomes (Davidson and Erwin, 2006; Swalla, 2006).

The ability to regenerate neural tissue is widespread among numerous animal lineages, like Ctenophora, Cnidaria, Playhelminthes, Annelida, and Nemertea to name a few (Bely and Nyberg, 2010; Brown et al., 2009; Giangrande and Licciano, 2014; Alvarado A.S., 2000; Somorjai et al., 2012). Within the deuterostome clade (Figure 1), however, few animals are capable of complete nervous system regeneration after total neural ablation. Echinoderms (sea stars, sea urchins, sand dollars, sea cucumbers, and sea lilies) have impressive regenerative abilities. Every class in this group of animals has members that are able to regenerate certain

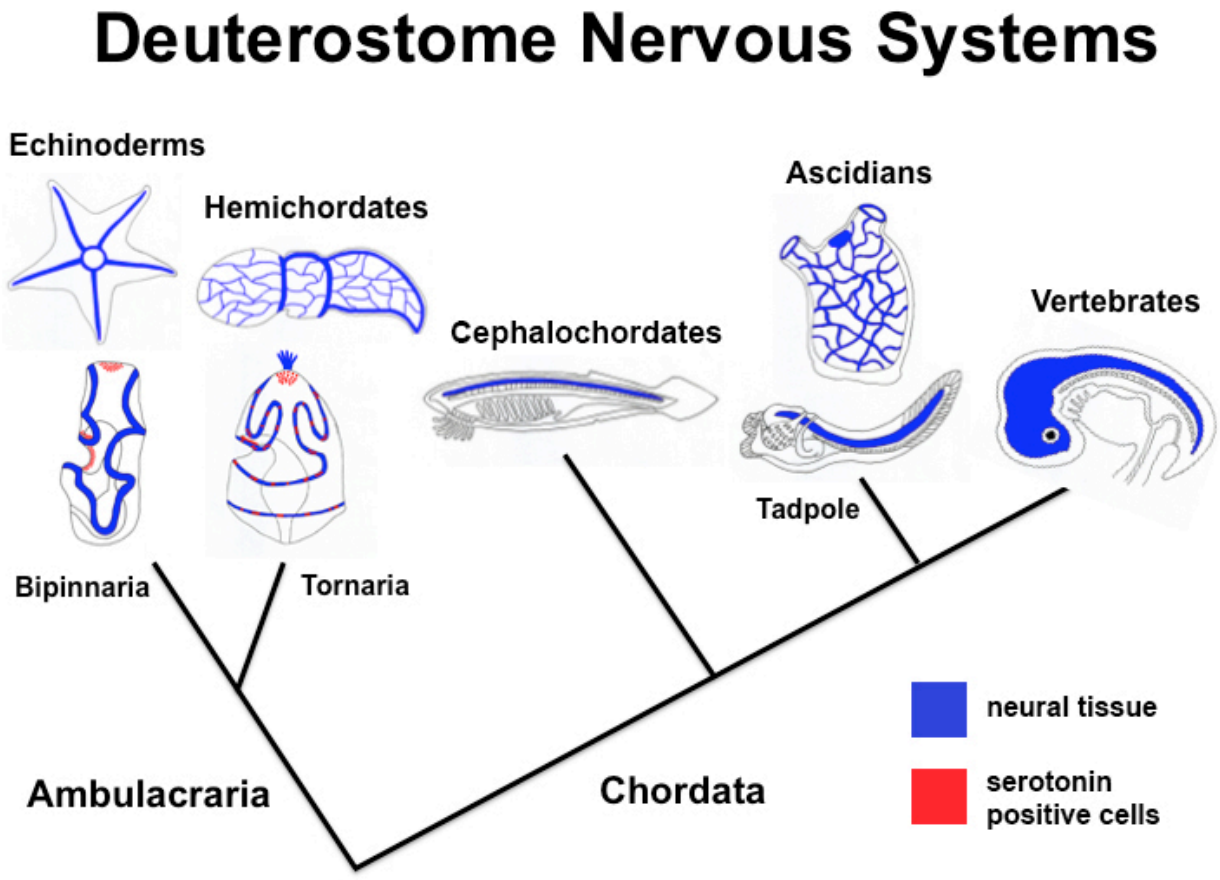

Figure 3.1. Deuterostome Nervous Systems. Echinoderms and hemichordates are sister groups and together form the Ambulacraria clade. Members of these groups have larval nervous systems consisting of ciliary bands, shown in blue, that wrap around the animal. Serotonin positive cells, shown in red, are grouped together in a cluster at the apical tuft, around the mouth, and throughout the ciliary bands. Upon metamorphosis to the adult body plan, echinoderms develop nerve cords in the arms and around the central disk. Hemichordates develop nerve cords along the dorsal and ventral trunk and circumferential nerve rings around the posterior collar and posterior proboscis. Some ptychoderid hemichordates also develop a hollow, dorsal neural tube in the collar region only. Hemichordates also possess a diffuse nerve net throughout the ectoderm. The chordates, consisting of lancelets, ascidians, and vertebrates, develop a dorsal, hollow neural tube. The neural tube of ascidian tadpole larvae undergoes apoptosis at metamorphosis and only the anterior-most region of the tube remains and becomes a neural gland between the two siphons. The adult ascidian also develops a nerve net throughout the ectoderm. Neural tissue shown in blue. Serotonin positive cells shown in red in the Ambulacraria.

tissues and structures in the larval and adult life stages, including nerve cords, innervated guts and even the central disk, or radial nerve cord (Carnevali et al., 2009; Mashanov and Heinzeller, 2008; Vickery et al., 2002; Vickery and McClintock, 1998). The echinoderm nervous system and body plan, however, is highly derived, with radial symmetry, lacking many features consistent with vertebrate body plans (Figure 1). Echinoderms develop their adult nerve cords post metamorphosis and they do not develop a neural tube in either the larval or adult stages of their life cycle (Garner et al., 2016; Mashanov et al., 2007). Furthermore, echinoderms lack an anterior head and instead possess a radial, oral-aboral body axis as opposed to the anterior-posterior body axis of chordates (Minsuk et al., 2005; Wygoda et al., 2014).

Cephalochordates also display robust regenerative capabilities within specific regions of the body. The caudal tail regenerates with high fidelity (Somorjai et al., 2012). The anterior most region of the animal also exhibits regenerative abilities with the notochord, fin, mouth, neural structures, and buccal cilia regenerating to some degree, but as the amputation plane moves toward the pharynx region, the regenerative abilities decline and are completely absent in the pharynx (Somorjai et al., 2012). Bisection within this region results in death for both halves of the animal. The cephalochordate model may provide great insight into some mechanisms underlying tissue regeneration, however these animals still have unknown barriers that block complete CNS regeneration.

Some chordate ascidians, which are sister group to the vertebrates (Bourlat et al., 2006; Delsuc et al., 2006), undergo whole-body regeneration, including their nervous system (Brown et al., 2009; Jeffery W., 2014; Kassmer et al., 2016; Rinkevich et al., 2010; Schultze LS., 1899; Zondag et al., 2016). Unfortunately, ascidian tadpole larvae, which possess several vertebrate

features, including a dorsal, hollow neural tube, do not regenerate during this early life stage (Jeffery, 2014). The remarkable regenerative abilities of ascidians appear to be activated post metamorphosis. When ascidians metamorphose from their tadpole larval stage and are competent for whole-body regeneration, the majority of their neural tube undergoes apoptosis and the anterior most part of the larval neural tube remains and becomes a neural gland situated between the incurrent and excurrent siphon of the adult (Horie et al., 2011; Manni et al., 2005). The adult ascidian also forms a rich nerve net throughout the ectoderm, but they lack a head, neural tube, and centralized nervous system similar to the vertebrates (Figure 1; Sasakura et al., 2012).

There are several groups of animals within the vertebrates that are capable of CNS regeneration, but these models also have unknown barriers preventing complete CNS regeneration after catastrophic injury. Teleost fish, newts, salamanders, lizards, and tadpole larval, anuran amphibians can regenerate portions of their spinal cord, but this is generally restricted to the caudal end of the spinal cord found in the tail of the animal (Beattie et al., 1990; Chernoff 1996; Duffy et al., 1992; Ghosh and Hui, 2016; Kizil et al., 2012; Sîrbulescua and Zupanca, 2011; Singer et al., 1979). The closer the spinal cord injury is to midline or the anterior head end of the animal, the less likely the injury will be corrected through regenerative mechanisms resulting in a fully functional animal. Furthermore, bisection of the animal in the transverse plane results in death and no vertebrate has been shown to regenerate an entire body half or head region. Humans do not have tails and therefore, these models may not be as informative for human CNS regeneration as models capable of robust regeneration throughout the entire CNS. Hemichordates are one deuterostome with remarkable CNS regenerative abilities that may provide insight into achieving more extensive neural regeneration in humans.

Hemichordates, also known as acorn worms, are marine invertebrates and sister group to

the echinoderms (Figure 1; Cameron et al., 2000; Wada and Satoh, 1994). Hemichordates share numerous developmental and morphological traits with the chordates, such are pharyngeal gill slits, a *Hox* specified anterior-posterior body plan, an endostyle, and a post-anal tail (Aronowicz and Lowe, 2006; Brown et al., 2008; Luttrell and Swalla, 2014). Acorn worms begin life as planktonic, feeding, tornaria larva that can remain in the water column for up to three hundred days (Hadfield, 1978). The larva progresses through various developmental stages throughout the long planktonic phase, progressing from a newly hatched Heider stage larva, to a Metchnikoff, Krohn, Spengel, and lastly Agassiz stage larva, or what is commonly known as the swimming head larva (Lin et al., 2016; Nakajima et al., 2004; Nishikawa, 1977; Rao, 1954; Tagawa et al., 1998). The nervous system of the larva consists of ciliary bands that wrap around the animal and move the larva through the water column (Figure 1). The ciliary bands contain serotonin positive cells and also stain positive for 1E11, an antibody raised against sea urchin synaptotagmin protein (Burke et al., 2006; Byrne et al., 2007; Nakajima et al., 2004). Synaptotagmin is a calcium-binding factor of synaptic vesicles and is expressed exclusively in neurons in some invertebrates (Augustine, 2001; Bai et al., 2002; Katsuyama et al., 2002; Littleton et al., 1993; Nonet et al., 1993). The apical organ, or brain of the larva, is found at the anterior end below the eyespots and contains a rich complex of serotonin and 1E11 positive cells (Burke et al., 2006; Byrne et al., 2007; Nakajima et al., 2004). The ciliary bands connect at the four corners of the apical organ (Figure 2).

The larva becomes competent for metamorphosis during the Spengel stage of development and transforms to a juvenile worm during the Agassiz stage (Lin et al., 2016). The tripartite body plan of the worm becomes apparent and the metamorphosing larva settles to the benthos for the remainder of its life span. The tripartite worm is composed of an anterior

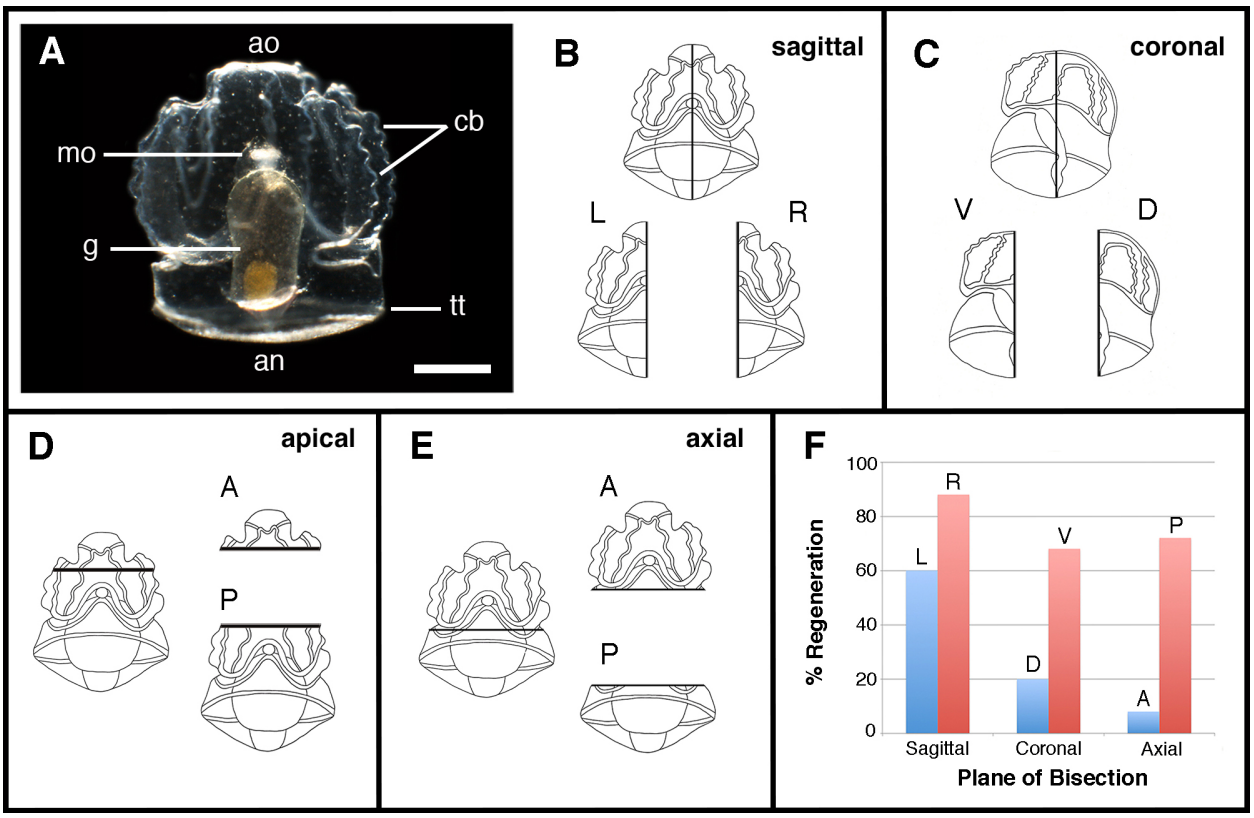

Figure 3.2. Sagittal, coronal, apical and axial cut Krohn stage *Ptychodera flava* larvae. **A.** Dorsal view of uncut Krohn stage larva **B**. Krohn stage larva with sagittal cut bisecting the left (L) and right (R) halves. **C**. Krohn stage larva cut through the coronal plane bisecting the ventral (V) and dorsal (D) halves. **D**. Krohn stage larva with apical cut separating the anterior (A) and posterior (P) halves **E.** Krohn stage larva with axial cut separating the anterior (A) and posterior (P) halves. **F**. Percent of larval halves showing complete regeneration after 28 days. N = 25 for each plane of bisection. A = anterior; an = anus; ao = apical organ; cb = ciliary band; D = dorsal; g = gut; L = left; mo = mouth; P = posterior; R = right; tt = telotroch; V = ventral.

proboscis, or head, a middle collar region and a long posterior trunk (Luttrell et al., 2016). Interestingly, the solitary hemichordate *Ptychodera flava* has a hollow, dorsal neural tube in the collar region that we, and others, have shown develops in a similar fashion to the chordate neural tube (Luttrell et al., 2012; Miyamoto and Wada, 2013). Even more striking, *P. flava* reliably regenerates all body structures, including their complete neural tube after total ablation and their anterior head region (Humphreys et al., 2010; Rychel and Swalla, 2008; Luttrell et al., 2016). It remains to be determined, however, at what point during development this regeneration program is activated. It may be that regeneration is initiated after the animal undergoes metamorphosis from a planktonic larva into a juvenile worm or it may be that the regeneration program becomes active at some point before metamorphosis. Does the metamorphosis program somehow initiate regeneration or is this capacity active at all stages of development in *P. flava,* similar to the regeneration program in some echinoderm larvae and adults? If *P. flava* larvae are capable of regeneration, do all regions of the larva regenerate with the same efficiency?

The present study shows that Krohn stage *Ptychodera flava* tornaria larvae are capable of robust regeneration in the sagittal, coronal, and axial planes (Figures 2, 3, and 4). We found that proliferating cells are abundant at the cut site in *P. flava* larvae and throughout the regenerating tissue. We also show that bisected larvae fully regenerate their nervous system and are indistinguishable from healthy, intact larvae, but they revert to an earlier developmental larval stage during regeneration. Though *P. flava* larvae do not possess a neural tube pre-metamorphosis, the regeneration program is likely the same for both larvae and adults. Functional studies aimed at uncovering the genetic and molecular mechanisms controlling the regeneration process may, in certain cases, be more tractable in the larvae due to their small size, transparency, and relatively simple body plan and tissues compared to adults acorn worms.

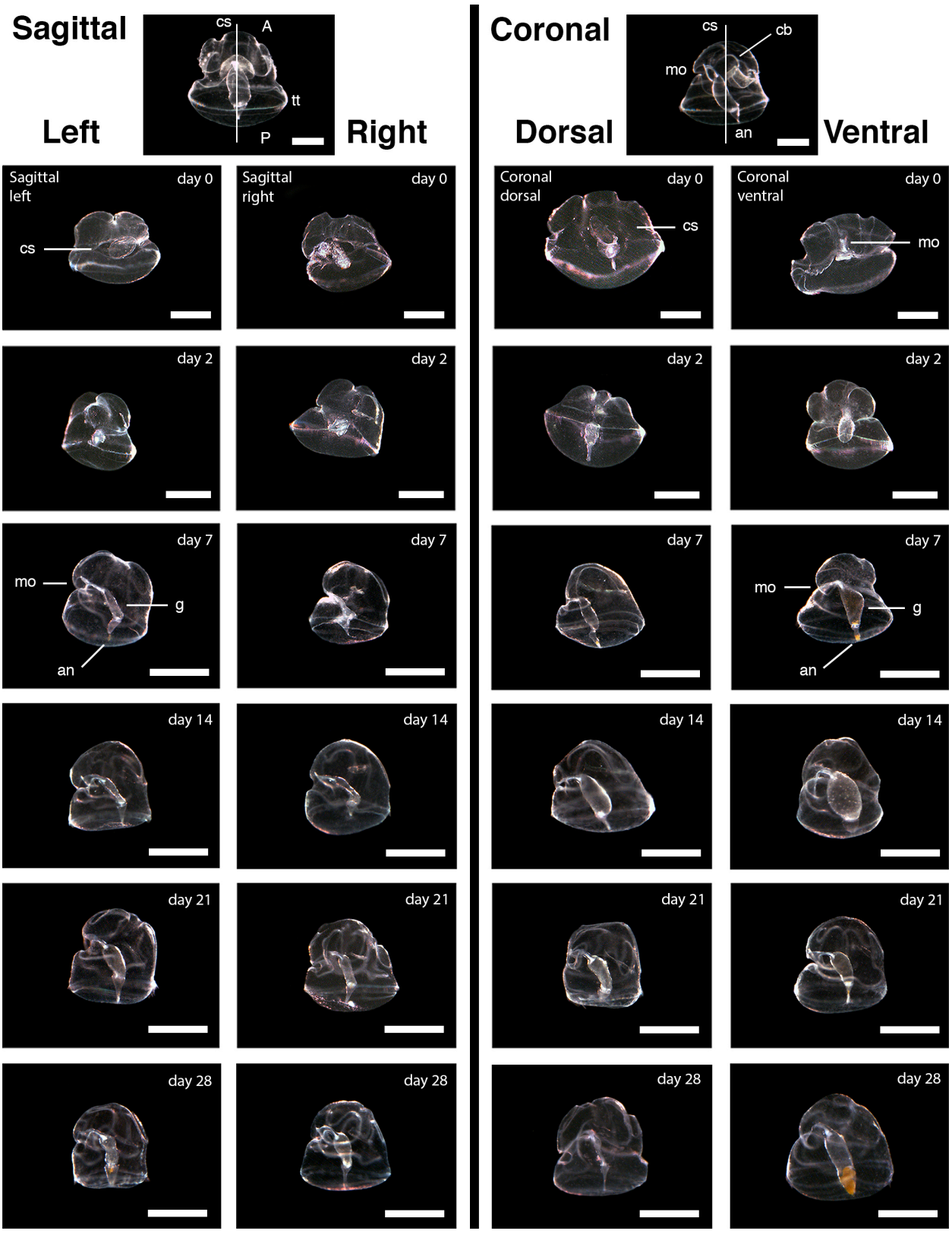
Sagittal
Left
Right
cs
A
tt
P
Coronal
Dorsal
Ventral
cb
mo
an
Sagittal left
Sagittal right
Coronal dorsal
Coronal ventral
day 0
day 2
day 7
day 14
day 21
day 28
g

Figure 3.3. Coronal and Sagittal Regeneration in *Ptychodera flava* Krohn larvae. Each column shows day zero through day twenty-eight of regeneration for the left and right halves of sagitally cut larvae and the dorsal and ventral halves of coronally cut larvae. All day zero and day 2 time points are lateral, cut site views. Day seven through day twenty-eight are lateral views with the mouth on the left side showing the gut and the anus is at the posterior end. Anterior is to the top in all views. Scales bars are 1mm for all images. A = anterior; an = anus; cb = ciliary band; cs = cut site; g = gut; mo = mouth; P = posterior; tt = telotroch.

Section 3: Materials and Methods

Animal Collection and Management

Ptychodera flava larvae were obtained from Dr. Yi-Hsien Su's lab at Academia Sinica in Taiwan, where they spawned gravid, adult worms and reared the embryos through hatching. Larvae were transported in a container of seawater from Taipei, Taiwan to the University of Washington, Friday Harbor Laboratories in Friday Harbor, Washington. Larvae were contained in 2 liter Erlenmeyer flasks filled with 0.2 μm filtered seawater (FSW) and kept at room temperature. Air was continuously bubbled into each flask and the water was changed every 4 days with fresh FSW. Larvae were fed after each water change with *Rhodomonas* sp. and *Isochrysis galbana* algae.

Larval Regeneration

Healthy, intact Krohn stage larvae were bisected through the midline in either the sagittal, coronal, or axial planes with a sterile micro-surgical blade (Figures 2, 3, and 4). A total of twenty-five larvae were bisected through each plane and allowed to regenerate at room temperature in 6-well plates filled with FSW. Left and right halves, dorsal and ventral halves, and anterior and posterior halves were separated into individual wells. Each well contained no more than 10 larval halves and all were fed starting from day one post bisection with one drop each of concentrated *Rhodomonas* sp. and *Isochrysis galbana* algae. FSW and algae was changed every two days during regeneration over the course of twenty-eight days.

In a second set of experiments we removed the anterior apical region in healthy Krohn stage larvae with a micro-surgical blade to determine the time required for larval brain regeneration. Both anterior and posterior pieces were incubated in EdU and fixed after two, five,

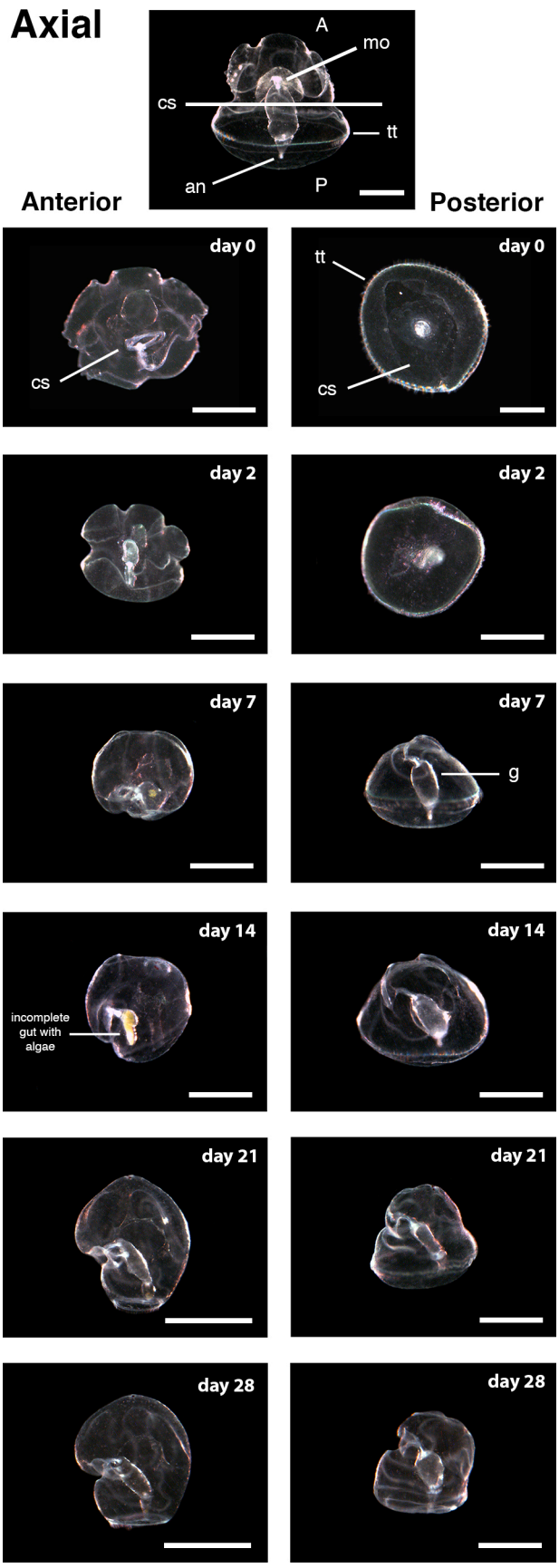
Axial
A
mo
cs
tt
an
P
Anterior
Posterior
day 0
cs
day 0
tt
cs
day 2
day 2
day 7
day 7
g
day 14
incomplete gut with algae
day 14
day 21
day 21
day 28
day 28

Figure 3.4. Axial Regeneration in *Ptychodera flava* Krohn Stage Larvae. Each column shows day zero through day twenty-eight of regeneration for the anterior and posterior halves of axially cut larvae. Day zero and day 2 anterior half time points are lateral, cut site views. Day zero and day 2 posterior half time points are top down, cut site views. All day seven through day twenty-eight time points are lateral views with the mouth on the left side and the anterior is to the top. Scales bars are 1mm for all images. A = anterior; an = anus; cs = cut site; g = gut; mo = mouth; P = posterior; tt = telotroch.

eight, and fifteen days post amputation. Fixed pieces were labeled with a Click-iT® reaction mixture, followed by anti-serotonin antibody staining. All live, regenerating larval pieces were photographed on a Nikon SMZ 1500 dissecting microscope and photographed with a QImaging MicroPublisher RTV camera.

EdU labeling

The apical region of Krohn stage larvae was removed and both pieces were allowed to regenerate at room temperature, approximately 24°C. After two, five, eight, and fifteen days, the regenerating larvae were immersed in 10 μM EdU in filtered seawater for 30 minutes at room temperature (RT). Larvae were then fixed in 3.2% paraformaldehyde in PBS for 1 hour at RT and then washed three times in PBST (PBS with 1% tween) for 15 minutes each. Larvae were then blocked for 30 minutes in 5% goat serum in PBST on a rocker at RT. Larvae were incubated for 2 hours in Click-iT® reaction mixture per the manufacturers guidelines at RT on a rocker and then washed three times in PBST for 10 minutes each. Larvae were subsequently stained with antibodies and mounted onto slides in Vectashield with DAPI (Vector Laboratories, Burlingame, CA), and photographed on a Nikon Eclipse E800 or a Zeiss LSM 800 confocal microscope.

Immunocytochemistry

Following EdU staining, larvae were incubated overnight (or in some cases up to two days) with 1:1000 rabbit polyclonal anti-serotonin (Sigma-Aldrich, St. Louis, MO). The following day larvae were washed five times in PBST for 30 minutes each and then incubated overnight in a 1:1000 dilution of Alexa Fluor 568 goat anti-rabbit IgG antibody (Invitrogen,

Eugene, OR). Larvae were then washed again five times for thirty minutes each in PBST and then mounted onto slides in Vectashield with DAPI (Vector Laboratories, Burlingame, CA).

Section 4: Results

Sagittal, Coronal and Axial regeneration

We defined complete regeneration as having a complete gut and feeding, normal morphology, and normal swimming behavior. Larvae that were cut through the sagittal plane into left and right halves displayed the most robust regeneration (Figure 2). In total, twenty-five krohn stage larvae were bisected and 74% of the halves regenerated normal larval morphology, were feeding, and swimming normally after twenty-eight days (Figures 2 and 3). There was a slight difference between the overall numbers of fully regenerated halves, with the right half outperforming the left. The right half of the bisected larvae experienced an 88% regeneration rate, with twenty-two of the twenty-five halves regenerating a complete gut and feeding within two weeks (Figures 2 and 3). Normal morphology and swimming was acquired for some of the larval halves within three weeks, but the final count was assessed after twenty-eight days because some halves were feeding, but had not yet acquired normal morphology. The left half displayed a 60% regeneration rate with fifteen of the twenty-five halves meeting fully regenerated benchmarks at 28 days (Figures 2 and 3). Nearly all of the larvae that achieved complete regeneration were feeding by two weeks post cut.

Larvae that were cut through the coronal plane separating dorsal and ventral halves displayed dramatically different regeneration rates between the two halves. The overall rate for this cut was 44% with the ventral half drastically outperforming the dorsal half (Figure 2). The ventral half of the animal regenerated normal morphology, feeding, and behavior in seventeen of

the twenty-five halves, or 68% of the cut larvae (Figures 2 and 3). This is a stark contrast to the dorsal half, which achieved a 20% regeneration rate and only five of the twenty-five halves regenerated a complete gut and began feeding to achieve normal morphology within twenty-eight days (Figures 2 and 3). Interestingly, all of the cut larval halves that fully regenerated, regardless of the plane of bisection, displayed morphology of the previous developmental larval stage. At the end of twenty-eight days, all regenerated Krohn stage larvae lacked tentacular buds on the ciliary bands. Collar and trunk coeloms that were present in the uncut animals were notably absent. All regenerated larval halves exhibited the morphological characteristics consistent with the Metschnikoff stage (Figures 3 and 5).

Axially cut larvae, separating the anterior and posterior halves displayed the lowest total regeneration rate at 40%, largely in part to a near lack of regeneration in the anterior half (Figures 2 and 4). Posterior halves completely regenerate a gut, feed, form eyespots, and develop normal swimming behavior 72% of the time. Eighteen of the twenty-five halves appeared normal after 28 days and some had regenerated eyespots at the apical tuft after only 17 days post cut (data not shown). This is in stark contrast to the anterior half that only fully regenerated in 8% of the cuts. Only two out of twenty-five anterior halves regenerated a complete gut and telotroch, or ciliated band at the posterior end of the animal (Figure 4). All of the remaining halves, twenty-three out of twenty-five, healed at the cut wound site and persisted through 2-4 weeks, but never regained complete guts and eventually shrank in size to small balls of cilia and degraded.

Wound healing for nearly all bisected larvae occurred within the first two days after amputation (Figures 3 and 4). It is worth noting that the tissue at the cut site was pinched together during bisection for some samples. In these cases, the larva was completely bisected, however, the wound at the cut site for one or both halves was sealed together and it did not

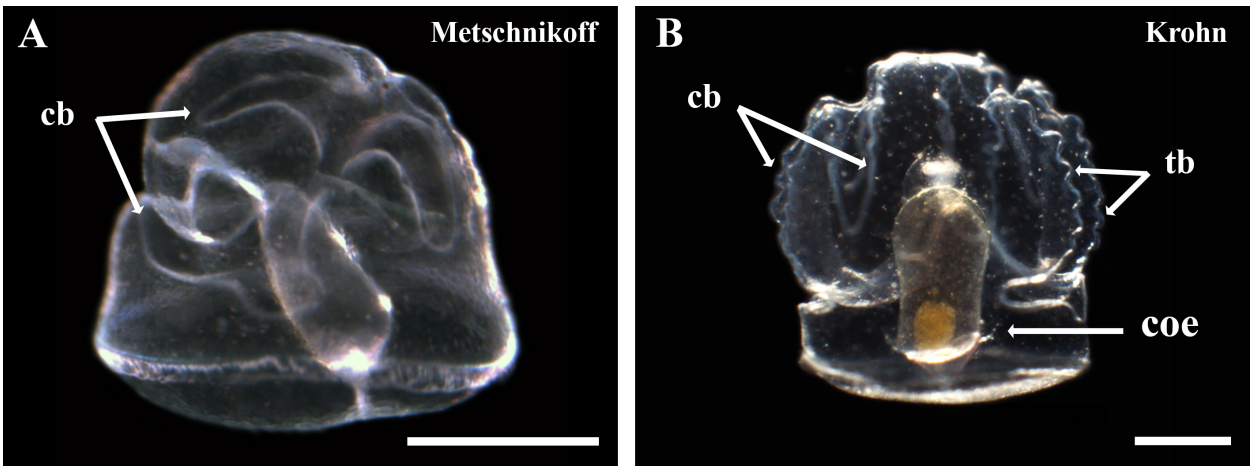

Figure 3.5. ***Ptychodera flava*** **Metschnikoff stage and Krohn Stage Larva**. A. Uncut Metschnikoff stage larva. Lateral view with the mouth to the left. B. Uncut Krohn stage larva. Ventral view with the mouth to the center. All scale bars are 1mm. cb = ciliary band, tb = tentacular bud on ciliary band, coe = coelom.

appear to re-open. It was not possible to accurately determine wound healing time in these cases as there was no open wound after cutting. The majority of animals, however, had open wounds that healed within two days, including larval halves that ultimately did not regenerate. This indicates that the wound healing program is different than the regeneration program in *Ptychodera flava*.

Apical Organ Regeneration

Apical regeneration closely resembled axial regeneration, however the anterior apical piece did not regenerate to a fully functional animal in any of the cut larvae. The apical organ did not die after the initial cut and persisted through wound healing and in a few samples up to 25 days post cut, depending on the original size of the fragment (Figure 6). The overall size of the apical tissue gradually shrinks over time and eventually becomes a small ball of ciliated cells typically after 2-3 weeks post amputation. Serotonin positive cells were found in the apical tuft after fifteen days and did not appear to undergo apoptosis and degrade although the tissue itself diminished in size throughout the time points (Figure 6). Proliferating cells labeled with EdU (5-ethynyl-2'-deoxyuridine) were detected throughout all time points, but the number of dividing cells declines over time and is severely reduced by day fifteen post amputation (Figure 6).

Regeneration from the posterior site was markedly different from the anterior piece. Significant cell proliferation was detected throughout the tissue at the cut site after two days post amputation, indicating that active cell division is contributing to wound healing and promoting regeneration (Figure 7). These dividing cells coalesced toward the center of the posterior piece where new tissue was replacing structures lost in amputation (Figure 7). Cell proliferation increased significantly at the 15 day time point after eyespots formed in the anterior apical end of

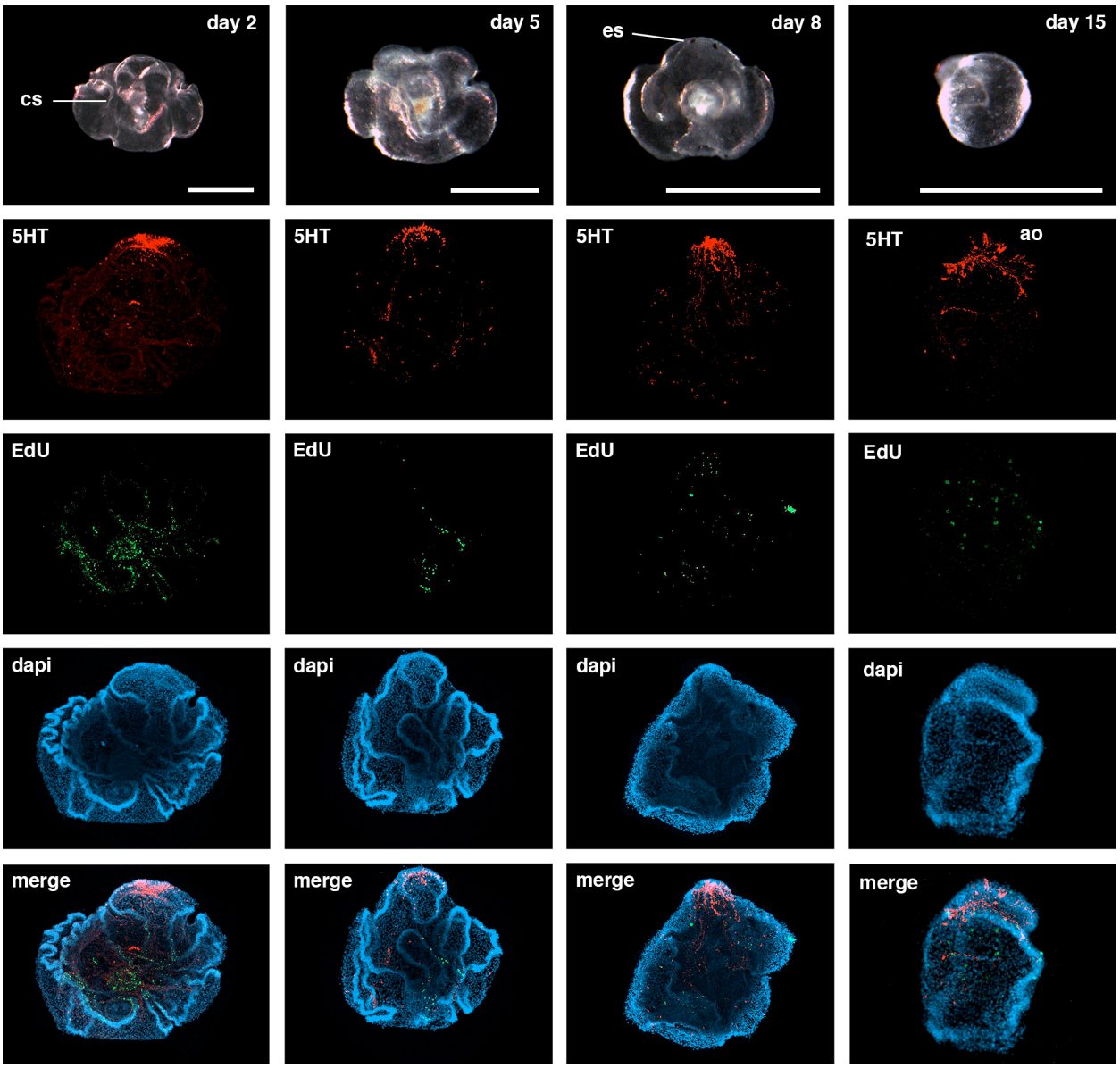

Figure 3.6. Regeneration in the amputated apical organ from Krohn stage *Ptychodera flava* larvae. Columns show day two, day five, day eight, and day fifteen of regeneration post amputation of the anterior apical organ from Krohn stage larvae. Live animal images are all cut site views. Serotonin, or 5-hydroxytryptamine (5HT), shows staining of neurons in the apical organ and surrounding tissue at all time points. EdU, or 5-ethynyl-2′-deoxyuridine, shows staining of proliferating cells at all time points. Dapi stains cell nuclei. All staining images are lateral views with anterior to the top. Scales bars are 1mm for all images. Blue = dapi; green = EdU; red = serotonin. ao = apical organ; cs = cut site; es = eyespots; pao = presumptive apical organ.

the animal (Figure 7). Serotonin positive cells were detected at two and five days post cut in the portions of ciliary bands that remained in the posterior pieces after amputation (Figure 7). Two distinct populations of serotonin positive cells were found near the midline in the regenerating presumptive apical organ at eight days post cut and these populations of cells likely merged at fifteen days post cut and formed a condensed, serotonin-rich apical organ (Figures 7 and 8).

Section 5: Discussion

This study shows that the regeneration program is active in *Ptychodera flava* pre-metamorphosis during the larval stage. This is consistent with the regeneration program in some echinoderm larvae. Certain species of sea urchin, sand dollar, and sea star larvae fully regenerate after bisection through the axial plane (Vickery and McClintock, 1998; Vickery et al., 2002). Both the anterior and posterior halves completely regenerate with no mortality within 12-14 days in the sea stars *Luidia foliolata* and *Pisaster ochraceus* and the sea urchin, *Lytechinus variegatus* (Vickery and McClintock, 1998; Vickery et al., 2002). The sand dollar, *Dendraster excentricus* also regenerates after bisection through the axial plane, but the anterior half experiences reduced regeneration compared to the posterior half, similar to axial regeneration observed in this study (Vickery et al., 2002). The regeneration time scale and overall capacity is comparable between echinoderm larvae and *P. flava* larvae, indicating that regeneration was probably an ancestral character in the Ambulacraria clade (Figure 1) and could possibly extend beyond to the common ancestor of the deuterostomes in general.

We also provide evidence that neurons in the apical sensory organ, or brain of the larvae, regenerate from posterior pieces after complete ablation. This confirms that the larval brain is not required for larval regeneration. Serotonin positive cells are absent in the center of the posterior

piece two days post amputation of the apical organ, but are shown to reform near the apical midline after only eight days of regeneration. A rich serotonin positive complex of cells is grouped together in the apical organ of the posterior piece after two weeks post amputation. Eyespots are visible in the apical region above the serotonin rich complex and indicate that sensory structures reliably regenerate from posterior halves of the larvae. While the functionality of these structures was not tested experimentally, the larvae displayed normal swimming behavior and motility through coordinated ciliary action.

We also show that the amputated apical organ does not die after removal from the larva and serotonin positive cells persist throughout all time points in this study. The apical tissue does not regenerate to form a complete animal, however, and over time the amputated apical organ shrinks in size and disintegrates. This indicates that neurons in the apical organ alone are not enough to promote regeneration and suggests that either some population of cells in the tissue

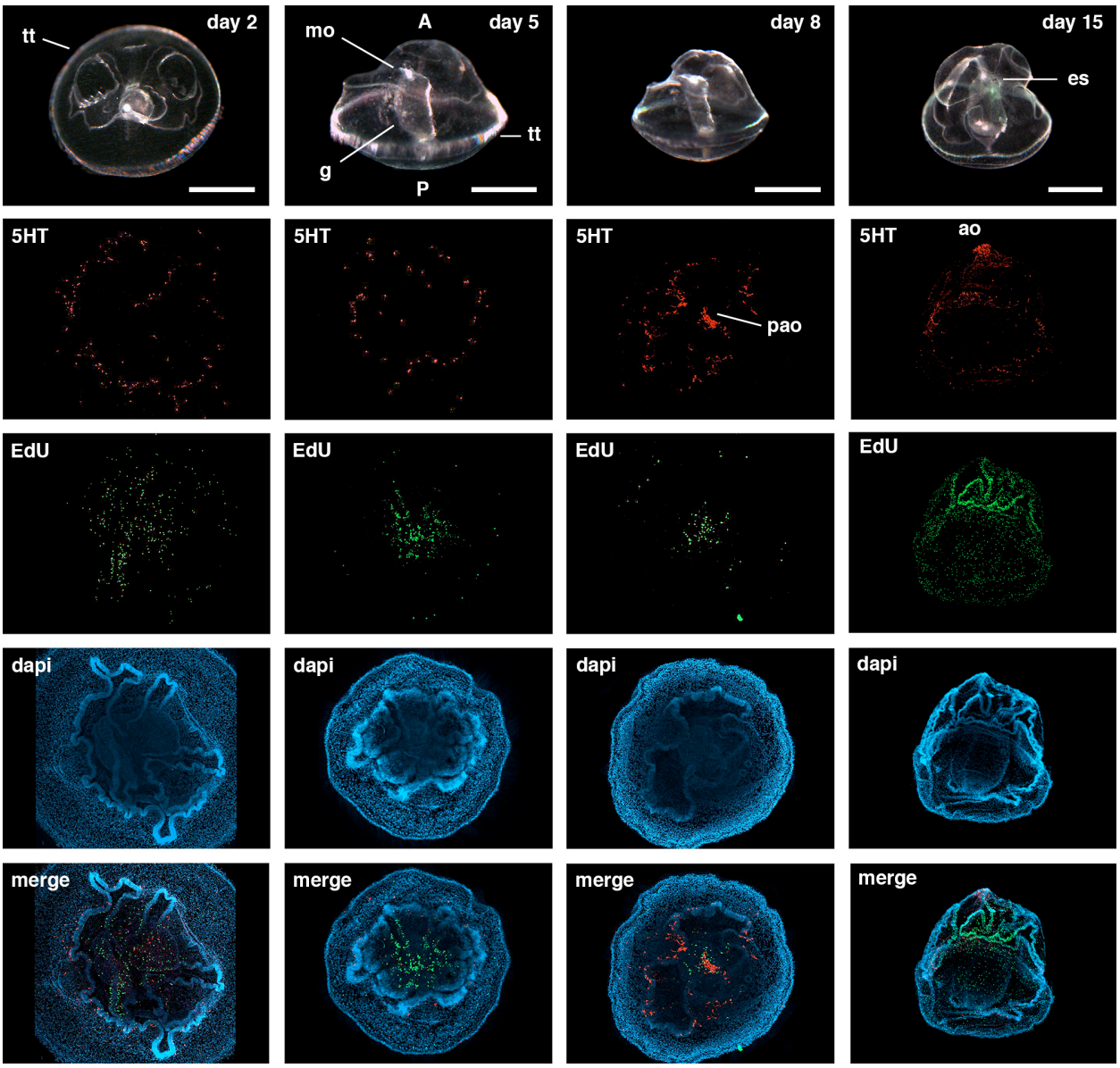

Figure 3.7. Anterior regeneration in Krohn stage *Ptychodera flava* larvae. Columns show day two, day five, day eight, and day fifteen of regeneration post amputation of the posterior piece from Krohn stage larvae. Live animal image of day two is a top down view showing the healed cut site. Live animal images of day five, day eight, and day fifteen are lateral views with the mouth on the left and anterior to the top. Serotonin, or 5-hydroxytryptamine (5HT), shows staining of neurons in the telotroch, ciliary bands and regenerating apical organ at all time points. EdU, or 5-ethynyl-2′-deoxyuridine, shows staining of proliferating cells at all time points. Dapi stains cell nuclei. All day two, day five, and day eight stains are top down views and day fifteen stains are lateral views with anterior to the top. Scales bars are 1mm for all images. Blue = dapi; green = EdU; red = serotonin. Scales bars are 1mm for all images. A = anterior; ao = apical organ; es = eyespots; g = gut; mo = mouth; P = posterior; pao = presumptive apical organ; tt = telotroch.

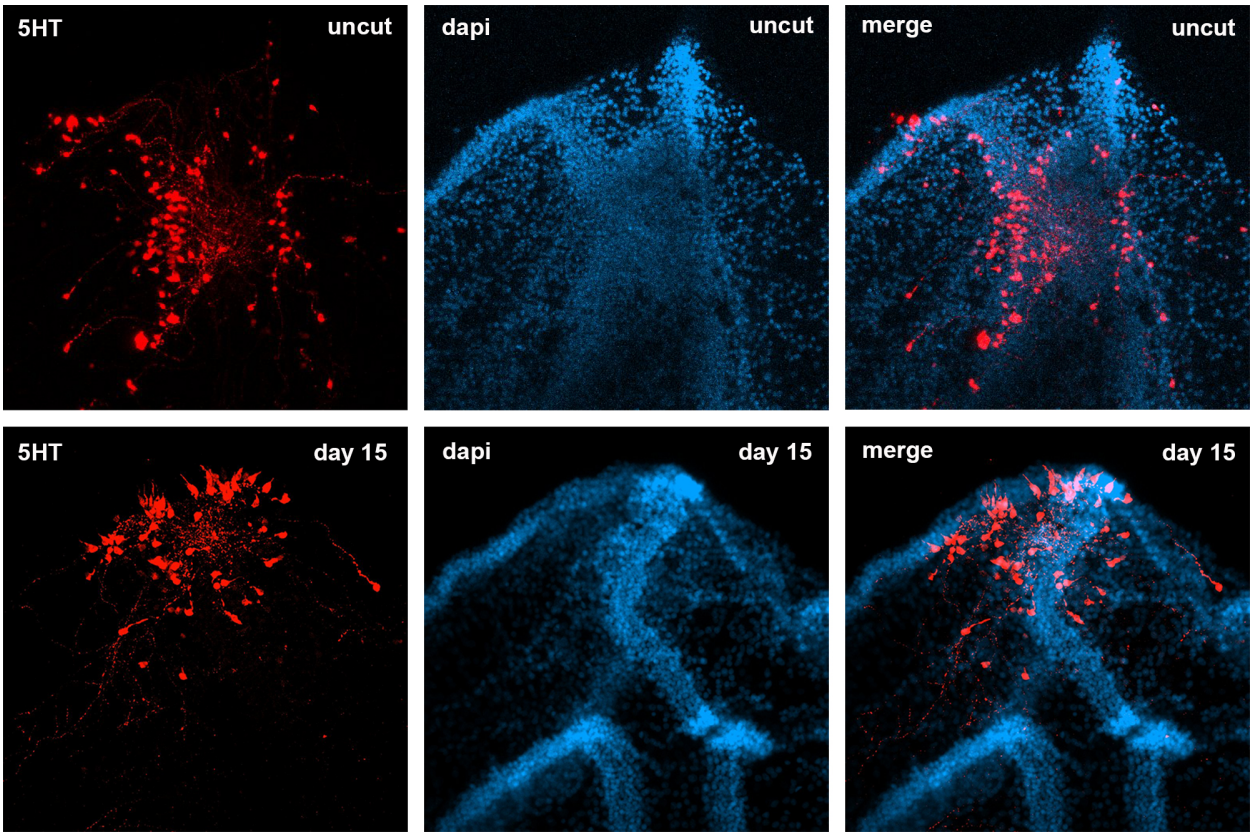

Figure 3.8. Regenerated serotonin positive cells in the apical organ. The top row shows the apical organ in an uncut Krohn stage larva stained with serotonin (5HT) and dapi marking cell nuclei. The bottom row shows serotonin positive cells in the regenerated apical organ fifteen days post amputation.

below the apical organ is required for regeneration or there is not enough energy stored in the amount of tissue remaining in the apical organ to support full posterior regeneration. Once the apical organ is removed from the larva, it does not have a mouth to feed and take in nutrients to provide energy to fuel the regeneration process. Proliferating cells are detected by EdU staining in the apical tissue from two days through fifteen days post amputation, but the amount of cell division diminishes over time. This implies that regenerative mechanisms may be activated on amputation, but as the tissue is not feeding, there is no compensation for the energetic requirements of regeneration and growth and these processes halt over time.

We also show that certain regions of the larva regenerate more efficiently than others. The dorsal half of the larva experiences reduced regeneration rates compared to the ventral half. The percentage of dorsal larval halves that regenerate a complete gut and begin feeding is nearly three fold less than ventral halves. This may indicate that having a mouth facilitates regeneration by allowing the animal to bring food into the body cavity at earlier times than the dorsal half of the larva. The gut is full of algae at seven days post bisection in some of the ventral halves of the larvae, while the dorsal half is feeding after two weeks. It is possible that bisection of the halves was not completely equal on the midline, conferring an advantage to the half with more tissue and likely, more gut present, resulting in less regeneration time to feeding. It is more likely, however, that the ventral half, by morphology (Figure 2C), has more gut tissue present than the dorsal half and therefore, requires less time to regenerate a complete gut. This results in earlier feeding times and supports the hypothesis that feeding facilitates regeneration by supplying energy to supplement the high metabolic cost of regeneration. Further support for this hypothesis can be seen in axially cut larvae.

Larvae that were bisected in the axial plane displayed the most disparate regeneration rates. Eighteen of the twenty-five posterior halves of the animal completely regenerated to form a normal, feeding larva. Many were feeding within one week and all were feeding within two weeks post amputation. All eighteen posterior halves regenerated eye spots in their apical region and displayed normal swimming behavior by twenty-eight days with most reaching this benchmark by three weeks. Posterior halves of the larvae retain the majority of the gut at bisection. They possess the mid and posterior gut and anus and, barring slight deviations from the midline during cutting, need only regenerate the anterior most part of their tripartite gut and mouth. The anterior half, on the other hand, must regenerate the mid gut, hindgut and anus in order to maximize the full benefit of feeding. Only two of the anterior halves out of twenty-five animals regenerated completely, acquiring normal morphology at the end of twenty-eight days. These two anterior halves were able to bring food into their incomplete guts at two weeks post bisection (Figure 5), which may have aided them in achieving complete regeneration. The remaining anterior halves did not feed and slowly diminished in size over time, resembling anterior apical cut tissue. While feeding seems to support robust regeneration in *P. flava* larvae, there may be other factors contributing to regeneration success.

The low regeneration rate observed in anterior halves and lack of regeneration in anterior apical fragments may also be due to the cellular composition of the tissue. We show through EdU staining that substantial cell proliferation occurs at the cut site of bisected larvae, particularly in the posterior piece. Rychel and Swalla (2008) showed that significant cell proliferation also occurs in adult *Ptychodera flava* acorn worms during anterior regeneration. It is an open question whether these dividing cells are originating from de-differentiated somatic cells that are returning to a progenitor cell state and then acquiring new cell fates in the newly

regenerated tissue or whether dividing cells are bona fide stem cells occupying an unknown niche. If the latter is true, then it is possible the larvae also possess an unknown stem cell niche, which would likely be in the posterior region of the larvae. This hypothesis would explain why anterior pieces of apical cut larvae do not regenerate and only a small fraction of the anterior pieces of axial cut larvae regenerate. It is possible that those cuts were made off center and each anterior piece retained a small portion of the posterior stem cell niche. Current work in our lab is aimed at using stem cell markers to answer this intriguing question.

Finally, we show that Krohn stage larvae display positional memory deficits during regeneration as all regenerated halves acquired morphological features of the previous developmental stage. All Krohn stage larvae completed regeneration resembling a Metchnikoff stage larva, lacking tentacular buds on the ciliary bands. Collar and trunk coeloms were absent at the end of twenty-eight days. They retained the protocoel, though not well developed in many specimens. Also, the final regeneration size of every larva was significantly smaller than the animal prior to cutting. This size difference can be explained by a lack of feeding during the early stages of regeneration. Adult acorn worms display the same size disparity after regeneration and this was attributed to a lack of feeding during the first week of regeneration after the anterior region, including the mouth and anterior gut was amputated (Luttrell et al, 2016).

Section 6: Conclusions

Krohn stage *Ptychodera flava* larvae regenerate all structures, including their nervous system, eyespots, gut, mouth, and ciliary bands. This study provides a framework for future research aimed at uncovering the cell types and genetic mechanisms underlying the regeneration

program in this basal deuterostome. Adult *P. flava* acorn worms also regenerate, however their large size and opacity makes them difficult to use in a variety of molecular assays. Sectioning is required to detail internal molecular markers and even then it is difficult to gain a clear picture of what is happening throughout all tissues. These obstacles can now be overcome by using the larvae to investigate regenerative mechanisms. Their tiny size means a smaller amount of reagents can be used resulting in lower experimental cost. More importantly, the larvae are transparent and easy to image using confocal microscopy. In situ hybridization protocols and many other techniques have been published for the larvae and the signal is easy to detect because of their clear tissues. Drug trials aimed at inhibiting regeneration to detect required genetic pathways are more feasible with the larvae as they require considerably less volume to submerge. Culturing techniques have been established for the larvae and therefore, they can easily be kept healthy and maintained in a small area of the lab for the duration of the larval stage. Methods to induce metamorphosis have proven highly successful and therefore, the larvae provide a system to study regeneration through all life stages in the lab. The *P. flava* model has the potential to reveal key molecular and genetic mechanisms underlying regeneration in the deuterostomes. The relatively simple body plan and tissue architecture of the larva compared to the adult will undoubtedly simplify future regeneration studies.

Section 7: Acknowledgements

We thank Dr. Yi-Hsien Su of Academia Sinica for providing tornaria larvae and care and maintenance protocols. We thank Drs. Olivia Bermingham McDonogh and Sharlene Santana of the University of Washington for their helpful comments on the manuscript. Drs. James Truman and Lynn Riddiford generously provided help with antibody staining

techniques and allowed us to use their Zeiss LSM800 confocal microscope. This material is based upon work supported by the National Science Foundation Graduate Research Fellowship Program, Grant number 1256082 to Shawn Luttrell, and BEACON NSF Science and Technology Center, Grant number 948, to Shawn Luttrell and Billie J. Swalla.

REFERENCES

Abitua PB, Wagner E, Navarrete IA, Levine M. (2012). Identification of a rudimentary neural crest in a non-vertebrate chordate. *Nature*. 492(7427): 104-107.

Adamska M, Matus DQ, Adamski M, Green K, Rokhsar DS, Martindale MQ, Degnan BM. (2007). The evolutionary origin of hedgehog proteins. *Curr Biol* 17: R836–R837.

Agata K, Saito Y, Nakajima E. (2007). Unifying principles of regeneration I: Epimorphosis versus morphallaxis. *Dev. Growth Diff*. 49: 73-78.

Alexa A, Rahnenfuhrer J. (2010). topGO: enrichment analysis for gene ontology. R package version 2.20.0.

Altaba A, Jessel TM, Roelink H. (1995). Restrictions to floor plate induction by hedgehog and winged-helix genes in the neural tube of frog embryos. *Mol Cell Neurosci* 6:106–121.

Alvarado AS. (2000). Regeneration in the metazoans: why does it happen? *Bioessays* 22: 578–590.

Arimoto A, Tagawa K. (2015). Hedgehog expression during development and regeneration in the hemichordate, *Ptychodera flava. Zoolog Sci* 32:33–37.

Aronowicz J, Lowe CJ. (2006). Hox gene expression in the hemichordate *Saccoglossus kowalevskii* and the evolution of deuterostome nervous systems. *Integr Comp Biol*. 46(6): 890-901.

Augustine GJ. (2001). How does calcium trigger neurotransmitter release? *Curr Opin Neurobiol* 11: 320–326.

Bai JH, Wang P, Chapman ER. (2002). C2A activates a cryptic Ca2+-triggered membrane penetration activity within the C2B domain of synaptotagmin I. *Proc Natl Acad Sci USA* 99: 1665–1670.

Balser EJ, Ruppert EE. (1990). Structure, ultrastructure, and function of the preoral heart-kidney in *Saccoglossus kowalevskii* (Hemichordata, Enteropneusta) including new data on the stomochord. *Acta Zool*. 71: 235-249.

Bardet SM, Ferran JL, Sanchez-Arrones L, Puelles L. (2010). Ontogenetic expression of sonic hedgehog in the chicken subpallium. *Front Neuroanat*. 4(28): 1-21.

Bassham S, Postlethwait JH. (2005). The evolutionary history of placodes: a molecular genetic investigation of the larvacean urochordate *Oikopleura dioica*. *Development* 132: 4259-4572.

Beattie BS, Bresnahan JC, Lopate G. (1990). Metamorphosis alters the response to spinal cord transection in *Xenopus laevis* frogs. *J. Neurobiol*. 21: 1108–1122.

Bely AE, Nyberg KG. (2010). Evolution of animal regeneration: reemergence of a field. *Trends Ecol Evol* 25: 161–170.

Benito J, Pardos F. (1997). Hemichordata. In: F Harrison F, Ruppert E, editors. Microscopic anatomy of invertebrates, Vol. 15, New York: Wiley-Liss. p 15–101.

Blair JE, Hedges SB. (2005). Molecular phylogeny and divergence times of deuterostome animals. *Mol Biol Evol*. 22: 2275-2284.

Bourlat SJ, Juliusdottir T, Lowe CJ, Freeman R, Aronowicz J, Kirschner M, Lander ES, Thorndyke M, Nakano H, Kohn AB, Heyland A, Moroz L, Copley RR, Telford MJ, (2006). Deuterostome phylogeny reveals monophyletic chordates and the new phylum Xenoturbellida. *Nature*. 444(7115): 85-8.

Bosch TCG. (2007). Why Polyps regenerate and we don't: towards a cellular and molecular framework for *Hydra* regeneration. *Dev Biol* 303: 421–433.

Briscoe J, Sussel L, Serup P, Hartigan-O'Connor D, Jessell TM, Rubenstein JL, Ericson J. (1999). Homeobox gene *Nkx2.2* and specification of neuronal identity by graded Sonic hedgehog signaling. *Nature* 398: 622–627.

Brown FD, Keeling EL, Le AD, Swalla BJ. (2009). Whole body regeneration in a colonial ascidian, *Botrylloides violaceus*. *J. Exp. Zool. B Mol. Dev. Evol*. 312B(8): 885-900.

Brown FD, Prendergast A, Swalla BJ. (2008). Man is but a worm: Chordate origins. *Genesis*. 46(11): 605-613.

Brown RC, Lockwood AH, Sonawane BR. (2005). Neurodegenerative diseases: an overview of environmental risk factors. Environ Health Perspect. 113(9): 1250-1256.

Burke R, Osborne L, Wang D, Murabe N, Yaguchi S, Nakajima Y. (2006). Neuron-specific expression of a *synaptotagmin* gene in the sea urchin *Strongylocentrotus purpuratus*. *J of Comp Neuro.* 496(2): 244-51.

Byrne M, Nakajima Y, Chee F, Burke R. (2007). Apical organs in echinoderm larvae: Insights into larval evolution in the Ambulacraria. *Evo Dev*. 9(5): 432-45.

Cameron CB, Garey JR, Swalla BJ. (2000). Evolution of the chordate body plan: new insights from phylogenetic analyses of deuterostome phyla. *Proc. Natl. Acad. Sci*. USA 97: 4469–4474.

Cameron RA, Rowen L, Nesbitt R, Bloom S, Rast J, Berney K, Arenas-Mena C, Martinez P, Lucas S, Richardson PM, Davidson EH, Peterson KJ, Hood L. (2006). Unusual gene order and organization of the sea urchin Hox cluster. *J. Exp. Zoolog. B Mol. Dev. Evol*. 306: 45-58.

Candia Carnevali MD. (2006). Regeneration in echinoderms: Repair, regrowth, cloning. *Invert Surv J*. 3: 64-76.

Candia Carnevali MD, Thorndyke MR, Matranga V. (2009). Regenerating in echinoderms: A promise to understand stem cells potential. In: Rinkevich R, Matranga V. (eds) Stem Cells in Marine Organisms. Springer, New York.

Camacho C, Coulouris G, Avagyan V, Ma N, Papadopoulos J, Bealer K, Madden TL. (2008). BLAST+: architecture and applications. *BMC Bioinformatics* 10: 421. PubMed

Chernoff EAG. (1996). Spinal cord regeneration: a phenomenon unique to urodeles? *Int. J. Dev. Biol.* 40: 823-831.

Chernoff EA, Sato K, Corn A, Karcavich RE. (2002). Spinal cord regeneration: intrinsic properties and emerging mechanisms. *Semin Cell Dev Biol*. 13(5): 361-368.

Chen SH, Li KL, Lu IH, Wang YB, Tung CH, Ting HC, Lin CY, Lin CY, Su YH, Yu JK. (2014). Sequencing and analysis of the transcriptomes of the acorn worm *Ptychodera flava*, an indirect developing hemichordate. *Mar Genomics* 15: 35–43.

Dahlberg C, Auger H, Dupont S, Sasakura Y, Thorndyke M, Joly J-S. (2009). Refining the *Ciona intstinalis* model of central nervous system regeneration. *PLoS ONE* 4(2): e4458. doi:10.1371/journal.pone.0004458.

Dahia CL, Mahoney EJ, Durrani AA, Wylie C. (2011). Intercellular signaling pathways active during and after growth and differentiation of the lumbar vertebral growth plate. *Spine* (Phila Pa 1976), 36(14): 1071-1080.

Dahia CL, Mahoney E, Wylie C. (2012). *Shh* signaling from the nucleus pulposus is required for the postnatal growth and differentiation of the mouse intervertebral disc. *PLoS One*. 7(4): e35944.

D'Ancona Lunetta G. (2009). Stem cells in *Holothuria polii* and *Sipunculus nudus*. In: Rinkevich R, Matranga V. (eds) Stem Cells in Marine Organisms. Springer, New York.

Dawydoff C. (1902). Utber die Regeneration der Eichel bei den Enteropneusten. *Zool. Anz*. 25: 551-556.

Davidson EH, Erwin DH. (2006). Gene regulatory networks and the evolution of animal body plans. Science. 311, 796-800.

Dehal P. et al., (2002). The draft genome of *Ciona intestinalis*: insights into chordate and vertebrate origins. *Science*. 298(5601): 2157-67.

Dehal P, Boore J. (2005). Two rounds of whole genome duplication in the ancestral vertebrate. *Plos Biol* 3: 1700–1708.

Delsuc F, Brinkmann H, Chourrout D, Philippe H. (2006). Tunicates and not cephalochordates are the closest living relatives of vertebrates. *Nature*. 439: 965-968.

Denoeud F. et al., (2010). Plasticity of animal genome architecture unmasked by rapid evolution of a pelagic tunicate. *Science*. 330(6009): 1381-1385.

Dubuc TQ, Traylor-Knowles N, Martindale MQ. (2014). Initiating a regenerative response, cellular and molecular features of wound healing in the cnidarian *Nematostella vectensis*. *BMC Biol* 12: 24.

Duffy MT, Liebich DR, Garner LK, Hawrych A, Simpson Jr. SB, Davis BM. (1992). Axonal sprouting and frank regeneration in the lizard tail spinal cord: correlation between changes in synaptic circuitry and axonal growth. *J. Comp. Neurol*, 316: 363–374.

Echevarria D, Vieira C, Gimeno L, Martinez S. (2003). Neuroepithelial secondary organizers and cell fate specification in the developing brain. *Brain Res Brain Res Rev* 43: 179–191.

Eddy SR. (2011). Accelerated profile HMM searches. *PLoS Comp Biol* 7: e1002195.

Eschscholtz F. (1825). Bericht über die zoologische Ausbeute während der Reise von Kronstadt bis St. Peter und Paul. Isis 733–747. Available at http://www.biodiversitylibrary.org/item/87983#page/403/mode/1up.

Finn RD, Bateman A, Clements J, Coggill P, Eberhardt RY, Eddy SR, Heger A, Hetherington K, Holm L, Mistry J, Sonnhammer ELL, Tate J, Punta M. (2014). Pfam: the protein families database. *Nucleic Acids Res* 42: D222–D230.

Freeman R, Ikuta T, Wu M, Koyanagi R, Kawashima T, Tagawa K, Humphreys T, Fang GC, Fujiyama A, Saiga H, Lowe C, Worley K, Jenkins J, Schmutz J, Kirschner M, Rokhsar D, Satoh N, Gerhart J. (2012). Identical genomic organization of two hemichordate *Hox* clusters. *Curr Biol*. 22(21): 2053-8.

Freeman RM Jr., Wu M, Cordonnier-Pratt MM, Pratt LH, Gruber CE, Smith M, Lander ES, Stange-Thomann N, Lowe CJ, Gerhart J, Kirschner M. (2008). cDNA sequences for transcription factors and signaling proteins of the hemichordate *Saccoglossus kowalevskii*: efficacy of the expressed sequence tag (EST) approach for evolutionary and developmental studies of a new organism. *Biol Bull*. 214(3): 284-302.

Fong JH, Murphy TD, Pruitt KD. (2013). Comparison of RefSeq protein-coding regions in human and vertebrate genomes. *BMC Genomics*. 14(1): 654.

Gans C, Northcutt RG. (1983). Neural crest and the origin of vertebrates: a new head. *Science*. 220: 268-274.

Garner S, Zysk I, Byrne G, Kramer M, Moller D, Taylor V, Burke RD. (2016). Neurogenesis in sea urchin embryos and the diversity of deuterostome neurogenic mechanisms. *Development* 143(2): 286-97. doi: 10.1242/dev.124503.

Garstang W. (1928). The morphology of the Tunicata and its bearing on the phylogeny of the Chordata. *Q. J. Micro. Sci*. 72: 51-187.

Gee H. Before the Backbone. Views on the Origin of the Vertebrates. (Chapman and Hall, London, 1996).

Gene Ontology C. (2015). Gene Ontology Consortium: going forward. *Nucleic Acids Res* 43: D1049–D1056.

Gerhart J, Lowe C, Kirschner M. (2005). Hemichordates and the origin of chordates. *Curr. Opin. Genet. Dev.* 15: 461-467.

Ghosh S, Hui SP. (2016). Regeneration of zebrafish CNS: adult neurogenesis. *Neural Plasticity*. 2016: ID 5815439. doi:10.1155/2016/5815439

Giangrande A, Licciano M. (2014). Regeneration and clonality in Metazoa. The price to pay for evolving complexity. *Invertebr Reprod Dev* 58: 1–8.

Gillis AJ, Fritzenwanker JH, Lowe CJ. (2012). A stem-deuterostome origin of the vertebrate pharyngeal transcriptional network. *Proc. R. Soc. B.* 279: 237-246.

Grabherr MG, Haas BJ, Yassour M, Levin JZ, Thompson DA, Amit I, Adiconis X, Fan L, Raychowdhury R, Zeng Q, Chen Z, Mauceli E, Hacohen N, Gnirke A, Rhind N, di Palma F, Birren BW, Nusbaum C, Lindblad-Toh K, Friedman N, Regev A. (2011). Fulllength transcriptome assembly from RNA-seq data without a reference genome. *Nat Biotechnol* 29: 644–652.

Hadfield MG. (1978). Growth and metamorphosis of planktonic larvae of *Ptychodera flava* (Hemichordata: Enteropneusta). In: Chia FS, Rice ME, editors. Settlement and metamorphosis of marine invertebrate larvae. New York: Elsevier. p 247–254.

Halanych KM. (2004). The new view of animal phylogeny. *Ann. Rev. Ecol. Evol. Syst*. 35: 229-256.

Hall BK, Gillis JA. (2013). Incremental evolution of the neural crest, neural crest cells and neural crest-derived skeletal tissues. *J Anat*. 222(1): 19-31.

Holland L, Carvalho J, Escriva H, Laudet V, Schubert M, Shimeld SM, Yu J. (2013). Evolution of bilaterian central nervous systems: a single origin? *Evodevo* 4: 27.

Holland ND, Holland LZ. (1995). An amphioxus Pax gene, *AmphiPax-1*, expressed in embryonic endoderm, but not in mesoderm: implications for the evolution of class I paired box genes. *Mol. Mar. Biol. Biotech*. 4: 206-214.

Holland PW, Koschorz B, Holland LZ, Herrmann BG. (1995). Conservation of *Brachyury (T)* genes in amphioxus and vertebrates: developmental and evolutionary implications. *Development*. 121: 4283-4291.

Horie T, Shinki R, Ogura Y, Kusakabe TG, Satoh N, Sasakura Y. (2011). Ependymal cells of chordate larvae are stem-like cells that form the adult nervous system. *Nature* 469: 525–528.

Houart C, Caneparo L, Heisenberg C, Barth K, Take-Uchi M, Wilson SW. (2002). Establishment of the telencephalon during gastrulation by local antagonism of *Wnt* signaling. *Neuron* 35: 255–265.

Huangfu D, Anderson KV. (2006). Signaling from *Smo* to *Ci/Gli*: conservation and divergence of Hedgehog pathways from *Drosophila* to vertebrates. *Development* 133: 3–14.

Hughes T, Liberles D. (2008). Whole-genome duplications in the ancestral vertebrate are detectable in the distribution of gene family sizes of tetrapod species. *J Mol Evol* 67: 343–357.

Humphreys T, Sasaki A, Uenishi G, Taparra K, Arimoto A, Tagawa K. (2010). Regeneration in the hemichordate *Ptychodera flava*. *Zoolog Sci*. 27(2): 91-95.

Hyman LH. (1959). Hemichordata. In "The Invertebrates: Smaller Coelomate Groups". pp. 72-207. McGraw–Hill, New York.

Jeffery W. (2014). The tunicate *Ciona*: A model system for understanding the relationship between regeneration and aging. *Invertebrate Reproduction & Development,* 1-6.

Jeffery WR. (2012). Siphon regeneration capacity is compromised during aging in the ascidian *Ciona intestinalis*. *Mech Ageing Dev*. 133(9-10): 629-36.

Jeffery WR, Chiba T, Krajka FR, Deyts C, Satoh N, Joly JS. (2008). Trunk lateral cells are neural crest-like cells in the ascidian *Ciona intestinalis*: insights into the ancestry and evolution of the neural crest. *Dev Biol*. 324(1): 152-160.

Jeffries RPS. (1986). "The Ancestry of Vertebrates". British Museum of Natural History, London.

Jollie M. (1973). The origin of the chordates. *Acta. Zool*. 54: 81-100.

Kassmer, Rodriguez, De Tomaso. (2016). Colonial ascidians as model organisms for the study of germ cells, fertility, whole body regeneration, vascular biology and aging. *Current Opinion in Genetics & Development*, 39: 101-106.

Katsuyama Y, Matsumoto J, Okada T, Ohtsuka Y, Chen L, Okado H, Okamura Y. (2002). Regulation of *synaptotagmin* gene expression during ascidian embryogenesis. *Dev Biol* 244: 293–304.

Kaul S, Stach T. (2010). Ontogeny of the collar cord: neurulation in the hemichordate *Saccoglossus kowalevskii*. *J Morphol* 271: 1240–1259.

Kaul-Strehlow S, Stach T. (2013). A detailed description of the development of the hemichordate *Saccoglossus kowalevskii* using SEM, TEM, histology and 3D-reconstructions. *Front Zool* 10: 53.

Kaul-Strehlow S, Urata M, Minokawa T, Stach T, Wanninger A. (2015). Neurogenesis in directly and indirectly developing enteropneusts: of nets and cords. *Org Divers Evol* 15: 405–422.

Kizil C, Kaslin J, Kroehne V, Brand M. (2012), Adult neurogenesis and brain regeneration in zebrafish. *Devel Neurobio*. 72: 429–461. doi:10.1002/dneu.20918.

Kolde R. (2013). pheatmap: pretty heatmaps. R package version 0.7.7. Available at: http://CRAN.R-project.org/package¼pheatmap.

Krogh A, Larsson B, von Heijne G, Sonnhammer ELL. (2001). Predicting transmembrane protein topology with a hidden Markov model: application to complete genomes. *J Mol Biol* 305: 567–580.

Kroehne V, Freudenreich D, Hans S, Kaslin J, Brand M. (2011). Regeneration of the adult zebrafish brain from neurogenic radial glia-type progenitors. *Development* 138: 4831–4841

Lacalli TC. (2005). Protochordate body plan and the evolutionary role of larvae: old controversies resolved? *Can. J. Zool*. 83: 216-224.

Langmead B, Salzberg S. (2012). Fast gapped-read alignment with Bowtie 2. *Nat Methods* 9: 357–359.

Lau BYB, Fogerson SM, Walsh RB, Morgan JR. (2013). Cyclic AMP promotes axon regeneration, lesion repair and neuronal survival in lampreys after spinal cord injury. *Exp Neurol* 250: 31–42.

Li H, Handsaker B, Wysoker A, Fennell T, Ruan J, Homer N, Marth G, Abecasis G, Durbin R, 1000 Genome Project Data Processing Subgroup. (2009). The Sequence alignment/map (SAM) format and SAMtools. *Bioinformatics* 25: 2078–2079.

Lin CY, Tung CH, Yu JK, Su YH. (2016). Reproductive periodicity, spawning induction, and larval metamorphosis of the hemichordate acorn worm *Ptychodera flava*. *J Exp Zool B Mol Dev Evol* 326: 47–60.

Littleton JT, Stern M, Schulze K, Perin M, Bellen HJ. (1993). Mutational analysis of *Drosophila* synaptotagmin demonstrates its essential role in Ca2+-activated neurotransmitter release. Cell 74: 1125–1134.

Love MI, Huber W, Anders S. (2014). Moderated estimation of fold change and dispersion for RNA-seq data with DESeq2. *Genome Biol* 15: 550.

Lowe CJ, Terasaki M, Wu M, Freeman RM Jr., Runft L, Kwan K, Haigo S, Aronowicz, J, Lander E, Gruber C, Smith M, Kirschner M, Gerhart J. (2006). Dorsoventral patterning in hemichordates: insights into early chordate evolution. *PLoS Biol*. 4(9): e291.

Lowe CJ, Wu M, Salic A, Evans L, Lander E, Stange-Thomann N, Gruber CE, Gerhart J, Kirschner M. (2003). Anteroposterior patterning in hemichordates and the origins of the chordate nervous system. *Cell*. 113: 853-65.

Lupas A, Van Dyke M, Stock J. (1991). Predicting coiled coils from protein sequences. *Science* 252: 1162–1164.

Luttrell SM, Gotting K, Ross E, Alvarado AS, Swalla BJ. (2016). Head regeneration in hemichordates is not a strict recapitulation of development. *Dev Dynamics* 245: 1159-1175.

Luttrell S, Konikoff C, Byrne A, Bengtsson B, Swalla B. (2012). Ptychoderid hemichordate neurulation without a notochord. *Integr Comp Biol* 52: 829–834.

Luttrell SM, Swalla BJ. (2014). Genomic and evolutionary insights into chordate origins. In: Moody S, editor. "Principles of Developmental Genetics", 2nd ed. San Diego: Elsevier. p 116–126.

Mahabaleshwarkar R, Khanna R. (2014). National hospitalization burden associated with spinal cord injuries in the United States. *Spinal Cord* 52: 139–144.

Manni L, Agnoletto A, Zaniolo G, Burighel P. (2005). Stomodeal and neurohypophysial placodes in *Ciona intestinalis*: Insights into the origin of the pituitary gland. *J of Exp Zool Part B: Mol and Dev Evol,* 304(4), 324-339

Manni L, Lane NJ, Joly JS, Gasparini F, Tiozzo S, Caicci F, Zaniolo G, Burighel P. (2004). Neurogenic and non-neurogenic placodes in ascidians. *J. Exp. Zool. B Mol. Dev. Evol*. 302: 483-504.

Martí E. (2000). Expression of chick *BMP-1/Tolloid* during patterning of the neural tube and somites. *Mech. Dev*. 91: 415-9.

Mashanov VS, Zueva OR, Heinzeller T. (2008). Regeneration of the radial nerve cord in a holothurian: A promising new model system for studying post-traumatic recovery in the adult nervous system. *Tissue and Cell*, 40(5): 351-372.

Mashanov VS, Zueva OR, Heinzeller T, Aschauer B, Dolmatov IY. (2007). Developmental origin of the adult nervous system in a holothurian: an attempt to unravel the enigma of neurogenesis in echinoderms. Evol & Dev. 9: 244–256.

Matthysse AG, Deschet K, Williams M, Marry M, White AR, Smith WC. (2004). A functional cellulose synthase from ascidian epidermis. *Proc Natl Acad Sci*.101(4): 986-91.

Mazet F. (2002). The Fox and the thyroid: the amphioxus perspective. *Bioessays*. 24: 696-699.

Mazet F, Hutt JA, Milloz J, Millard J, Graham A, Shimeld SM. (2005). Molecular evidence from *Ciona intestinalis* for the evolutionary origin of vertebrate sensory placodes. *Develop. Biol*. 282: 494-508.

Méndez AT, Roig-López JL, Santiago P, Santiago C, García-Arrarás JE. (2000). Identification of *Hox* Gene Sequences in the Sea Cucumber *Holothuria glaberrima* Selenka (Holothuroidea: Echinodermata). *Mar Biotechnol*. 2(3): 231-240.

Minsuk SB, Andrews ME, Raff RA. (2005). From larval bodies to adult body plans: patterning the development of the presumptive adult ectoderm in the sea urchin larva. *Dev Genes Evol*. 215(8): 383-92.

Mito T, Endo K. (2000). PCR survey of *Hox* genes in the crinoid and ophiuroid: evidence for anterior conservation and posterior expansion in the echinoderm *Hox* gene cluster. *Mol Phylogenet Evol*. 14(3): 375-88.

Miyamoto N, Saito Y. (2010). Morphological characterization of the asexual reproduction in the acorn worm *Balanoglossus simodensis*. *Dev Growth Differ* 52: 615–627.

Miyamoto N, Nakajima Y, Wada H, Saito Y. (2010). Development of the nervous system in the acorn worm *Balanoglossus simodensis*: insights into nervous system evolution. *Evol Dev* 12: 416–424.

Miyamoto N, Wada H. (2013). Hemichordate neurulation and the origin of the neural tube. *Nature Communications* 4: 2713 1-8.

Moody S, Saint-Jeannet JP. (2014). Genomic and evolutionary insights into chordate origins. In: Moody S, editor. “Principles of Developmental Genetics”, 2nd ed. San Diego: Elsevier. p 331-349.

Morgan T. (1894). The development of *Balanoglossus*. *J Morphol* 9: 1–86.

Morgan TH. (1898). Experimental studies of the regeneration of *Planaria maculate*. *Arch Entw Mech Org*. 7: 364-397.

Morgan TH. (1901). Regeneration. The Macmillan Company, New York.

Moroz LL, Kocot KM, Citarella MR, Dosung S, Norekian TP, Povolotskaya IS, Grigorenko AP, Dailey C, Berezikov E, Buckley KM, Ptitsyn A, Reshetov D, Mukherjee K, Moroz TP, Bobkova Y, Yu F, Kapitonov VV, Jurka J, Bobkov YV, Swore JJ, Girardo DO, Fodor A, Gusev F, Sanford R, Bruders R, Kittler E, Mills CE, Rast JP, Derelle R, Solovyev VV, Kondrashov FA, Swalla BJ, Sweedler JV, Rogaev EI, Halanych KM, Kohn AB. (2014). The ctenophore genome and the evolutionary origins of neural systems. *Nature* 510: 109–114.

Morris VB, Byrne M. (2005). Involvement of two *Hox* genes and *Otx* in echinoderm body-plan morphogenesis in the sea urchin *Holopneustes purpurescens*. *J. Exp. Zool. B Mol. Dev. Evol*. 304: 456-467.

Nakajima Y, Humphreys T, Kaneko H, Tagawa K. (2004). Development and neural organization of the Tornaria larva of the Hawaiian hemichordate, *Ptychodera flava*. *Zool Sci*, 21(1): 69-78.

Nakashima K, Sugiyama J, Satoh N. (2008). A spectroscopic assessment of cellulose and the molecular mechanisms of cellulose biosynthesis in the ascidian *Ciona intestinalis*. *Mar Genomics*. 1(1): 9-14.

Neubüser A, Koseki H, Balling R. (1995). Characterization and developmental expression of *Pax 9*, a paired-box-containing gene related to *Pax1*. *Develop. Biol*. 170: 701-716.

Nielsen C, Hay-Schmidt A. (2007). Development of the Enteropneust *Ptychodera flava*: ciliary bands and nervous system. *J Morphol* 268: 551–570.

Nishida H. (2005). Specification of embryonic axis and mosaic development in ascidians. *Dev. Dynamics* 233: 1177-1193.

Nishikawa T. (1977). Preliminary report on the biology of the enteropneust, *Ptychodera flava* Eschscholtz, in the vicinity of Kushimoto, Japan. *Publ Seto Marine Biol Lab* 23: 393–419.

Nonet ML, Grundahl K, Meyer BJ, Rand JB. (1993). Synaptic function is impaired but not eliminated in *C-elegans* mutants lacking synaptotagmin. *Cell.* 73: 1291–1305.

Norenburg JL, Barrett JM. (1987). Steedman's polyester wax embedment and deembedment for combined light and scanning electron microscopy. *J Electron Microsc Tech* 6: 35–41.

Ogasawara M, Wada H, Peters H, Satoh N. (1999). Developmental expression of *Pax1/9* genes in urochordate and hemichordate gills: insight into function and evolution of the pharyngeal epithelium. *Development*. 126: 2539-2550.

Ogasawara M, Shigetani Y, Hirano S, Satoh N, Kuratani S. (2000a). *Pax1/Pax9*-related genes in an agnathan vertebrate, *Lampetra japonica*: expression pattern of *LjPax9* implies sequential evolutionary events toward the gnathostome body plan. *Develop. Biol*. 223: 399-410.

Ogasawara M, Shigetani Y, Suzuki S, Kuratani S, Satoh N. (2000b). Expression of thyroid transcription factor (*TTF-1*) gene in the ventral forebrain and endostyle of the agnathan vertebrate, *Lampetra japonica*. *Genesis*. 30: 51-58.

Paek H, Gutin G, Hebert JM. (2009). FGF signaling is strictly required to maintain early telencephalic precursor cell survival. *Development* 136: 2457–2465.

Pani AM, Mullarkey EE, Aronowicz J, Assimacopoulos S, Grove EA, Lowe CJ. (2012). Ancient deuterostome origins of vertebrate brain signalling centres. *Nature*. 483(7389): 289-94.

Pascual-Anaya J, Aniello SD, Kuratani S, Garcia-Fernàndez J. (2013). Evolution of *Hox* gene clusters in deuterostomes. *BMC Dev. Biol*. 13(1): 26.

Passamaneck YJ, Di Gregorio A. (2005). *Ciona intestinalis*: Chordate development made simple. *Develop. Dynamics* 233: 1-19.

Peters H, Neubüser A, Kratochwil K, Balling R. (1998). *Pax9*-deficient mice lack pharyngeal pouch derivatives and teeth and exhibit craniofacial and limb abnormalities. *Genes Dev*. 12: 2735-2747.

Petersen TN, Brunak S, von Heijne G, Nielsen H. (2011). SignalP 4.0: discriminating signal peptides from transmembrane regions. *Nat Methods* 8: 785–786.

Peterson KJ. (2004). Isolation of *Hox* and *Parahox* genes in the hemichordate *Ptychodera flava* and the evolution of deuterostome *Hox* genes. *Mol. Phy. Evol*. 31: 1208-1215.

Peterson KJ, Cameron RA, Tagawa K, Satoh N, Davidson EH. (1999). A comparative molecular approach to mesodermal patterning in basal deuterostomes: the expression pattern of *Brachyury* in the enteropneust hemichordate *Ptychodera flava*. *Development.* 126: 85-95.

Poss KD. (2010). Advances in understanding tissue regenerative capacity and mechanisms in animals. *Nat Rev Genet* 11: 710–722.

Presnell JK, Schreibman MP. (1997). Humason's animal tissue techniques. Baltimore: Johns Hopkins University Press. p. 572.

Putnam NH et al., (2008). The amphioxus genome and the evolution of the chordate karyotype. *Nature.* 453: 1064-1071.

Rando TA, Wyss-Coray T. (2014). Stem cells as vehicles for youthful regeneration of aged tissues. *J Gerontol A Biol Sci Med Sci* 69: S39–S42.

Rao K. (1954). The early development of an Enteropneusta *Ptychodera flava* Eschsholtz. *J Zool Soc India* 6: 145–152.

Rickmann M, Fawcett J, Keynes R. (1985). The migration of neural crest cells and the growth of motor axons through the rostral half of the chick somite. *J Embryol Exp Morphol* 90: 437–55.

Rink JC, Gurley KA, Elliott SA, Alvarado AS. (2009). Planarian Hh signaling regulates regeneration polarity and links Hh pathway evolution to cilia. *Science* 326: 1406–1410.

Rinkevich Y, Rosner A, Rabinowitz C, Lapidot Z, Moiseeva E, Rinkevich B. (2010). Piwi positive cells that line the vasculature epithelium, underlie whole body regeneration in a basal chordate. *Dev Biol*, 345(1): 94-104.

Romer AS. (1967). Major steps in vertebrate evolution. *Science.* 158: 1629-1637.

Röttinger E, Lowe CJ. (2012). Evolutionary crossroads in developmental biology: hemichordates. *Development*. 139(14): 2463-75.

Röttinger E, Martindale MQ. (2011). Ventralization of an indirect developing hemichordate by $NiCl_2$ suggests a conserved mechanism of dorso-ventral (D/V) patterning in Ambulacraria (hemichordates and echinoderms). *Dev Biol* 354: 173–190.

Ruppert EE, Cameron CB, Frick JE. (1999). Endostyle-like features of the dorsal epibranchial ridge of an enteropneust and the hypothesis of dorsal-ventral axis inversion in chordates. *Invert. Biol*. 118: 202-212.

Ruppert EE. (2005). Key characters uniting hemichordates and chordates: homologies or homoplasies? *Can. J. Zool*. 83: 8-23.

Ryan JF, Pang K, Schnitzler CE, Nguyen AD, Moreland RT, Simmons DK, Koch BJ, Francis WR, Havlak P, Smith SA, Putnam NH, Haddock SH, Dunn CW, Wolfsberg TG, Mullikin JC, Martindale MQ, Baxevanis AD. (2013). The genome of the ctenophore *Mnemiopsis leidyi* and its implications for cell type evolution. *Science* 342: 1242592.

Rychel AL, Smith SE, Shimamoto HT, Swalla BJ. (2006). Evolution and development of the chordates: Collagen and pharyngeal cartilage. *Mol. Biol. Evol*. 23: 1-9.

Rychel AL, Swalla BJ. (2007). Development and evolution of chordate cartilage. *J. Exp. Zool. Part B*. 308(3): 325-35.

Rychel AL, Swalla BJ. (2008). Anterior regeneration in the hemichordate *Ptychodera flava. Dev. Dyn*. 237(11): 3222-3232.

Salic A, Mitchison TJ. (2008). A chemical method for fast and sensitive detection of DNA synthesis in vivo. *Proc Natl Acad Sci U S A*. 105(7): 2415-20.

Sasaki A, Miyamoto Y, Satou Y, Satoh N, Ogasawara M. (2003). Novel endostyle specific genes in the ascidian *Ciona intestinalis*. *Zoolog Sci*. 20: 1025-1030.

Sasakura Y, Mita K, Ogura Y, Horie T. (2012). Ascidians as excellent chordate models for studying the development of the nervous system during embryogenesis and metamorphosis. *Dev Growth & Diff*. 54(3): 420-437.

Satoh N, Tagawa K, Lowe CJ, Yu JK, Kawashima T, Takahashi H, Ogasawara M, Kirschner M, Hisata K, Su YH, Gerhart J. (2014). On a possible evolutionary link of the stomochord of hemichordates to pharyngeal organs of chordates. *Genesis* 52: 925–934.

Schaeffer B. (1987). Deuterostome monophyly and phylogeny. *Evol. Biol*. 21: 179-235.

Schneider C, Wicht H, Enderich J, Wegner M, Rohrer H. (1999). Bone morphogenetic proteins are required in vivo for the generation of sympathetic neurons. *Neuron*. 24: 861-70.

Schultze LS. (1899). Die Regeneration des Ganglions von *Ciona intestinalis* [The regeneration of the ganglion in *Ciona intestinalis*]. *Jena Z f Naturwiss*. 33:263–344.

SeqClean. (2011). Available at: http://sourceforge.net/projects/seqclean/.

Simakov O, Kawashima T, Marletaz F, Jenkins J, Koyanagi R, Mitros T, Hisata K, Bredeson J, Shoguchi E, Gyoja F, Yue JX, Chen YC, Freeman RM Jr, Sasaki A, Hikosaka-Katayama T, Sato A, Fujie M, Baughman KW, Levine J, Gonzalez P, Cameron C, Fritzenwanker JH, Pani AM, Goto H, Kanda M, Arakaki N, Yamasaki S, Qu J, Cree A, Ding Y, Dinh HH, Dugan S, Holder M, Jhangiani SN, Kovar CL, Lee SL, Lewis LR, Morton D, Nazareth LV, Okwuonu G, Santibanez J, Chen R, Richards S, Muzny DM, Gillis A, Peshkin L, Wu M, Humphreys T, Su YH, Putnam NH, Schmutz J, Fujiyama A, Yu JK, Tagawa K, Worley KC, Gibbs RA, Kirschner MW, Lowe CJ, Satoh N, Rokhsar DS, Gerhart J. (2015). Hemichordate genomes and deuterostome origins. *Nature* 527: 459–465.

Singer M, Nordlander RH, Egar M. (1979). Axonal guidance during embryogenesis and regeneration in the spinal cord of newt: the blueprint hypothesis of neuronal pathway patterning. *J. Comp. Neurol*. 185: 1–22.

Sîrbulescu R, Zupanc G. (2011). Spinal cord repair in regeneration competent vertebrates: adult teleost fish as a model system. *Brain Res Rev* 67: 73–93.

Slack JMW, Lin G, Chen Y. (2008). The *Xenopus* tadpole: a new model for regeneration research. *Cell Mol Life Sci* 65: 54–63.

Sly BJ, Hazel JC, Popodi EM, Raff RA. (2002). Patterns of gene expression in the developing adult sea urchin central nervous system reveal multiple domains and deep-seated neural pentamery. *Evol Dev* 4: 189–204.

Sodergren et al., (2006). The genome of the sea urchin *Strongylocentrotus purpuratus*. *Science*. 314(5801): 941-952.

Somorjai IML, Somorjai RL, Garcia-Fernandez J, Escriva H. (2012). Vertebrate-like regeneration in the invertebrate chordate *amphioxus*. *Proc Natl Acad Sci USA* 109: 517–522.

Spagnuolo A, Ristoratore F, Di Gregorio A, Aniello F, Branno M, Di Lauro R. (2003). Unusual number and genomic organization of *Hox* genes in the tunicate *Ciona intestinalis*. *Gene*. 309: 71-79.

Smith AB, Peterson KJ, Wray G, Littlewood DTJ. (2004). From bilateral symmetry to pentaradiality: The phylogeny of hemichordates and echinoderms. In "Assembling the Tree of Life" (J. Cracraft and M. J. Donoghue eds), pp 365-383. Oxford Press, New York.

Smith SE, Douglas R, Da Silva KB, Swalla BJ. (2003). Morphological and molecular identification of *Saccoglossus* species (Hemichordata: Harrimaniidae) in the Pacific Northwest. *Can. J. Zool*. 81: 133-141.

Steedman HF. (1957). Polyester wax: a new ribboning embedding medium for histology. *Nature* 179: 1345.

Stocum D. (2006). Regenerative Biology and Medicine. London: Academic Press.

Swalla BJ. (2004). Protochordate gastrulation: lancelets and ascidians. In "Gastrulation" (C. Stern, ed.) pp 139-149. Cold Spring Harbor Press, New York.

Swalla BJ. (2006). Building divergent body plans with similar genetic pathways. *Heredity* 97: 235-243.

Swalla BJ. (2007). "New insights into vertebrate origins" In: Principles of Developmental Genetics, Sally Moody, ed. Elsevier Press (San Diego, Elsevier) pp. 114-128.

Swalla BJ, Cameron CB, Corley LS, Garey JR. (2000). Urochordates are monophyletic within the deuterostomes. *Syst. Biol*. 49: 122-134.

Swalla BJ, Smith AB. (2008). Deciphering deuterostomes phylogeny: molecular, morphological and palaeontological perspectives. *Phil. Trans. R. Soc. B*. 363(1496): 1557-1568.

Tagawa K, Arimito A, Sasaki A, Izumi M, Fujita S, Humphreys T, Fujiyama A, Kagoshima H, Shin-I T, Kohara Y, Satoh N, Kawashima T. (2014). A cDNA resource for gene expression studies of a hemichordate, *Ptychodera flava. Zoolog Sci* 31: 414–420.

Tagawa K, Nishino A, Satoh N, Humphreys T. (1998). The spawning and early development of the Hawaiian acorn worm (hemichordate), *Ptychodera flava*. *Zool Sci*. 15(1): 85-91.

Takacs CM, Moy VN, Peterson KJ. (2002). Testing putative hemichordate homologues of the chordate dorsal nervous system and endostyle: expression of *NK2.1* (*TTF-1*) in the acorn worm *Ptychodera flava* (Hemichordata, Ptychoderidae). *Evol. Dev*. 4: 405-417.

Takahashi K, Tanabe K, Ohnuki M, Narita M, Ichisaka T, Tomoda K, Yamanaka S. (2007). Induction of pluripotent stem cells from adult human fibroblasts by defined factors. *Cell*. 131(5): 861-72.

Theveneau E, Mayor R. (2014). Genomic and evolutionary insights into chordate origins. In: Moody S, editor. "Principles of Developmental Genetics", 2nd ed. San Diego: Elsevier. p 315–327.

Turbeville JM, Schulz JR, Raff RA. (1994). Deuterostome phylogeny and the sister group of the chordates: evidence for molecules and morphology. *Mol. Biol. Evol*. 11: 648-655.

Tsagkogeorga G, Turon X, Hopcroft RR, Tilak MK, Feldstein T, Shenkar N, Loya Y, Huchon D, Douzery EJ, Delsuc F. (2009). An updated 18S rRNA phylogeny of tunicates based on mixture and secondary structure models. *BMC Evol Biol*. 9: 187.

UniProt C. (2015). UniProt: a hub for protein information. *Nucleic Acids Res* 43: D204–D212.

Urata M, Iwasaki S, Ohtsuka S. (2012). Biology of the swimming acorn worm *Glandiceps hacksi* from the Seto Inland Sea of Japan. *Zoolog Sci*. 29(5): 305-310.

Urata M, Yamaguchi M. (2004). The development of the enteropneust hemichordate *Balanoglossus misakiensis* KUWANO. *Zoolog. Sci*. 21: 533-540.

Vickery MS, McClintock JB. (1998). Regeneration in metazoan larvae. Nature 394: 140.

Vickery MS, Vickery MCL, Mcclintock JB. (2002). Morphogenesis and Organogenesis in the Regenerating Planktotrophic Larvae of Asteroids and Echinoids. Biol Bull. 203(2): 121-133.

Vinson JP, Jaffe DB, O'Neill K, Karlsson EK, Stange-Thomann N, Anderson S, Mesirov JP, Satoh N, Satou Y, Nusbaum C, Birren B, Galagan JE, Lander ES. (2005). Assembly of polymorphic genomes: Algorithms and application to *Ciona savignyi*. *Genome Res*. 15: 1127-1135.

Wada H, Satoh N. (1994). Details of the evolutionary history from invertebrates to vertebrates, as deduced from the sequences of 18S rDNA. *Proc. Natl. Acad. Sci. U.S.A.* 91: 1801-1804.

Wallin J, Eibel H, Neubüser A, Wilting J, Koseki H, Balling R. (1996). *Pax1* is expressed during development of the thymus epithelium and is required for normal T-cell maturation. *Development.* 122: 23-30.

Wilkinson DG, Bhatt S, Herrmann BG. (1990). Expression pattern of the mouse *T* gene and its role in mesoderm formation. *Nature.* 343: 657-659.

Willey A. (1899). Enteropneusta from the South Pacific, with notes on the West Indian Species. In: Willey A, editor. Zoological results, Part 3. Cambridge.

Wilson SW, Houart C. (2004). Early steps in the development of the forebrain. *Dev Cell* 6: 167–181.

Wygoda JA, Yang Y, Byrne M, Wray GA. (2014). Transcriptomic analysis of the highly derived radial body plan of a sea urchin. *Genome Biol Evol*. 6(4): 964-73. doi: 10.1093/gbe/evu070.

Yannas IV. (2001) Tissue and organ regeneration in adults. Springer-Verlag New York, Inc pp. 138–185.

Yasuo H, Satoh N. (1993). Function of the vertebrate *T* gene. *Nature* 364: 582-583.

Young HM, Anderson RB, Anderson CR. (2004). Guidance cues involved in the development of the peripheral autonomic nervous system. *Auton Neurosci*. 112(1-2): 1-14.

Zhang G, Miyamoto MM, Cohn MJ. (2006). Lamprey type II collagen and *Sox9* reveal an ancient origin of the vertebrate collagenous skeleton. *Proc. Natl. Acad. Sci. USA*. 103(9): 3180-3185.

Ziegler-Graham K, MacKenzie EJ, Ephraim PL, Travison TG, Brookmeyer R. (2008). Estimating the Prevalence of Limb Loss in the United States: 2005 to 2050. *Arch Phys Med Rehabil* 89: 422–429.

Zondag L, Rutherford K, Gemmell N, Wilson M. (2016). Uncovering the pathways underlying whole body regeneration in a chordate model, *Botrylloides leachi* using de novo transcriptome analysis. *BMC Genomics*. 17: 114.